



NUREG/CR-3805, Vol. 5

Engineering Characterization of Ground Motion

Engineering Characterization of Ground Motion

Task II: Summary Report

Manuscript Completed: June 1986

Date Published: August 1986

Prepared by

M.S. Power, C.-Y. Chang, I.M. Idriss, Woodward-Clyde Consultants
R.P. Kennedy, Structural Mechanics Associates, Inc.

Woodward-Clyde Consultants
Walnut Creek, CA 94596

Structural Mechanics Associates, Inc.
Newport Beach, CA 92660

NRC Job Code B6680

NOTICE

This report was prepared as an account of work sponsored by an agency of the United States Government. Neither the United States Government nor any agency thereof, or any of their employees, makes any warranty, expressed or implied, or assumes any legal liability of responsibility for any third party's use, or the results of such use, of any information, apparatus, product or process disclosed in this report, or represents that its use by such third party would not infringe privately owned rights.

NOTICE

Availability of Reference Materials Cited in NRC Publications

Most documents cited in NRC publications will be available from one of the following sources:

1. The NRC Public Document Room, 1717 H Street, N.W.
Washington, DC 20555
2. The Superintendent of Documents, U.S. Government Printing Office, Post Office Box 37082,
Washington, DC 20013-7082
3. The National Technical Information Service, Springfield, VA 22161

Although the listing that follows represents the majority of documents cited in NRC publications, it is not intended to be exhaustive.

Referenced documents available for inspection and copying for a fee from the NRC Public Document Room include NRC correspondence and internal NRC memoranda; NRC Office of Inspection and Enforcement bulletins, circulars, information notices, inspection and investigation notices; Licensee Event Reports; vendor reports and correspondence; Commission papers; and applicant and licensee documents and correspondence.

The following documents in the NUREG series are available for purchase from the GPO Sales Program: formal NRC staff and contractor reports, NRC-sponsored conference proceedings, and NRC booklets and brochures. Also available are Regulatory Guides, NRC regulations in the *Code of Federal Regulations*, and *Nuclear Regulatory Commission Issuances*.

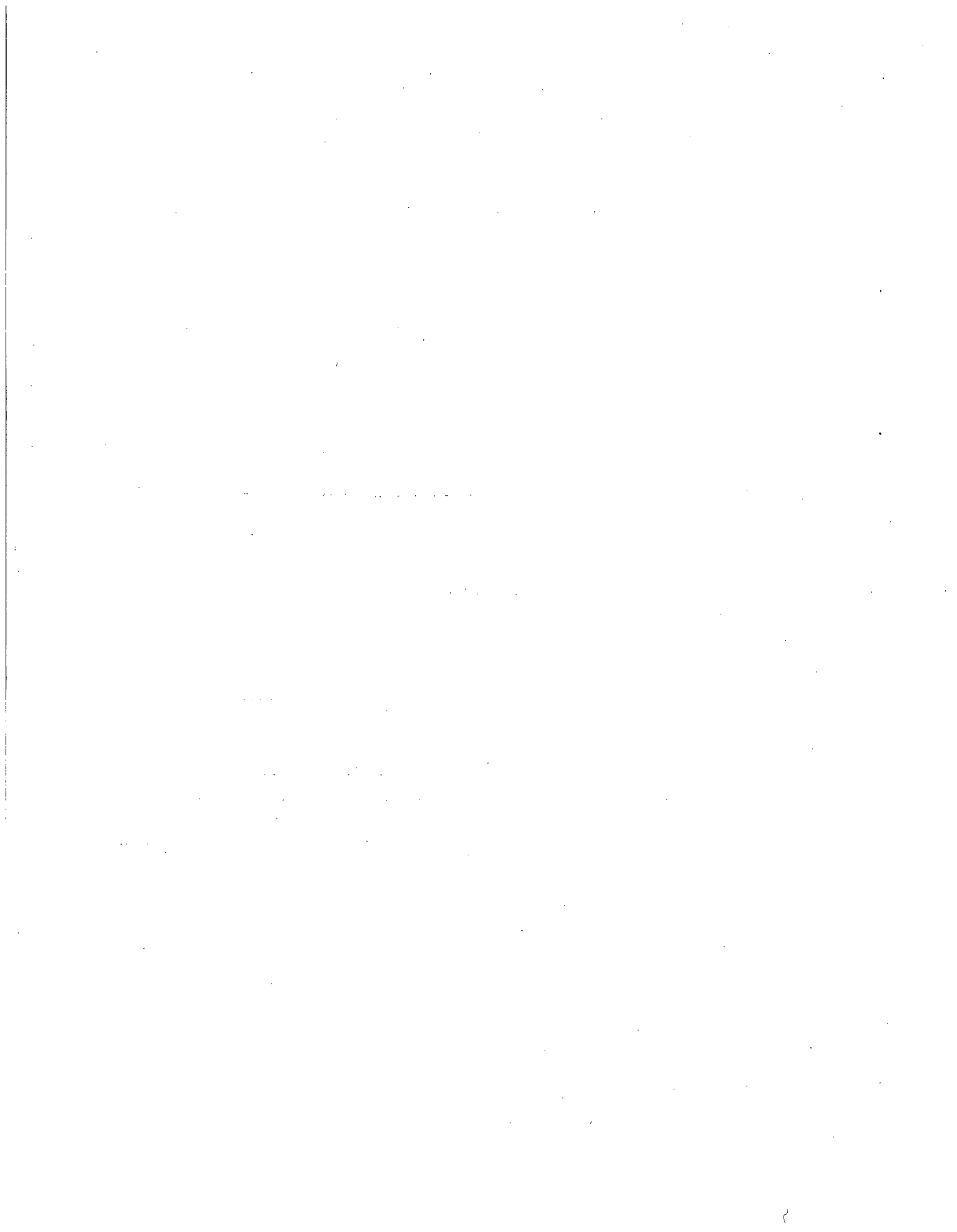
Documents available from the National Technical Information Service include NUREG series reports and technical reports prepared by other federal agencies and reports prepared by the Atomic Energy Commission, forerunner agency to the Nuclear Regulatory Commission.

Documents available from public and special technical libraries include all open literature items, such as books, journal and periodical articles, and transactions. *Federal Register* notices, federal and state legislation, and congressional reports can usually be obtained from these libraries.

Documents such as theses, dissertations, foreign reports and translations, and non-NRC conference proceedings are available for purchase from the organization sponsoring the publication cited.

Single copies of NRC draft reports are available free, to the extent of supply, upon written request to the Division of Technical Information and Document Control, U.S. Nuclear Regulatory Commission, Washington, DC 20555.

Copies of industry codes and standards used in a substantive manner in the NRC regulatory process are maintained at the NRC Library, 7920 Norfolk Avenue, Bethesda, Maryland, and are available there for reference use by the public. Codes and standards are usually copyrighted and may be purchased from the originating organization or, if they are American National Standards, from the American National Standards Institute, 1430 Broadway, New York, NY 10018.



FOREWORD

This report presents the results of part of a two-task study on the engineering characterization of earthquake ground motion for nuclear power plant design. The overall objective of this research program sponsored by the U.S. Nuclear Regulatory Commission (USNRC) is to develop recommendations for methods for selecting design response spectra or acceleration time histories to be used to characterize motion at the foundation level of nuclear power plants.

Task I of the study, which is presented in Vol. 1 of NUREG/CR-3805, developed a basis for selecting design response spectra taking into account the characteristics of free-field ground motion found to be significant in causing structural damage. Task II incorporates additional considerations of effects of spatial variations of ground motions and soil-structure interaction on foundation motions and structural response. The results of Task II are presented in Vols. 2 through 5 of NUREG/CR-3805 as follows: Vol. 2, effects of ground motion characteristics on structural response considering localized structural nonlinearities and soil-structure interaction effects; Vol. 3, observational data on spatial variations of earthquake ground motions; Vol. 4, soil-structure interaction effects on structural response; and Vol. 5, summary based on Tasks I and II studies. This report presents the results of the Vol. 5 studies.

This study was conducted under Contract No. NRC 04-80-192 with the USNRC. Woodward-Clyde Consultants (WCC) was the prime contractor for the project. Project Subcontractors were Structural Mechanics Associates, Newport Beach, California, Structural and Earthquake Engineering Consultants, Inc., Sierra Madre, California, Interpacific Technology, Inc., Oakland, California, and NCT Engineering, Inc., Lafayette, California.

Project Consultants, W. J. Hall of the University of Illinois, Champaign, J. E. Luco of the University of California, San Diego, J. M. Roeset of the University of Texas, Austin, H. B. Seed of the University of California, Berkeley, and N. C. Tsai of NCT Engineering, Inc., Lafayette, California, provided a detailed review of a draft of the report and made many valuable comments. J. F. Costello provided overall technical guidance and review as the technical representative of the USNRC for this research project.

TABLE OF CONTENTS

	<u>Page</u>
1. <u>INTRODUCTION</u>	1-1
2. <u>ENGINEERING CHARACTERIZATION OF GROUND MOTION AS RELATED TO THE INELASTIC RESPONSE AND PERFORMANCE OF STRUCTURES</u>	2-1
2.1 GROUND MOTION CHARACTERISTICS INFLUENCING STRUCTURAL INELASTIC BEHAVIOR	2-2
2.2 CHARACTERIZATION OF GROUND MOTION FOR STRUCTURAL INELASTIC DEFORMATIONS	2-7
2.2.1 Construction of Inelastic Response Spectra	2-7
2.2.2 Characterization of Ground Motion Using Reg. Guide 1.60	2-11
2.3 ESTIMATING INELASTIC RESPONSE OF MULTI-DEGREE-OF-FREEDOM SYSTEMS	2-13
2.3.1 Estimating Story Drift Ductilities	2-15
2.3.2 Inelastic Response in Fixed-base and Soil-structure Interaction Cases	2-17
2.3.3 Response of Equipment	2-19
3. <u>ENGINEERING CHARACTERIZATION OF GROUND MOTION AS RELATED TO SPATIAL VARIATIONS OF GROUND MOTION AND SOIL-STRUCTURE INTERACTION</u>	3-1
3.1 CHARACTERIZATION OF FREE-FIELD CONTROL MOTION	3-2
3.1.1 Effects of Soil-structure Interaction on Structural Response for Different Free-field Motions	3-2
3.1.2 Effects of Free-field Motion on Structural Response for Given Foundation Conditions	3-6
3.1.3 Free-field Ground Motion Characterization	3-8
3.2 CHARACTERIZATION OF VARIATIONS OF GROUND MOTION WITH DEPTH	3-11
3.2.1 Analytical Predictions of Ground Motion Variations with Depth	3-11
3.2.2 Observational Data on Variations of Earthquake Ground Motion with Depth	3-13
3.2.3 Effects on Structural Response of Neglecting Ground Motion Variations with Depth	3-18

TABLE OF CONTENTS (concluded)

	<u>Page</u>
3.2.4 Ground Motion Characterization	3-21
3.3 CHARACTERIZATION OF VARIATIONS OF GROUND MOTION IN A HORIZONTAL PLANE	3-23
3.3.1 Phase Differences in Ground Motion in a Horizontal Plane	3-23
3.3.1.1 Apparent Horizontal Wave Propagation Velocity	3-23
3.3.1.2 Effects on Structural Response of Non-Vertically Incident Waves	3-25
3.3.2 Incoherence of Ground Motion	3-32
3.3.3 Ground Motion Characterization	3-35
4. <u>SUMMARY AND CONCLUSIONS</u>	4-1
REFERENCES	R-1
APPENDIX A <u>CALCULATIONS OF ACCIDENTAL ECCENTRICITY</u>	A-1

LIST OF TABLES

<u>Table</u>		<u>Page</u>
2-1	LIST OF EARTHQUAKE/STRUCTURE-TYPES INCLUDED IN REVIEW/DAMAGE DOCUMENTATION	2-22
2-2	ACCELEROGRAMS USED IN NONLINEAR ANALYSES	2-23
2-3	SCALE FACTORS FOR LOW AND HIGH DUCTILITIES	2-24
2-4	CORRELATION BETWEEN DURATION, T'_D AND EFFECTIVE NUMBER OF STRONG NONLINEAR CYCLES, N	2-25
2-5	COMPARISON OF MAXIMUM STORY DRIFT DUCTILITIES FROM ELASTIC AND NONLINEAR ANALYSES - REACTOR BUILDING ON FIXED BASE	2-26
2-6	COMPARISON OF MAXIMUM STORY DRIFT DUCTILITIES FROM ELASTIC AND NONLINEAR ANALYSES - REACTOR BUILDING EMBEDDED IN STIFF SOIL	2-27
3-1	CHARACTERISTICS OF SOIL PROFILES I THROUGH IV	3-38
3-2	ACCELEROGRAMS USED IN SOIL-STRUCTURE INTERACTION ANALYSES	3-39
3-3	EFFECTS OF SOIL-STRUCTURE INTERACTION ON BASE SHEAR FORCE IN CONTAINMENT SHELL	3-40
3-4	EFFECTS OF INPUT MOTION ON BASE SHEAR FORCE IN CONTAINMENT SHELL FROM SOIL-STRUCTURE INTERACTION ANALYSIS	3-41
3-5	EFFECT OF EXCLUDING KINEMATIC INTERACTION ON BASE SHEAR FORCE IN CONTAINMENT SHELL	3-42
3-6	CHARACTERISTICS OF SOIL PROFILES V AND VI	3-43
3-7	EFFECTS OF RELATIVELY SMALL VARIATIONS IN SOIL PROPERTIES ON STRUCTURAL RESPONSE FROM SOIL-STRUCTURE INTERACTION ANALYSIS	3-44
3-8	SUMMARY OF APPARENT HORIZONTAL PROPAGATION VELOCITIES	3-45
A-1	ACCIDENTAL ECCENTRICITY FOR NON-VERTICALLY INCIDENT EXCITATIONS	A-4

LIST OF FIGURES

<u>Figure</u>		<u>Page</u>
2-1	SHEAR WALL STRUCTURAL MODEL FOR NONLINEAR ANALYSES	2-28
2-2	ACCELEROGRAM SCALE FACTORS REQUIRED TO ATTAIN DUCTILITY OF 4.3 VERSUS STRONG MOTION DURATION	2-29
2-3	EFFECT OF FREQUENCY SHIFT DUE TO NONLINEAR RESPONSE	2-30
2-4	ACCELEROGRAM SCALE FACTORS REQUIRED TO ATTAIN DUCTILITY OF 4.3 VERSUS MAGNITUDE	2-31
2-5	INELASTIC RESPONSE SPECTRA CORRESPONDING TO REG. GUIDE 1.60 RESPONSE SPECTRA	2-32
2-6	INELASTIC RESPONSE SPECTRA FOR MELENDY RANCH ACCELEROGRAM	2-33
2-7	COMPARISON OF INELASTIC RESPONSE SPECTRA FOR TAFT AND MELENDY RANCH ACCELEROGRAMS	2-34
2-8	COMPARISON OF TAFT SPECTRA WITH REG. GUIDE 1.60 SPECTRA ANCHORED TO "EFFECTIVE" DESIGN ACCELERATION	2-35
2-9	COMPARISON OF MELENDY RANCH SPECTRA WITH REG. GUIDE 1.60 SPECTRA ANCHORED TO "EFFECTIVE" DESIGN ACCELERATION	2-36
2-10	REACTOR BUILDING MAXIMUM STORY DRIFT DUCTILITY VERSUS MAXIMUM DEMAND/CAPACITY RATIO FOR FIXED-BASE AND SOIL-STRUCTURE INTERACTION CASES	2-37
2-11	COMPARISON OF IN-STRUCTURE RESPONSE SPECTRA FROM ELASTIC AND INELASTIC ANALYSIS OF REACTOR BUILDING - FIXED-BASE CASE, ARTIFICIAL ACCELEROGRAM (0.5G) INPUT	2-38
2-12	COMPARISON OF IN-STRUCTURE RESPONSE SPECTRA FROM ELASTIC AND INELASTIC ANALYSIS OF REACTOR BUILDING - SOIL-STRUCTURE INTERACTION (STIFF SOIL) CASE, PARKFIELD ACCELEROGRAM (0.5G) INPUT	2-39
3-1	FREQUENCY CONTENT OF MELENDY RANCH (N29W) INPUT MOTION IN RELATION TO CHARACTERISTIC FREQUENCY OF SOIL-STRUCTURE SYSTEMS (REACTOR BUILDING, 40 FT EMBEDMENT, VERTICALLY INCIDENT WAVES)	3-46

LIST OF FIGURES (Continued)

<u>Figure</u>		<u>Page</u>
3-2	FREQUENCY CONTENT OF PARKFIELD INPUT MOTION IN RELATION TO CHARACTERISTIC FREQUENCIES OF SOIL-STRUCTURE SYSTEMS (REACTOR BUILDING, 40 FT EMBEDMENT, VERTICALLY INCIDENT WAVES)	3-47
3-3	COMPARISON OF FLOOR RESPONSE SPECTRA OF REACTOR BUILDING FOR RIGID SOIL, SOIL PROFILES I, II, III AND IV USING ARTIFICIAL R.G. 1.60 MOTION AS CONTROL MOTION (VERTICAL INCIDENCE, 40 FT EMBEDMENT)	3-48
3-4	EFFECTS OF SOIL-STRUCTURE INTERACTION ON FLOOR RESPONSE SPECTRA (REACTOR BUILDING, 40 FT EMBEDMENT, SOIL PROFILE II, VERTICALLY INCIDENT WAVES)	3-49
3-5	EFFECTS OF SOIL-STRUCTURE INTERACTION ON FLOOR RESPONSE SPECTRA (REACTOR BUILDING, 40 FT EMBEDMENT, SOIL PROFILE IV, VERTICALLY INCIDENT WAVES)	3-50
3-6	COMPARISON OF RESPONSE SPECTRA OF DIFFERENT CONTROL MOTIONS USED IN THE SOIL-STRUCTURE INTERACTION ANALYSES	3-51
3-7	RELATIVE FREQUENCY CONTENT OF PARKFIELD AND REG. GUIDE 1.60 INPUT MOTIONS IN RELATION TO CHARACTERISTIC FREQUENCIES OF SOIL-STRUCTURE SYSTEMS AND BASE SHEAR RESPONSE (REACTOR BUILDING, 40 FT EMBEDMENT, VERTICALLY INCIDENT WAVES)	3-52
3-8	RELATIVE FREQUENCY CONTENT OF MELENDY RANCH (N29W) AND REG. GUIDE 1.60 INPUT MOTIONS IN RELATION TO CHARACTERISTIC FREQUENCIES OF SOIL-STRUCTURE SYSTEMS AND BASE SHEAR RESPONSE (REACTOR BUILDING, 40 FT EMBEDMENT, VERTICALLY INCIDENT WAVES)	3-53
3-9	COMPARISON OF FLOOR RESPONSE SPECTRA AT TOP OF BASEMAT OF REACTOR BUILDING FOR DIFFERENT CONTROL MOTIONS, (VERTICAL INCIDENCE, 40 FT EMBEDMENT)	3-54
3-10	COMPARISON OF FLOOR RESPONSE SPECTRA AT TOP OF CONTAINMENT SHELL OF REACTOR BUILDING FOR DIFFERENT CONTROL MOTIONS, (VERTICAL INCIDENCE, 40 FT EMBEDMENT)	3-55
3-11	COMPARISON OF FLOOR RESPONSE SPECTRA AT TOP OF INTERNAL STRUCTURE OF REACTOR BUILDING FOR DIFFERENT CONTROL MOTIONS, (VERTICAL INCIDENCE, 40 FT EMBEDMENT)	3-56

LIST OF FIGURES (Continued)

<u>Figure</u>		<u>Page</u>
3-12	ILLUSTRATION OF EFFECT OF LOCAL SOIL CONDITIONS ON RESPONSE SPECTRAL SHAPES FROM STATISTICAL ANALYSIS	3-57
3-13	ILLUSTRATION OF EFFECT OF EARTHQUAKE MAGNITUDE ON RESPONSE SPECTRAL SHAPE FROM STATISTICAL ANALYSIS	3-58
3-14	COMPARISON OF RESPONSE SPECTRA OF REG. GUIDE 1.60 HORIZONTAL CONTROL MOTION, HORIZONTAL FREE-FIELD FOUNDATION-LEVEL MOTION, AND FOUNDATION INPUT MOTIONS, (REACTOR BUILDING, 40 FT EMBEDMENT, SOIL PROFILE IV, VERTICALLY INCIDENT WAVES)	3-59
3-15	COMPARISON OF RESPONSE SPECTRA OF REG. GUIDE 1.60 VERTICAL CONTROL MOTION, VERTICAL FREE-FIELD FOUNDATION-LEVEL MOTION, AND VERTICAL FOUNDATION INPUT MOTION, (REACTOR BUILDING, 40 FT EMBEDMENT, SOIL PROFILE IV, VERTICALLY INCIDENT WAVES)	3-60
3-16	COMPARISON OF RESPONSE SPECTRA OF HORIZONTAL FOUNDATION INPUT MOTION WITH HORIZONTAL FOUNDATION MOTION FROM COMPLETE SOIL-STRUCTURE INTERACTION ANALYSIS (REACTOR BUILDING, 40 FT EMBEDMENT, SOIL PROFILE IV, REG. GUIDE 1.60 CONTROL MOTION, VERTICALLY INCIDENT WAVES)	3-61
3-17	COMPARISON OF RESPONSE SPECTRA OF VERTICAL FOUNDATION INPUT MOTION WITH VERTICAL FOUNDATION MOTION FROM COMPLETE SOIL-STRUCTURE INTERACTION ANALYSIS (REACTOR BUILDING, 40 FT EMBEDMENT, SOIL PROFILE IV, REG. GUIDE 1.60 CONTROL MOTION, VERTICALLY INCIDENT WAVES)	3-62
3-18	COMPARISON OF RESPONSE SPECTRA OF ROCKING FOUNDATION INPUT MOTION WITH ROCKING FOUNDATION MOTION FROM COMPLETE SOIL-STRUCTURE INTERACTION ANALYSIS (REACTOR BUILDING, 40 FT EMBEDMENT, SOIL PROFILE IV, REG. GUIDE 1.60 CONTROL MOTION, VERTICALLY INCIDENT WAVES)	3-63
3-19	VARIATIONS OF RECORDED PEAK ACCELERATION WITH DEPTH-NARIMASU DOWNHOLE ARRAY DATA	3-64
3-20	RESPONSE SPECTRA OF RECORDED MOTIONS - NARIMASU DOWNHOLE ARRAY DATA (DAMPING=0.05)	3-65
3-21a	COMPARISON OF CALCULATED AND RECORDED VARIATIONS OF PEAK ACCELERATION WITH DEPTH, DECONVOLUTION ANALYSIS, NS COMPONENTS, NARIMASU SITE	3-66

LIST OF FIGURES (Continued)

<u>Figure</u>		<u>Page</u>
3-21b	COMPARISON OF CALCULATED AND RECORDED VARIATIONS OF PEAK ACCELERATION WITH DEPTH, DECONVOLUTION ANALYSIS, EW COMPONENTS, NARIMASU SITE	3-67
3-22a	COMPARISON OF RESPONSE SPECTRA OF RECORDED AND COMPUTED MOTIONS, DECONVOLUTION ANALYSIS, NS COMPONENTS, NARIMASU SITE	3-68
3-22b	COMPARISON OF RESPONSE SPECTRA OF RECORDED AND COMPUTED MOTIONS, DECONVOLUTION ANALYSIS, EW COMPONENTS, NARIMASU SITE	3-69
3-23	COMPARISON OF RESPONSE SPECTRA OF RECORDED AND COMPUTED MOTIONS, DECONVOLUTION ANALYSIS WITH PARAMETRIC VARIATION IN SOIL PROPERTIES, EW COMPONENTS, NARIMASU SITE	3-70
3-24	COMPARISON OF RESPONSE SPECTRA OF ACCELEROGRAMS RECORDED AT FINISHED GRADE IN THE FREE FIELD AND AT THE BASE OF THE REACTOR CAISSON AT THE HUMBOLDT BAY PLANT DURING THE JUNE 6, 1975, FERNDAL, CALIFORNIA EARTHQUAKE (HORIZONTAL COMPONENTS)	3-71
3-25	COMPARISON OF RESPONSE SPECTRA OF ACCELEROGRAMS RECORDED AT FINISHED GRADE IN THE FREE FIELD AND AT THE BASE OF THE REACTOR CAISSON AT THE HUMBOLDT BAY PLANT DURING THE JUNE 6, 1975, FERNDAL, CALIFORNIA EARTHQUAKE (VERTICAL COMPONENT)	3-72
3-26	COMPARISON OF RECORDED AND COMPUTED SPECTRA IN REFUELING BUILDING, HUMBOLDT BAY POWER PLANT (AFTER VALERA ET AL., 1977)	3-73
3-27a	COMPARISON OF RESPONSE SPECTRA OF MOTIONS RECORDED AT STATIONS 199 (WITHOUT BASEMENT) AND 208 (WITH BASEMENT) DURING THE 1971 SAN FERNANDO EARTHQUAKE	3-74
3-27b	COMPARISON OF RESPONSE SPECTRA OF MOTIONS RECORDED AT STATIONS 199 (WITHOUT BASEMENT) AND 208 (WITH BASEMENT) DURING THE 1971 SAN FERNANDO EARTHQUAKE	3-75
3-28	COMPARISON OF RESPONSE SPECTRA OF MELENDY RANCH CONTROL MOTION AND CORRESPONDING FOUNDATION INPUT MOTION (REACTOR BUILDING, SOIL PROFILE IV, 40 FT EMBEDMENT, VERTICALLY INCIDENT WAVES)	3-76

LIST OF FIGURES (Continued)

<u>Figure</u>		<u>Page</u>
3-29	COMPARISON OF RESPONSE SPECTRA OF PARKFIELD CONTROL MOTION AND CORRESPONDING FOUNDATION INPUT MOTION (REACTOR BUILDING, SOIL PROFILE IV, 40 FT EMBEDMENT, VERTICALLY INCIDENT WAVES)	3-77
3-30	COMPARISON OF FLOOR RESPONSE SPECTRA OF REACTOR BUILDING FROM ANALYSES WITH AND WITHOUT CONSIDERATION OF KINEMATIC INTERACTION, ARTIFICIAL REG. GUIDE 1.60 EXCITATION, SOIL PROFILE III (40 FT EMBEDMENT, VERTICAL INCIDENCE)	3-78
3-31	COMPARISON OF RESPONSE SPECTRA OF COMBINED TRANSLATIONAL AND TORSIONAL MOTION AND TRANSLATIONAL COMPONENT, AUXILIARY BUILDING, SOIL PROFILE III, NONVERTICALLY INCIDENT WAVES ($C_Y = 3\text{KM/SEC}$), ARTIFICIAL REG. GUIDE 1.60 EXCITATION	3-79
3-32	COMPARISON OF RESPONSE SPECTRA OF COMBINED TRANSLATIONAL AND TORSIONAL MOTION AND TRANSLATIONAL COMPONENT, REACTOR BUILDING, 40 FT EMBEDMENT, SOIL PROFILE II, NONVERTICALLY INCIDENT WAVES ($C_Y = 3\text{KM/SEC}$), MELENDY RANCH EXCITATION	3-80
3-33	COMPARISON OF RESPONSE SPECTRA OF COMBINED TRANSLATIONAL AND TORSIONAL MOTION AND TRANSLATIONAL COMPONENT, AUXILIARY BUILDING, SOIL PROFILE III, NONVERTICALLY INCIDENT WAVES ($C_Y = 3\text{KM/SEC}$), MELENDY RANCH EXCITATION	3-81
3-34	TIME HISTORIES OF BASE SHEAR AND TORQUE (NORMALIZED BY $D = 160\text{ FT}$), AUXILIARY BUILDING, SOIL PROFILE III, NONVERTICALLY INCIDENT WAVES ($C_Y = 3\text{KM/SEC}$), ARTIFICIAL REG. GUIDE 1.60 EXCITATION	3-82
3-35	ACCELERATION TIME HISTORIES FOR CHANNEL 2 (EAST-WEST COMPONENT), EL CENTRO DIFFERENTIAL ARRAY, THE 1979 IMPERIAL VALLEY EARTHQUAKE (AFTER SMITH ET AL., 1982)	3-83
3-36	RATIO OF THE RESPONSE SPECTRA FOR THE ARRAY SUM TO THE AVERAGE OF THE INDIVIDUAL RESPONSE SPECTRA FOR THE HORIZONTAL COMPONENTS (CHANNELS 2 AND 3), EL CENTRO DIFFERENTIAL ARRAY (AFTER SMITH ET AL., 1982)	3-84
A-1a	TIME HISTORIES OF BASE SHEAR AND TORQUE (NORMALIZED BY $D = 100\text{ FT}$), REACTOR BUILDING, 40 FT EMBEDMENT, SOIL PROFILE II, NONVERTICALLY INCIDENT WAVES ($C_Y = 3\text{KM/SEC}$), ARTIFICIAL REG. GUIDE 1.60 EXCITATION	A-5

LIST OF FIGURES (Concluded)

<u>Figure</u>		<u>Page</u>
A-1b	TIME HISTORIES OF BASE SHEAR AND TORQUE (NORMALIZED BY D = 100 FT) REACTOR BUILDING, 40 FT EMBEDMENT, SOIL PROFILE II, NONVERTICALLY INCIDENT WAVES ($C_V = 3\text{KM/SEC}$), ARTIFICIAL REG. GUIDE 1.60 EXCITATION	A-6
A-2a	TIME HISTORIES OF BASE SHEAR AND TORQUE (NORMALIZED BY D = 100 FT), REACTOR BUILDING, 40 FT EMBEDMENT, SOIL PROFILE II, NONVERTICALLY INCIDENT WAVES ($C_V = 3\text{KM/SEC}$), MELENDY RANCH EXCITATION	A-7
A-2b	TIME HISTORIES OF BASE SHEAR AND TORQUE (NORMALIZED BY D = 100 FT), REACTOR BUILDING, 40 FT EMBEDMENT, SOIL PROFILE II, NONVERTICALLY INCIDENT WAVES ($C_V = 3\text{ KM/SEC}$), MELENDY RANCH EXCITATION	A-8
A-3	TIME HISTORIES OF BASE SHEAR AND TORQUE (NORMALIZED BY D = 160 FT), AUXILIARY BUILDING, SOIL PROFILE III, NONVERTICALLY INCIDENT WAVES ($C_V = 3\text{ KM/SEC}$), ARTIFICIAL REG. GUIDE 1.60 EXCITATION	A-9
A-4	TIME HISTORIES OF BASE SHEAR AND TORQUE (NORMALIZED BY D = 160 FT), AUXILIARY BUILDING, SOIL PROFILE III, NONVERTICALLY INCIDENT WAVES ($C_V = 3\text{ KM/SEC}$), MELENDY RANCH EXCITATION	A-10

1. INTRODUCTION

This report summarizes the main findings of a study that has the objective of providing guidance on the engineering characterization of earthquake ground motion to be used for the design of nuclear power plant structures. The results of the detailed studies conducted for this research project are presented in earlier reports, including Kennedy et al. (1984), Kennedy et al. (1985), Chang et al. (1986), and Luco et al. (1986).

In this study, the engineering characterization of earthquake ground motion has been related to two general considerations: the inelastic response and performance of structures; and spatial variations of ground motion and soil-structure interaction. With regard to the first consideration, observations from past earthquakes suggest that elastic response spectra are an insufficient descriptor of the damage potential of ground motions. In the first part of this study, the characteristics of ground motion that relate to the response of structures beyond the elastic range have been examined, and an engineering characterization of ground motion has been developed as a function of structural inelastic deformations and the key ground motion characteristics found to influence inelastic response.

With regard to the second consideration, evidence from past earthquakes and analytical studies indicate that the phenomena of spatial variations of ground motion and soil-structure interaction can cause the motions input to a structure foundation to differ from the free-field motions at a point on the ground surface. In the second part of the study, these phenomena have been examined and conclusions have been arrived at regarding characterizing the variations of ground motion with depth and variations of ground motion in a horizontal plane. Also, based on findings from both parts of the study on the free-field ground motion

characteristics significantly affecting elastic and inelastic structural responses, conclusions pertaining to the characterization of the free-field control motion have been developed.

The remainder of this report summarizes the two parts of the study outlined above. In Section 2, the engineering characterization of ground motion as related to the inelastic response and performance of structures is addressed. In Section 3, the engineering characterization of ground motion as related to spatial variations of ground motion and soil-structure interaction is addressed. These sections contain the main results and conclusions of the study. A summary of the main findings is presented in Section 4.

2. ENGINEERING CHARACTERIZATION OF GROUND MOTION AS RELATED TO THE INELASTIC RESPONSE AND PERFORMANCE OF STRUCTURES

The studies conducted in this part included, first, an examination of the earthquake ground motion characteristics influencing structural inelastic behavior. This was accomplished primarily through a series of analyses of simple, nonlinear structural models subjected to a variety of earthquake accelerograms. The analytical studies were supported by a review of performance of structures in past earthquakes. From these studies, earthquake ground motion characteristics having primary and secondary influence on the development of structural inelastic deformations were identified.

On the basis of these studies, the scaling of accelerograms required to attain certain inelastic deformations (attain certain ductilities) was correlated to the characteristics of the accelerograms. From these correlations, procedures were developed to construct and characterize "effective" or "inelastic" response spectra corresponding to selected ductilities (i.e. to provide an engineering characterization of ground motion with respect to structural damage potential).

The methodology for constructing inelastic response spectra was developed from analyses of simple structures having a single elastic frequency. The methodology was then applied to estimating the inelastic response of a typical multi-degree-of-freedom reactor building having localized nonlinearities. These evaluations were made both for the building supported on a rigid rock (fixed-base analyses) and embedded in soil (analyses including soil-structure interaction). As part of these analyses, the effects of structural nonlinear behavior on floor spectra, as pertinent to the response of equipment, were also examined.

The main elements of the approaches and key conclusions from these studies are summarized in the following sections.

2.1 GROUND MOTION CHARACTERISTICS INFLUENCING STRUCTURAL INELASTIC BEHAVIOR

A summary of the earthquakes and types of structures that were included in the literature review of the performance of existing structures during past earthquakes (Kennedy et al., 1984) is presented in Table 2-1. When information was available, the elastic computed forces were compared with the design forces or the estimated ultimate capacities of the structures.

The review indicated that the characterization of ground motion by low-damped elastic response spectra is not sufficient to fully describe the structural damage potential of the ground motion. It appeared that well-designed structures could experience ground motions at least 2.5 times those that would just cause structural yielding (just reach elastic capacity) without significant structural damage, even for ground motions of relatively long duration.

This review supported the need for studies to identify those ground motion characteristics important to structural damage potential and to correlate the damage potential with the ground motion characteristics. However, the empirical data base, while providing the impetus, does not contain a sufficient number and range of cases where both input ground motions and structural response are known in detail to allow damage potential to be quantitatively correlated to ground motion characteristics. A series of analyses described below was made to identify significant ground motion characteristics and provide a quantitative correlation.

The analytical studies consisted of nonlinear, inelastic analyses of simple models of structural types typical of those in nuclear power plants (Kennedy et al., 1984). Most of the analyses were for shear wall structures and a limited number for braced frame structures. Each structural model was a single-degree-of-freedom model in the elastic

range and exhibited nonlinear, degrading stiffness, hysteretic behavior following yield. The force-deformation characteristics of the model are illustrated in Figure 2-1. The models were designed to have elastic frequencies of 2.1, 3.2, 5.3, and 8.5 Hz, considered representative of stiff nuclear power plant structures (i.e., structures having elastic frequencies in the 1.8 to 10 Hz range). Nonlinear, inelastic time history analyses were made of these models using eleven recorded accelerograms plus an artificial accelerogram having spectra that fit the Reg. Guide 1.60 spectra. The accelerograms were selected to cover a wide range of earthquake magnitudes and ground motion frequency content and duration of shaking. Table 2-2 summarizes the accelerograms used.

For a given accelerogram, each structural model was designed to be at the onset of yielding for that accelerogram, i.e., the spectral acceleration of the accelerogram at the structural elastic frequency was equal to the spectral acceleration required to just reach the elastic capacity of the structural model. The accelerogram was then scaled by a factor, F_{μ} to attain a certain amount of inelastic deformation in the structure. The measure of structural damage selected was the displacement ductility, μ (ratio of maximum displacement to yield displacement). Ductility levels of 1.85 and 4.3 were selected as "low" and "high" ductilities. The low ductility level corresponds roughly to the ductility attained when code allowable loads are reached for walls designed in accordance with ACI-349. The high ductility level is judged to represent a conservative lower bound for the onset of significant structural damage. The accelerogram scale factor, F_{μ} , may be viewed either as: (a) a factor by which an accelerogram must be multiplied to attain a ductility, μ , for a structure designed to yield at a certain elastic spectral acceleration of the unscaled accelerogram; or (b) a factor by which an elastic spectral acceleration may be divided (inelastic spectral deamplification factor) to obtain an "inelastic" spectral acceleration corresponding to ductility, μ (i.e., to obtain a spectral acceleration that if designed for elastically would result in a ductility, μ , when the structure was subjected to the actual unscaled accelerogram).

The scale factors, F_{μ} , obtained for the low and high ductility levels are summarized in Table 2-3. In Figure 2-2, the factors for the high ductility level ($\mu=4.3$) are plotted versus the duration of strong shaking. The table and figure indicate that the scale factors are widely scattered, ranging for $\mu = 4.3$ from a low value of 1.29 for the Parkfield accelerogram and a 5.3 Hz structure to a high value of 8.49 for the Gavilan College accelerogram and a 2.1 Hz structure. There is a tendency for the scale factors to decrease with increasing duration (Figure 2-2), but the tendency is not pronounced and is overwhelmed by the scatter in the F_{μ} values. There is a distinct trend for the lower frequency structures to have higher scale factors. It is clear from these results that there must be some ground motion characteristics strongly influencing the attainment of displacements beyond yield, and it appears that the influence of duration is secondary.

Analysis of the results indicates that the factor that mainly determines the magnitude of the scale factor for a given ductility is the frequency content of the accelerogram relative to the elastic frequency of the structure. As the structure goes into the inelastic range during response to the scaled accelerogram, its effective frequency shifts (decreases) from the elastic frequency, f , toward a secant frequency, f_s , that corresponds to a certain ductility. As this occurs, energy is fed into the structure over this frequency range, and it is therefore the spectral content of the accelerogram over this frequency range that determines the inelastic structural response. If the accelerogram has a response spectrum that is characterized by increasing spectral accelerations as the structure softens from frequency f to f_s , then scale factors will be low. On the other hand, if the accelerogram is characterized by decreasing spectral accelerations with decreasing frequency over this range, then scale factors will be high.

The importance of the frequency content of the accelerogram to the scale factors for nonlinear response is illustrated in Figure 2-3, in which response spectra for the Parkfield, Melendy Ranch, and artificial

accelerograms are compared. For this comparison, an initial scaling of each accelerogram was made so that each has the same spectral acceleration (0.5 g) at a structural elastic frequency of 5.3 Hz. The question is, if the structure is designed to yield at the common spectral acceleration of 0.5 g, what further scale factors, F_{μ} , would be required for each accelerogram to attain a certain ductility? Because the Parkfield accelerogram has a response spectrum that shows increasing spectral values as the structure softens from the elastic frequency, f , of 5.3 Hz to a secant frequency, f_s , of 2.8 Hz (for μ equal to 4.3) (Figure 2-3), it would be expected that the scale factor for this accelerogram would be relatively low. On the other hand, because the response spectrum of the Melendy Ranch accelerogram decreases in going from 5.3 to 2.8 Hz, a relatively high scale factor would be expected for this accelerogram. A scale factor for the artificial accelerogram intermediate between those for Parkfield and Melendy Ranch would be expected based on the relatively flat spectral response for the artificial accelerogram over the f to f_s range. The scale factors determined from the nonlinear analyses (Table 2-3) are in accord with these expected results, being equal to approximately 1.3, 5.5, and 1.9 for the Parkfield, Melendy Ranch, and artificial accelerograms, respectively. For all the accelerograms used in the analyses (Table 2-3), it was found that the scale factor exceeded 2.7 for every case in which spectral acceleration decreased as the structure softened and was less than 1.7 for every case in which spectral acceleration increased (for μ of 4.3).

It is clear that the average spectral acceleration between f and f_s has a more significant influence on inelastic response than does the spectral acceleration at the elastic frequency, f . Thus the response spectrum frequency content over the frequency range for inelastic response appears to be the dominant ground motion characteristic influencing attainment of structural deformations. This frequency content effect over the range from f to f_s is also termed herein the "spectral averaging" effect.

The frequency content or spectral averaging effect appears to be much more important than the duration effect in influencing inelastic structural response. In fact, it is the spectral averaging effect which creates most of the apparent duration effect shown in Figure 2-2. Records of short duration tend to have narrow-banded spectra with the spectral peak occurring at high frequencies. When the structural elastic frequency is equal to or lower than this spectral peak frequency, large scale factors will be required to attain inelastic deformations.

Because earthquake magnitude tends to correlate with both ground motion frequency content and duration (lower magnitude events tending to have narrow-banded, relatively high frequency content spectra and short duration), it was thought that the scale factors might correlate better with earthquake magnitude than with duration. A plot of the scale factors in Table 2-3 for $\mu = 4.3$ against M_s magnitude is presented in Figure 2-4. Comparison of this figure with Figure 2-2 indicates that the correlation with magnitude is in fact better than with duration. However, the data are still widely scattered. (It is noted that for this data set the correlation with M_s magnitude appeared to be somewhat better than with M_L magnitude.)

The results of these analyses indicate the importance of frequency content (spectral amplifications, frequencies at which maximum amplifications occur, and band width) in any engineering characterization of ground motion for inelastic structural response. Further discussion of the effects of frequency content on soil-structure interaction response and implications of both inelastic structural behavior and soil-structure interaction response to the characterization of free-field ground motion is contained in Section 3.2.

It should be noted that the fact that duration has been found to have a secondary effect on inelastic structural response (relative to the effect of frequency content) is partly a result of the selection of the displacement ductility as the measure of structural damage. It is felt

that this is the most appropriate measure of the onset of structural damage (onset of behavior that might be considered unacceptable for a nuclear power plant structure). However, a better measure for structural collapse would be the total hysteretic energy absorbed by a structure during inelastic response. For this damage measure, duration or the number of strong nonlinear cycles would increase in importance. A correlation developed during this study between the duration of strong shaking (refer to Table 2-2 for definition of duration used in this study) and the number of strong nonlinear cycles is presented in Table 2-4. It should also be noted that in some extreme cases, such as earthquake ground motions in Mexico City during the 1985 Mexico earthquake, duration may play a larger role in affecting inelastic structural response than for the ground motions used in this study.

2.2 CHARACTERIZATION OF GROUND MOTION FOR STRUCTURAL INELASTIC DEFORMATIONS

2.2.1 Construction of Inelastic Response Spectra

Inelastic response spectra for selected levels of ductility are constructed by dividing elastic response spectra by the appropriate F_{μ} values. On the basis of the findings described in the preceding section on the significant ground motion characteristics influencing structural inelastic response, it was found that inelastic response spectra could be predicted from elastic response spectra with estimates of the frequency shift (a function of the ductility) and approximate knowledge of the duration of strong shaking (Kennedy et al., 1984). Two approaches were developed for constructing inelastic response spectra (Kennedy et al., 1984)--a point estimate approach, and a spectral averaging approach.

Using the point estimate approach, the inelastic spectral reduction factor F_{μ} , at any frequency, f , is given by

$$F_{\mu} = \mu \left(\frac{f'_e}{f} \right)^2 \left[\frac{S_a(f, \beta)}{S_a(f'_e, \beta'_e)} \right] \quad (2-1)$$

f and β are the elastic frequency and damping, respectively. f'_e and β'_e are the effective frequency and damping that account for frequency shifting and damping increase during inelastic response, i.e., the frequency and damping of an equivalent linear system that would have the same displacement as a nonlinear model. f'_e is somewhere between the elastic frequency, f , and the secant frequency, f_s . $S_a(f, \beta)$ is spectral acceleration of the elastic response spectrum at the elastic frequency and damping, and $S_a(f'_e, \beta'_e)$ is spectral acceleration of the elastic response spectrum at the effective frequency and damping. Procedures to calculate f'_e and β'_e are given in Kennedy et al. (1984). They are somewhat dependent on the strong motion duration, T'_D , and number of strong nonlinear cycles, N . Except for the shortest duration records having T'_D less than 1.0 second and N equal to 1, f'_e/f is approximately equal to 0.6 and β'_e approximately equal to 10% (for β equal to 7%) for a ductility of $\mu = 4.3$. For T'_D less than 1.0 second and $N=1$, f'_e/f increases to approximately 0.7 and β'_e to 12.5%.

It was found that the point-estimate procedure predicted scale factors that were in close agreement with the scale factors obtained from nonlinear analyses. For the twelve acceleration time histories and four model structures considered (48 cases in Table 2-3), the total range of the ratio of predicted scale factor to actual scale factor from nonlinear analyses was 0.75 to 1.29 for μ equal to 4.3. The mean ratio was 0.98 and the standard deviation of the ratios was 0.12.

Estimates of the scale factors could be improved slightly using a spectral averaging approach instead of the point estimate approach. In this approach, the spectral acceleration for the softened inelastic system is averaged over the frequency range from f to f_s rather than taken at the effective point value of f'_e . In general, the very minor improvement in accuracy for this approach as compared to the point

estimate approach does not warrant the substantial additional effort involved in using it.

The recommended procedures developed using this study have been compared to estimated F_{μ} values based on the Sozen (Gulkan and Sozen, 1974; Shibata and Sozen, 1976) and Iwan (1980) methods for predicting f'_e and β' and from the Newmark (Newmark and Hall, 1978) and Riddell (Riddell and Newmark, 1979) methods for directly estimating F_{μ} . From these comparisons, it is concluded that for the shear wall type resistance functions used in this study, either the point averaging approach or the spectral averaging approach provides significantly more accurate estimates for F_{μ} than do these other commonly used approaches. Although the specific relationships developed during this study were for shear walls, it is also concluded, based on parametric studies conducted during the study, that these relationships can be conservatively used for braced frames and other structural systems, as long as these systems do not exhibit greater stiffness degradation and pinching behavior than the resistance-deformation function used in this study for shear walls.

Typical inelastic response spectra constructed using the procedures developed during this study are shown in Figures 2-5 and 2-6. The spectra in Figure 2-5 were constructed for the Reg. Guide 1.60 smooth spectrum anchored to a peak ground acceleration of 1.0 g. The spectra in Figure 2-6 are for the Melendy Ranch accelerogram described in Table 2-2. As a matter of interest, note that the inelastic spectral deamplification factors for the Reg. Guide 1.60 smooth spectrum in Figure 2-5 are constant factors in the acceleration amplification region ($f > 2.5$ Hz) and velocity amplification region ($f < 2.5$ Hz) in Figure 2-5, as follows:

<u>Ductility, μ</u>	<u>Inelastic Spectral Deamplification Factor, F_{μ}</u>	
	<u>Acceleration Region</u>	<u>Velocity Region</u>
1.85	1.44	1.63
4.3	1.81	2.75

These factors were calculated assuming three strong nonlinear cycles ($N=3$). The factors are insignificantly different for other numbers of cycles, except for $N = 1$ for which the calculated values of F_y would be significantly larger. However, $N = 1$ would not be appropriate for a broad-banded spectra such as Reg. Guide 1.60 since such spectra would be associated with relatively long duration motions. Section 2.2.2 contains further discussion of ground motion characterization using the Reg. Guide 1.60 spectra.

Some general characteristics of inelastic response spectra are illustrated by the spectra in Figures 2-5 and 2-6. The inelastic spectral deamplification factors (ratios of elastic to inelastic spectral values) are larger at frequencies equal to or less than the frequency at which the elastic spectrum peaks than at higher frequencies, due to the spectral averaging effect. As a result of this difference in the factors on each side of the elastic spectral peak, the peak inelastic spectral accelerations occur at frequencies higher than the frequency at which the elastic spectrum peaks. The higher the ductility, the higher is the frequency of peak inelastic spectral response. It can also be noted that at frequencies less than the spectrum peak frequencies, the deamplification factors are greater for the Melendy Ranch spectra than for the Reg. Guide 1.60 spectra. This is due mainly to the fact that the elastic spectral accelerations decrease more rapidly with decreasing frequency for the Melendy Ranch spectrum than for the Reg. Guide 1.60 spectrum, thus resulting in a greater reduction due to the spectral averaging effect for the Melendy Ranch accelerogram.

One of the uses of inelastic response spectra is to compare the structural damage potential of different accelerograms. An example of such a comparison is shown in Figure 2-7 for the Taft and Melendy Ranch accelerograms summarized in Table 2-2. The Taft accelerogram was obtained at a distance of approximately 40 km from an M_s 7.7 earthquake and is characterized by a peak acceleration of 0.18 g, a relatively broad-banded response spectrum, and a relatively long duration of strong

shaking (T_D' of 10.3 seconds). The Melendy Ranch accelerogram was obtained at a distance of approximately 5 km from an M_S 4.3 earthquake and is characterized by a peak acceleration of 0.52 g, a relatively narrow-banded response spectrum (peak elastic response at about 6 Hz) and a relatively short duration of strong shaking (T_D' of 0.8 seconds). For each accelerogram, elastic ($\mu=1.0$) and inelastic ($\mu=1.85$ and 4.3) response spectra are shown in Figure 2-7. The figure indicates, for example, for a 5 Hz structure, that the Melendy Ranch accelerogram would be a much more severe loading than the Taft accelerogram if elastic response were required (elastic spectral acceleration for Melendy Ranch being about 4 times higher than elastic spectral accelerations for Taft at a frequency of 5 Hz). However, for a damage measure of ductility 4.3, Melendy Ranch is no more damaging than Taft to a 5 Hz structure (inelastic spectral accelerations of the two accelerograms being approximately equal at 5 Hz). For a structure having a frequency exceeding 5 Hz, Figure 2-7 indicates that Melendy Ranch is more damaging than Taft even at the higher ductility level of 4.3. As another example, for a 3 Hz structure, Melendy Ranch and Taft would have equal damage potential considering elastic response, but Melendy Ranch would be much less damaging than Taft considering a ductility of 4.3. In fact, for a ductility of 4.3 caused by the Taft accelerogram, the corresponding ductility caused by the Melendy Ranch accelerogram would be only about 2, based on Figure 2-7.

2.2.2 Characterization of Ground Motion Using Reg. Guide 1.60

As a further step in the engineering characterization of ground motion for structural inelastic response, an assessment was made as to whether a standard smooth response spectrum, namely the Reg. Guide 1.60 spectrum, could be used as a basis for satisfactorily approximating inelastic response spectra of recorded motions. It was found in this study that for stiff structures (frequency range 1.8 to 10 Hz) and at least over the ductility range 1.0 to 4.3, the Reg. Guide 1.60 spectral shapes for elastic and inelastic response (Figure 2-5), anchored to an "effective" ground acceleration, provide an adequate engineering

characterization of ground motion for longer duration motions ($T_D' > 3.0$ seconds) that are characterized by relatively broad-banded response spectra. The "effective" acceleration, denoted A_{DE1} herein, can be defined as an rms-based acceleration, as follows:

$$A_{DE1} = a_{rms} \sqrt{2 \ln(2.8 T_D' \Omega')} \quad (2-2)$$

in which the rms acceleration, a_{rms} , is evaluated over the strong motion duration, T_D' , and Ω' is the central or mean frequency of the motion. Ω' was found to be in the range of 3.6 to 4.7 Hz for the longer-duration motions used in the study. Values of A_{DE1} for the different accelerograms used in the study are summarized in Table 2-2.

An example of the characterization of a recorded motion using Reg. Guide 1.60 is shown in Figure 2-8. In the figure, elastic and inelastic response spectra for the Taft accelerogram are compared with smooth response spectra based on Reg. Guide 1.60 anchored to the effective acceleration for the Taft motion (Table 2-2). It can be seen that the spectra based on Reg. Guide 1.60 for $\mu = 1.0, 1.85,$ and 4.3 provide a reasonable and somewhat conservative fit to the spectra of the recorded Taft motion. For the six records used in the study that were characterized by relatively broad frequency content spectra and strong motion duration $T_D' > 3.0$ seconds (Table 2-2), it was found that the maximum factor of conservatism using Reg. Guide 1.60 anchored to A_{DE1} , i.e. the maximum ratio at any frequency in the range 1.8 to 10 Hz between the Reg. Guide spectrum and the spectrum of the recorded motion, was approximately 2.0 for spectra covering the ductility range 1.0 to 4.3. Similarly, the maximum factor of unconservatism was found to be about 1.3. On the average, considering the response for the six accelerograms over the frequency range from 1.8 to 10 Hz, the characterization of ground motion using Reg. Guide 1.60 introduced a slight conservative bias (factor of about 1.15) for elastic response ($\mu=1.0$) to essentially no bias for inelastic response ($\mu=1.85$ and 4.3).

Although it was found that use of Reg. Guide 1.60 provided an adequate engineering characterization of ground motion for the longer-duration records, this was not the case for the shorter duration records ($T_D' \leq 3.0$ seconds) that are typically characterized by narrow-banded spectra. The inadequacy of a Reg. Guide 1.60-type of characterization for these records is illustrated in Figure 2-9, in which elastic and inelastic response spectra for the Melendy Ranch accelerogram ($T_D'=0.8$ seconds, Table 2-2) are compared with the spectra obtained using Reg. Guide 1.60 and the effective acceleration for the Melendy Ranch accelerogram (Table 2-2). The characterization using Reg. Guide 1.60 would be grossly conservative at lower frequencies in this case, for example by a factor of about 5 at a frequency of 3 Hz for $\mu = 4.3$.

For the recorded accelerograms used in this study (Table 2-2), the six recorded during earthquakes having M_L of 6.4 or greater were characterized both by longer duration ($T_D' > 3.0$ seconds) and relatively broad-banded response spectra. The five accelerograms recorded during earthquakes having M_L of 5.7 or less were characterized both by shorter duration ($T_D' \leq 3.0$ seconds) and relatively narrow-banded response spectra. However, specific correlations with magnitude are not well defined by the limited data set.

2.3 ESTIMATING INELASTIC RESPONSE OF MULTI-DEGREE-OF-FREEDOM SYSTEMS

The methodology described in Section 2.2 for characterizing ground motions with respect to their structural damage potential was developed based on analyses of nonlinear models of simple structures. To demonstrate the adequacy of this ground motion characterization for more complex structures, the methodology was applied to estimating the response of a typical PWR reactor building having localized nonlinearities (Kennedy et al., 1985). The structure analyzed had been designed to remain elastic for a 0.2 g peak acceleration, broad-banded response spectrum input similar to the Reg. Guide 1.60 spectrum. The structure was subjected to four earthquake inputs scaled to 0.5 g peak

acceleration, resulting in varying degrees of structural inelastic response.

The PWR reactor building includes both a prestressed concrete containment and a reinforced concrete internal structure. The containment and internal structure have fixed-base fundamental natural frequencies of 4.5 and 5.2 Hz, respectively. The containment has very high seismic capacity so only the internal structure is susceptible to inelastic response. The internal structure is characterized by relatively high ratios of shear demand to shear capacity (i.e. elastic computed shear loads to shear strength) near its base, which results in that location being a "weak link" in which all the nonlinear, inelastic behavior occurs. The internal structure analyzed is representative of many nuclear plant structures that have nonuniform demand/capacity ratios with height, but the structure has more nonuniform ratios than most structures. The "weak-link" nature of the structure results in substantially greater localized ductilities than would occur in a structure with relatively uniform demand to capacity ratios. Thus, the detrimental influence of localized weak links and nonlinearities are emphasized. The measure of structural damage used in the study was the story drift ductility, μ_s , which is the ratio of maximum interstory shear inelastic deformation to interstory shear deformation at yield. For shear wall structures such as the structure analyzed, story drift ductilities in the range of 4 to 6 would be expected to represent the onset of serious structural strength degradation and damage.

The structure was analyzed for both fixed-base and soil foundation conditions. In the latter cases, 40 feet of foundation embedment (embedment depth to foundation diameter ratio approximately equal to 0.3) was assumed in soil profiles of two stiffnesses, designated "intermediate" and "stiff." Both soil profiles consist of soil layers to a depth of 250 ft overlying rock. The shear wave velocity of the soils in the intermediate soil profile is approximately 1,000 ft/sec. The soils of the stiff soil profile consist of a 40-ft layer with a shear wave velocity of approximately 900 ft/sec overlying a material with a

shear wave velocity of approximately 1,800 ft/sec. The shear wave velocity of the underlying rock is 3,600 ft/sec. Variations of ground motions with depth and kinematic and inertial soil-structure interaction were included for the soil foundation cases. Soil and structural models are described in detail by Kennedy et al. (1985). Free-field earthquake input excitation (all scaled to 0.5 g peak acceleration) consisted of an artificial accelerogram with spectra conforming to Reg. Guide 1.60, and the El Centro No. 5, Parkfield, and Melendy Ranch recorded accelerograms described in Table 2-2. These input accelerograms were applied directly to the foundation in fixed-base cases and were applied to the ground surface in the free field in soil-structure interaction cases.

2.3.1 Estimating Story Drift Ductilities

The story drift ductilities in yielding elements of the internal structure were determined from nonlinear structural analysis and were compared with ductilities estimated from linear elastic analyses using the methodology described in Section 2.2. Two techniques were utilized in estimating ductilities from elastic analyses. In the first technique, a single elastic analysis was made and ratios of induced elastic loads (elastic demand) to elastic capacity (i.e. demand/capacity ratios, F_{μ_s}) were obtained for elements corresponding to different stories throughout the height of the structure. Story drift ductilities were estimated using these elastic analysis results along with plots of F_{μ} versus μ prepared using the previously developed methodology. In the second technique, multiple pseudo elastic analyses were made using element properties in the yielding elements (effective stiffnesses and damping ratios) adjusted from the elastic values to account for the developed ductilities. The reduced stiffnesses and increased damping ratios were estimated using the previously developed methodology. An iterative approach was used in which subsequent analyses improve the agreement between the calculated pseudo elastic loads and those required to produce the estimated ductilities. The estimating techniques are described in detail by Kennedy et al. (1985).

Maximum story drift ductilities (occurring at the base of the internal structure) obtained from nonlinear analyses are compared with the estimated ductilities in Tables 2-5 and 2-6. Table 2-5 contains results for fixed-base cases and Table 2-6 for stiff soil cases incorporating soil-structure interaction effects. Estimates using the single elastic analysis technique are shown in the two left-hand columns of each table. The column labeled "lower bound" shows ductility estimates that would pertain to a structure having uniform demand-capacity ratios with height, such that the relationships between F_u and μ from the previously developed methodology would be directly applicable. However, for the structure analyzed here, with highly nonuniform demand to capacity ratios, these relationships will underestimate the maximum story drift ductility. As a result, the estimated ductilities were judgmentally increased, as summarized in the column labeled "estimated μ_s ". The resulting increase in the estimated ductilities is by a factor typically about 1.5 to 2. Note that a range of ductilities is estimated for each case, reflecting significant uncertainties when the procedure is applied to multi-degree-of-freedom structures with localized nonlinearities. The actual nonlinear result for μ_s is within the estimated range in each case, but the ranges are quite broad in some cases. As shown in the tables, improved estimates of μ_s , having substantially narrower ranges than those estimated from a single elastic analysis, are obtained using the multiple pseudo elastic analysis technique.

In general, the uncertainty in these estimates of ductility increases for input time histories in which the ductility changes relatively rapidly with changes in demand/capacity ratio. For this reason, a high uncertainty is indicated for the Parkfield excitation in Tables 2-5 and 2-6. In fact, the uncertainty is so great for Parkfield that the estimating procedure is not useful for this excitation, particularly for the single elastic analysis method. On the other hand, when the ductility is relatively insensitive to the demand/capacity ratio, the uncertainty band is relatively narrow. Thus, a narrow range of estimates

is shown in Table 2-5 for the Melendy Ranch excitation. (The relative sensitivity of ductility to demand/capacity ratio for different excitations can be seen by comparing scaling factors for ductilities of 1.85 and 4.3 shown in Table 2-3 for the simple nonlinear models analyzed.) The uncertainty in the ductility estimates also increases somewhat for soil-structure interaction cases (Table 2-6) as compared to fixed-base cases (Table 2-5). As mentioned previously, a greater uncertainty is also associated with the highly nonuniform demand/capacity structure analyzed in this study as compared to one having more uniform demand/capacity ratios.

An advantage of these techniques for estimating maximum story drift ductilities is that time history analyses are not needed. It is only necessary to have the elastic response spectrum along with a rough estimate of the strong motion duration. Another advantage is that the methods provide insight into reasons for different amounts of nonlinear response due to different input excitations. The methods are also quite efficient when a number of parametric studies are to be conducted. However, if only one or a few inelastic analyses are needed, it is equally or more efficient to conduct a nonlinear time history analysis than to use these procedures, particularly the more time consuming multiple analysis procedure, to estimate the inelastic response.

2.3.2 Inelastic Response in Fixed-base and Soil-structure Interaction Cases

In Figure 2-10, the maximum story drift ductility, μ_s , at the base of the internal structure determined from nonlinear analysis is plotted versus the corresponding maximum demand/capacity ratio, $F\mu_s$. The ductility values shown therein are the nonlinear results from fixed base and stiff soil-structure interaction cases in Tables 2-5 and 2-6 plus two additional data points (for Parkfield and artificial [Reg. Guide 1.60] excitations) from soil-structure interaction cases of the intermediate soil profile. One of the results that is apparent in

Figure 2-10 is the relatively higher demand/capacity ratios found for Melendy Ranch excitation than for the other excitations for fixed base cases, a finding that is consistent with the scale factors, F_{μ} , discussed previously for simple structures and shown in Table 2-3. Another trend that appears in Figure 2-10, although the number of data is limited, is that for a given ductility, lower scale factors or demand/capacity ratios are obtained for soil-structure interaction cases than for fixed-base cases. The trend of the data have been approximated by the curves shown in the figure. It is considered that two factors may contribute to a trend for lower F_{μ_s} values in soil-structure interaction cases than in fixed-base cases. The first is that, in fixed-base cases, structural yielding results in substantial decreases in the effective structural frequency and increases in the effective damping. This results in substantially reduced structural loads. The internal structure base shears from nonlinear analysis were 0.46, 0.66, 0.76, and 0.93 of the base shears from linear analysis for Melendy Ranch, El Centro No. 5, artificial, and Parkfield excitations, respectively, for fixed base cases. However, in soil-structure interaction cases, the effects of structural yielding on further changes in the soil-structure system frequency and damping were very small compared to the relatively large effects that had occurred due to soil-structure interaction. In these cases, structural yielding did not significantly reduce structural loads even when substantial inelastic behavior occurred resulting in large ductilities. In soil-structure interaction cases, internal structure base shears from nonlinear analysis ranged from 0.95 to 1.18 of the base shears from linear analysis.

The second factor that may contribute to lower F_{μ_s} values for soil-structure interaction cases than fixed-base cases is the effects of soil-structure interaction on the shape of the response spectrum of the foundation base motion. As will be discussed more in Section 3, the spectrum of the foundation motion tends to be reduced in the high-frequency portion relative to the spectrum of the free-field input motion. The resulting spectral shape of the foundation motion for a

structure embedded in soil is thus relatively low in the high frequency part as compared to a structure on a fixed base. As the embedded structure yields and its effective frequency lowers, the seismic excitation is thus increased somewhat as compared to a structure on a fixed base, resulting in increased ductilities for given demand/capacity ratios.

The tendency for lower scale factors to apply for soil-structure interaction cases than for fixed-base cases is important to consider when evaluating the seismic safety margin of a structure. That portion of the seismic safety margin due to structural inelastic response capacity may be smaller for a structure embedded in soil than for a structure on rigid rock. If seismic margins due to soil-structure interaction effects and structural inelastic response capacity are being combined, this needs to be done carefully in order not to double-count in obtaining the overall seismic margin. To take an example, assume that for the reactor building analyzed herein, it was determined that the margin due to soil-structure interaction effects corresponded to a factor, F , of 1.6. If it were assumed that an acceptable story drift ductility is $\mu_s = 5$, then Figure 2-10 would indicate an inelastic response margin factor, $F\mu_s$, equal to about 1.3 for soil-structure interaction cases and 1.8 or more for fixed-base cases. The overall seismic safety margin factor would thus be $1.6 \times 1.3 = 2.1$. For this example, it would be inappropriate and unconservative to combine the factor for soil-structure interaction (1.6) with the factor for inelastic response determined from fixed base analysis (≥ 1.8).

2.3.3 Response of Equipment

As part of the analysis of the reactor building described herein, the effects of structural inelastic response on low-damped floor response spectra were examined. Seismic response of equipment is generally evaluated using such spectra. For elastic analyses of the structure on a fixed-base, floor spectra high in the structure showed very high spectral

amplifications at the fixed-base fundamental frequency of the structure in cases where the input excitation was strong at that frequency. A typical result high in the internal structure is shown in Figure 2-11. The maximum spectral amplification factor (ratio of maximum spectral acceleration to peak floor acceleration) is almost a factor of 10 in this case. In general, maximum amplification factors of 7 to 10 were obtained in such cases. Spectra such as the highly amplified spectrum in Figure 2-11 could be damaging to equipment, even if well-anchored, without special seismic design provisions.

The effect of structural inelastic response in fixed-base cases was to substantially reduce the high amplification of floor response spectra found in the elastic analyses. The structural yielding and frequency shifting during inelastic response prevented the high amplifications from developing. In Figure 2-11, the effect is clearly shown in the comparison of spectra from elastic and inelastic analyses. In this case and in other inelastic analyses conducted, maximum spectral amplifications of 4 to 5 times were obtained, compared to 7 to 10 times in the elastic analysis cases. Note also the shifting of maximum response to lower frequencies in Figure 2-11. Most well-anchored equipment could withstand the spectral accelerations for the inelastic response case in Figure 2-11, even without special seismic design provisions.

The beneficial effects of structural inelastic response in reducing high peaks of floor response spectra were obtained only in the fixed-base cases and not in the soil-structure interaction cases. A typical comparison of floor response spectra from elastic and inelastic analyses for soil-structure interaction cases is shown in Figure 2-12, from which it can be seen that inelastic structural response had very little effect on the spectrum. Independent of whether structural inelastic response occurs, soil-structure interaction can result in substantial reduction of high peaks of floor response spectra due to system frequency shifting and high radiation damping. As was noted in Section 2.3.2, the additional

frequency shifting and damping associated with structural inelastic response was small in comparison with the changes due to soil-structure interaction. Thus, the floor spectra were changed very little by structural inelastic behavior in the soil-structure interaction cases.

In general, this study indicates that if floor spectra show highly amplified narrow spikes, then inelastic structural response will reduce them. On the other hand, if such spectral spikes are not present either because of soil-structure interaction effects or lack of frequency content of the input motion, then the effects of structural inelastic response on floor spectra will be small.

Table 2-1

LIST OF EARTHQUAKE/STRUCTURE-TYPES
INCLUDED IN REVIEW/DAMAGE DOCUMENTATION

<u>EARTHQUAKE</u>	<u>STRUCTURE-TYPE</u>
<u>Cases with Damage Documentation</u>	
1952 Kern County, CA	General, Kern County Steam Plant, Elevated Tanks
1966 Parkfield, CA	General
1971 San Fernando, CA	General Medical Facilities, High-Rise Buildings, Industrial, O. View, VA
1972 Bear Valley, CA	General
1972 Managua, Nicaragua	General, ESSO Refinery, ENALUF Thermal Plant
1975 Oroville, CA	General, State Water Project
1978 Santa Barbara, CA	General
1979 Coyote Lake, CA	General
1979 Imperial Valley, CA	General, El Centro Steam Plant
1980 Greenville, CA	General, LLNL
<u>Other Cases Reviewed</u>	
1906 San Francisco, CA	Major High-Rise Buildings
1940 Imperial Valley, CA	General
1949 Olympia, WA	General
1960 Agadir, Morocco	General
1960 Chile	Huachipato Steel Plant
1964 Alaska	General
1967 Caracas, Venezuela	General, High Rise
1967 Koyna, India	Koyna Dam
1972 Ancona, Italy	General
1974 Lima, Peru	General
1975 Ferndale, CA	General, Humboldt Bay, Nuclear Power Plant
1976 Friuli, Italy	General
1977 Romania	General
1978 Miyagi-Ken-Oki, Japan	Fukushima Nuclear Power Plant
1978 Monticello Reservoir	Virgil C. Summer Nuclear Plant
1980 Mammoth Lake, CA	General
1980 Eureka, CA	General, Humboldt Bay Nuclear Power Plant
1980 Sharpsburg	Wm. Zimmer Nuclear Power Plant

From Appendix A of Kennedy et al. (1984) (Vol. 1 of NUREG/CR-3805).

Table 2-2
ACCELEROGRAMS USED IN NONLINEAR ANALYSES

EARTHQUAKE	MAGNITUDE		RECORDING STATION AND ACCELEROGRAM COMPONENT	FAULT DISTANCE (km)	PEAK ACCELERATION a (g)	STRONG DURATION T _D [*] (sec)	RMS-BASED ACCELERATION A _{DE1} ^{**} (g)
	M _L	M _S					
21 July 1952 Kern County, CA	7.2	7.7	Taft Lincoln School (S69E)	40	0.180	10.3	0.155
13 April 1949 Olympia, WA	7.0	7.0	Highway Test Lab (N86E)	29	0.281	15.6	0.202
15 Oct. 1979 Imperial Valley, CA	6.6	6.9	El Centro Array No. 12 (140)	18	0.142	9.6	0.133
15 Oct. 1979 Imperial Valley, CA	6.6	6.9	El Centro Array No. 5 (140)	1	0.530	3.4	0.404
09 Feb. 1971 San Fernando, CA	6.4	6.6	Pacoima Dam (S14W)	3	1.170	6.1	0.795
09 Feb. 1971 San Fernando, CA	6.4	6.6	Hollywood Stg.P.E. Lot (N90E)	21	0.211	5.4	0.213
06 Aug. 1979 Coyote Lake, CA	5.7	5.6	Gilroy Array No. 2 (050)	7	0.191	2.2	0.202
27 June 1966 Parkfield, CA	5.6	6.4	Cholame-Shandon No.2 (N65E)	< 1	0.490	1.4	0.514
28 Nov. 1974 Hollister, CA	5.2	4.5	Gavilan College (S67W)	13	0.138	1.1	0.106
13 Aug. 1978 Santa Barbara, CA	5.1	5.6	UCSB Goleta (180)	4	0.347	3.0	0.332
04 Sept. 1972 Bear Valley, CA	4.7	4.3	Melendy Ranch (N29W)	6	0.520	0.8	0.435
-- -----	--	--	Artificial Accelerogram	--	0.200	9.4	---

* Strong motion duration, T_D^{*} used in this study = T_M - T_{0.05}, where T_{0.05} is the time associated with 5% of the cumulative energy of the accelerogram; and T_M is either the time associated with 75% of the cumulative energy, or the first zero crossing following the peak acceleration of the accelerogram, whichever occurs later.

** Refer to Section 2.2.2 for definition of A_{DE1}

From Kennedy et al. (1984) (Vol. 1 of NUREG/CR-3805).

Table 2-3
SCALE FACTORS FOR LOW AND HIGH DUCTILITIES

(a) Scale Factors for High Ductility ($\mu = 4.27$)

Earthquake Record (Comp)		Model Structure Frequency				Mean <F>	Std. Dev. σ	C.O.V. σ/F
		8.54 Hz	5.34 Hz	3.20 Hz	2.14 Hz			
1	Olympia, WA., 1949 (N86E)	1.56	1.54	2.61	3.75	2.37	1.05	0.44
2	Taft, Kern Co., 1952 (S69E)	1.25	1.65	2.05	3.38	2.08	0.92	0.44
3	El Centro Array No. 12 Imperial Valley, 1979, (140)	1.56	2.29	2.10	2.14	2.02	0.32	0.16
4	Artificial (R.G. 1.60)	1.89	1.88	2.84	2.75	2.34	0.53	0.23
5	Pacoima Dam San Fernando, 1971 (S14W)	1.70	1.86	2.67	3.89	2.53	1.00	0.40
6	Hollywood Storage PE Lot, San Fernando, 1971 (N90E)	1.94	2.50	2.60	2.05	2.27	0.33	0.15
7	El Centro Array No. 5, Imperial Valley, 1979, (140)	2.38	2.66	2.33	3.45	2.71	0.52	0.19
8	UCSB Goleta Santa Barbara, 1978 (180)	1.52	2.05	2.05	1.96	1.90	0.25	0.13
9	Gilroy Array No. 2, Coyote Lake, 1979, (050)	1.56	3.85	4.36	3.03	3.20	1.22	0.38
10	Cholame Array No. 2, Parkfield 1966 (N65E)	1.55	1.29	1.48	2.65	1.74	0.61	0.35
11	Gavilan College Hollister, 1974 (S67W)	2.84	2.97	2.71	8.49	4.25	2.83	0.67
12	Melendy Ranch Barn, Bear Valley, 1972 (N29W)	1.89	5.48	5.16	3.36	3.97	1.67	0.42
Mean, <F>		1.8	2.5	2.75	3.41	Overall:		
Std. Dev., σ		0.43	1.17	1.03	1.73	<F> = 2.62		
C.O.V., σ/F		0.24	0.47	0.37	0.51	σ = 1.28		
						C.O.V. = 0.49		

(b) Scale Factors for Low Ductility ($\mu = 1.85$)

Earthquake Record (Comp)		Model Structure Frequency				Mean <F>	Std. Dev. σ	C.O.V. σ/F
		8.54 Hz	5.34 Hz	3.20 Hz	2.14 Hz			
1	Olympia, WA., 1949 (N86E)	1.36	1.11	1.49	1.70	1.41	0.25	0.18
2	Taft, Kern Co., 1952 (S69E)	1.20	1.25	1.50	1.78	1.43	0.27	0.19
3	El Centro Array No. 12 Imperial Valley, 1979, (140)	1.34	1.56	1.29	1.48	1.42	0.12	0.08
4	Artificial (R.G. 1.60)	1.50	1.33	1.60	1.73	1.54	0.17	0.11
5	Pacoima Dam San Fernando, 1971 (S14W)	1.25	1.38	1.26	2.19	1.52	0.45	0.29
6	Hollywood Storage PE Lot, San Fernando, 1971 (N90E)	1.45	1.65	1.58	1.39	1.52	0.12	0.08
7	El Centro Array No. 5, Imperial Valley, 1979, (140)	1.58	1.60	1.34	1.51	1.51	0.12	0.08
8	UCSB Goleta Santa Barbara, 1978 (180)	1.35	1.65	1.41	1.49	1.48	0.13	0.09
9	Gilroy Array No. 2, Coyote Lake, 1979, (050)	1.36	1.93	2.00	1.86	1.79	0.29	0.16
10	Cholame Array No. 2, Parkfield 1966 (N65E)	1.22	1.21	1.21	1.59	1.31	0.19	0.15
11	Gavilan College Hollister, 1974 (S67W)	1.61	1.55	1.62	1.93	1.68	0.17	0.10
12	Melendy Ranch Barn, Bear Valley, 1972 (N29W)	1.45	1.96	2.18	1.98	1.89	0.31	0.16
Mean, <F>		1.39	1.52	1.54	1.72	Overall:		
Std. Dev., σ		0.13	0.27	0.29	0.24	<F> = 1.54		
C.O.V., σ/F		0.09	0.18	0.19	0.14	σ = 0.26		
						C.O.V. = 0.17		

From Kennedy et al. (1984) (Vol. 1 of NUREG/CR-3805)

Table 2-4
CORRELATION BETWEEN DURATION, T_D' ,
AND EFFECTIVE NUMBER OF STRONG NONLINEAR CYCLES, N

Strong Duration T_D' (Sec.)	Effective Number of Strong Nonlinear Cycles, N
less than 1.0	1
1.0 - 7.0	2
9.0 - 11.0	3
greater than 15.0	4

From Kennedy et al. (1984) (Vol. 1 of NUREG/CR-3805)

Table 2-5

COMPARISON OF MAXIMUM STORY DRIFT DUCTILITIES FROM ELASTIC
AND NONLINEAR ANALYSES - REACTOR BUILDING ON FIXED BASE

<u>Maximum Story Drift Ductility Estimates</u>				
Earthquake Record	<u>From Single Elastic Analysis</u>		From Multiple Pseudo-elastic Analyses, Improved μ_s Estimate	Actual Nonlinear Result, μ_s
	Lower Bound on μ_s, μ_e	Estimated μ_s , $\mu_s \approx M_e(\mu_e - 1) + 1$ $M_e = 1.8 \text{ to } 2.0$		
Artificial	5.7 - 14.2	9.5 - 27	9.4 - 15.5	11.9
El Centro #5	2.9 - 5.9	4.4 - 10.8	5.0 - 7.8	5.6
Parkfield	1.8 - >15.0	2.4 - >30	1.3 - 6.8	3.2
Melendy Ranch	2.1 - 3.0	3.0 - 5.0	3.2 - 4.8	4.7

From Kennedy et al. (1985) (Vol. 2 of NUREG/CR-3805)

Table 2-6

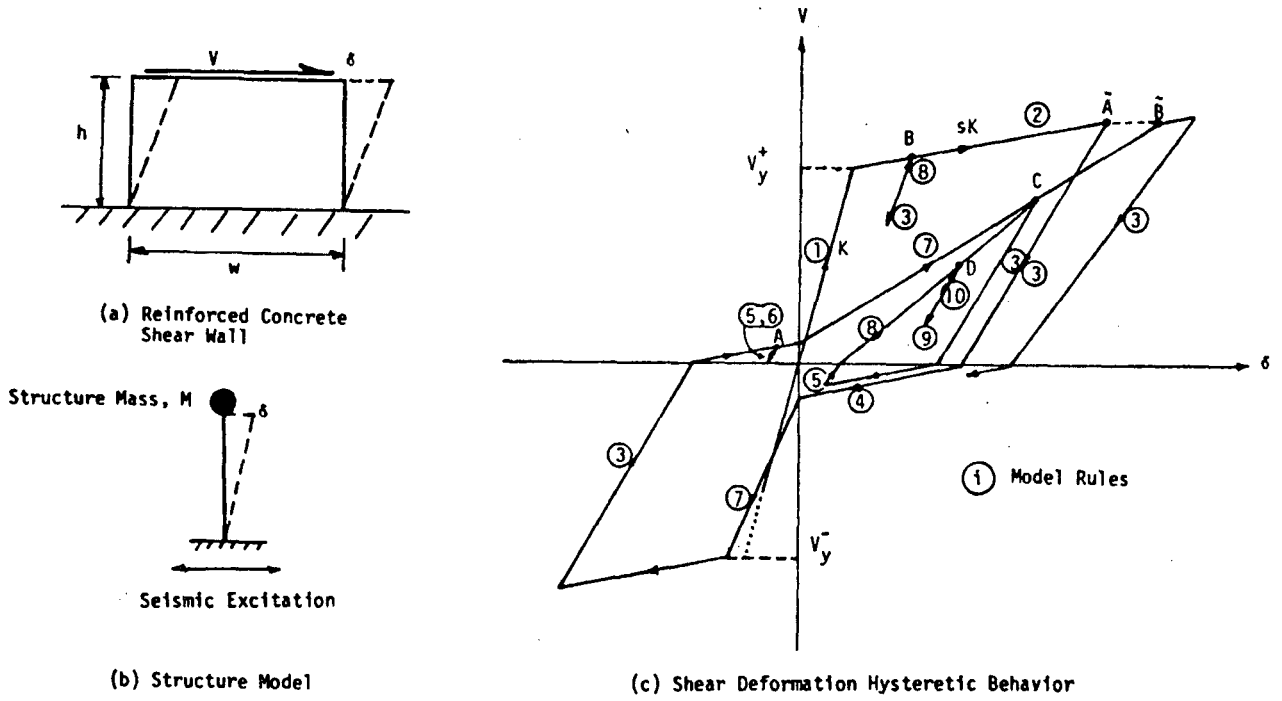
COMPARISON OF MAXIMUM STORY DRIFT DUCTILITIES FROM ELASTIC
AND NONLINEAR ANALYSES - REACTOR BUILDING EMBEDDED IN STIFF SOIL

Maximum Story Drift Ductility Estimates

Earthquake Record*	<u>From Single Elastic Analysis</u>		From Multiple Pseudo-elastic Analyses, Improved μ_s Estimate	Actual Nonlinear Result, μ_s
	Lower Bound on μ_s, μ_e	Estimated μ_s , $\mu_s \approx M_e(\mu_e - 1) + 1$ $M_e = 1.8 \text{ to } 2.0$		
Artificial	2.2 - 7.5	3.2 - 14.0	3.5 - 11.0	9.2
El Centro #5	1.2 - 1.5	1.4 - 2.0	1.2 - 1.8	1.7
Parkfield	3.2 - >15	5.0 - >30	5.4 - 14.3	12.9

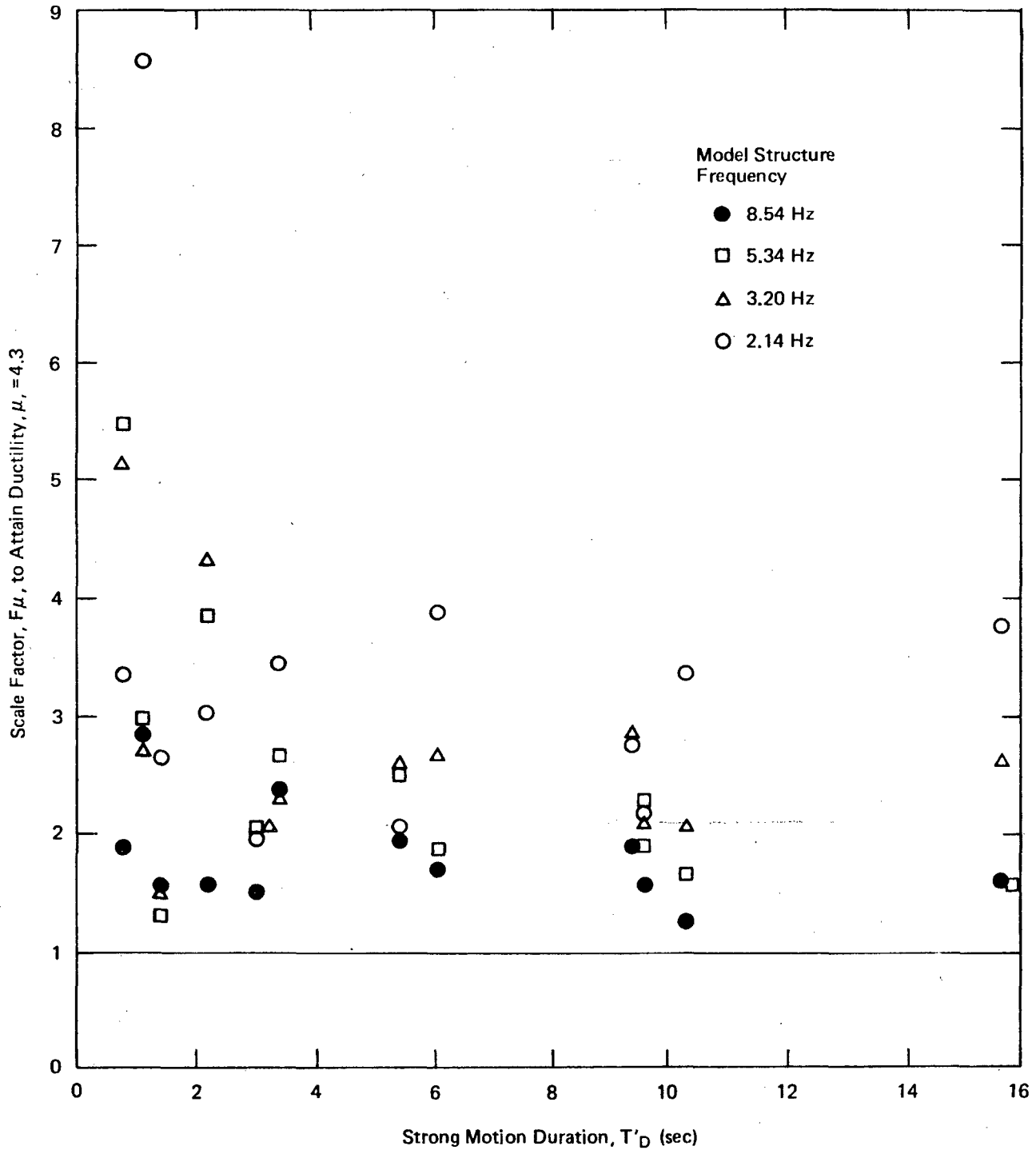
*Melendy Ranch record resulted in elastic response

From Kennedy et al. (1985) (Vol. 2 of NUREG/CR-3805)



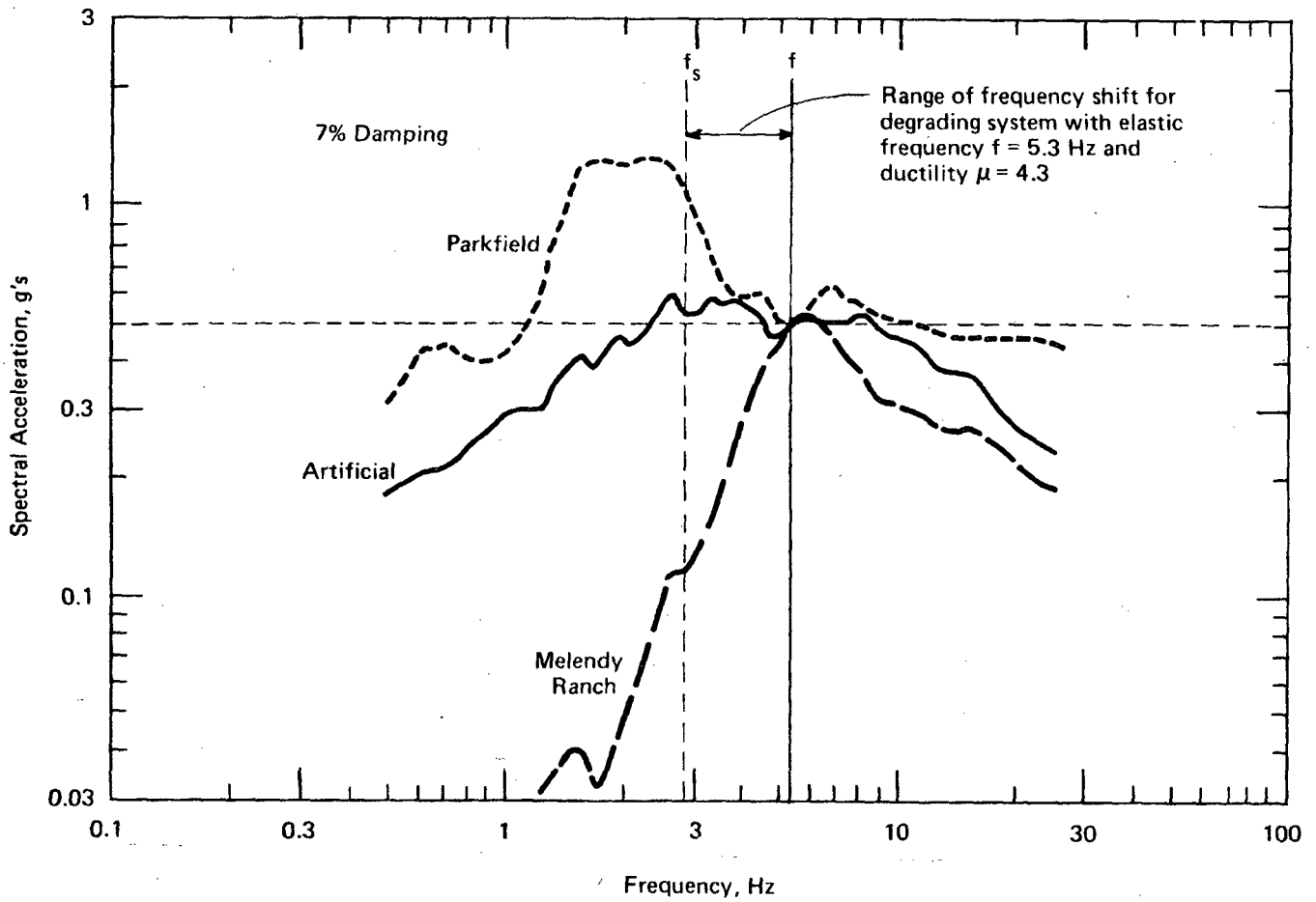
From Kennedy et al. (1984)
 (Vol. 1 of NUREG/CR-3805)

Figure 2-1. Shear Wall Structural Model for Nonlinear Analyses



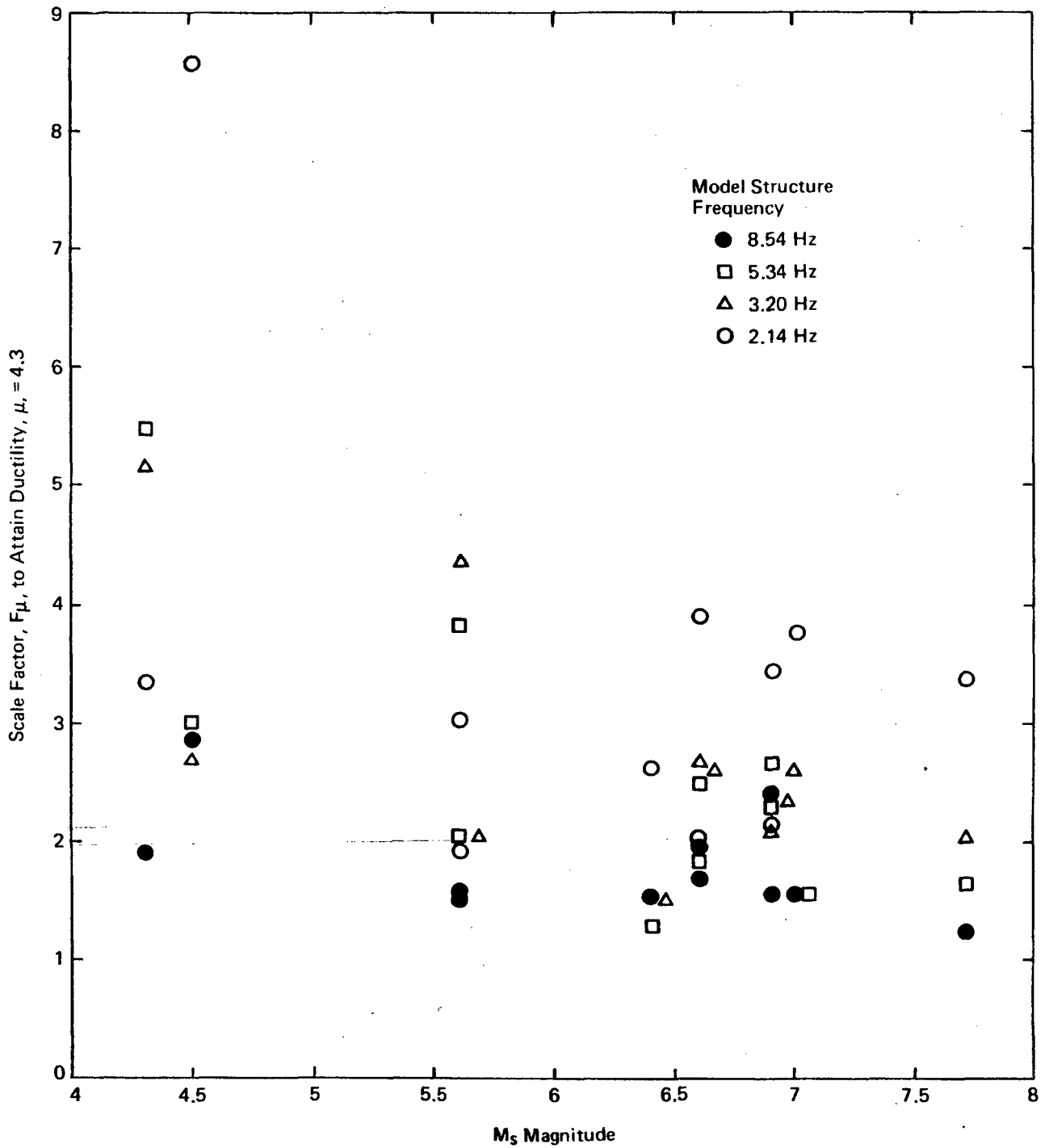
From Kennedy et al. (1984)
 (Vol. 1 of NUREG/CR-3805)

Figure 2-2. Accelerogram Scale Factors Required to Attain Ductility of 4.3 versus Strong Motion Duration



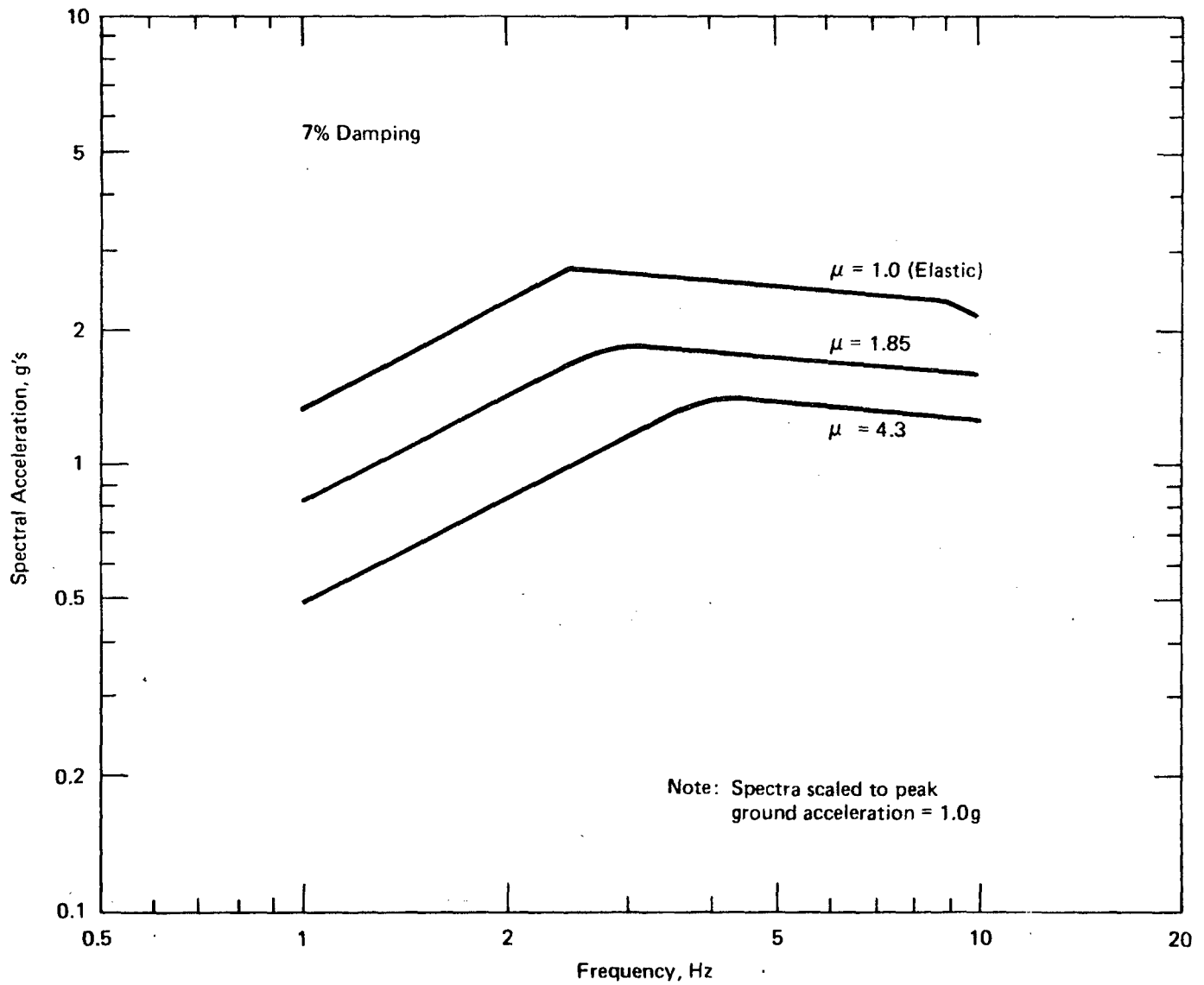
Based on Kennedy et al. (1984)
 (Vol. 1 of NUREG/CR-3805)

Figure 2-3. Effect of Frequency Shift Due to Nonlinear Response



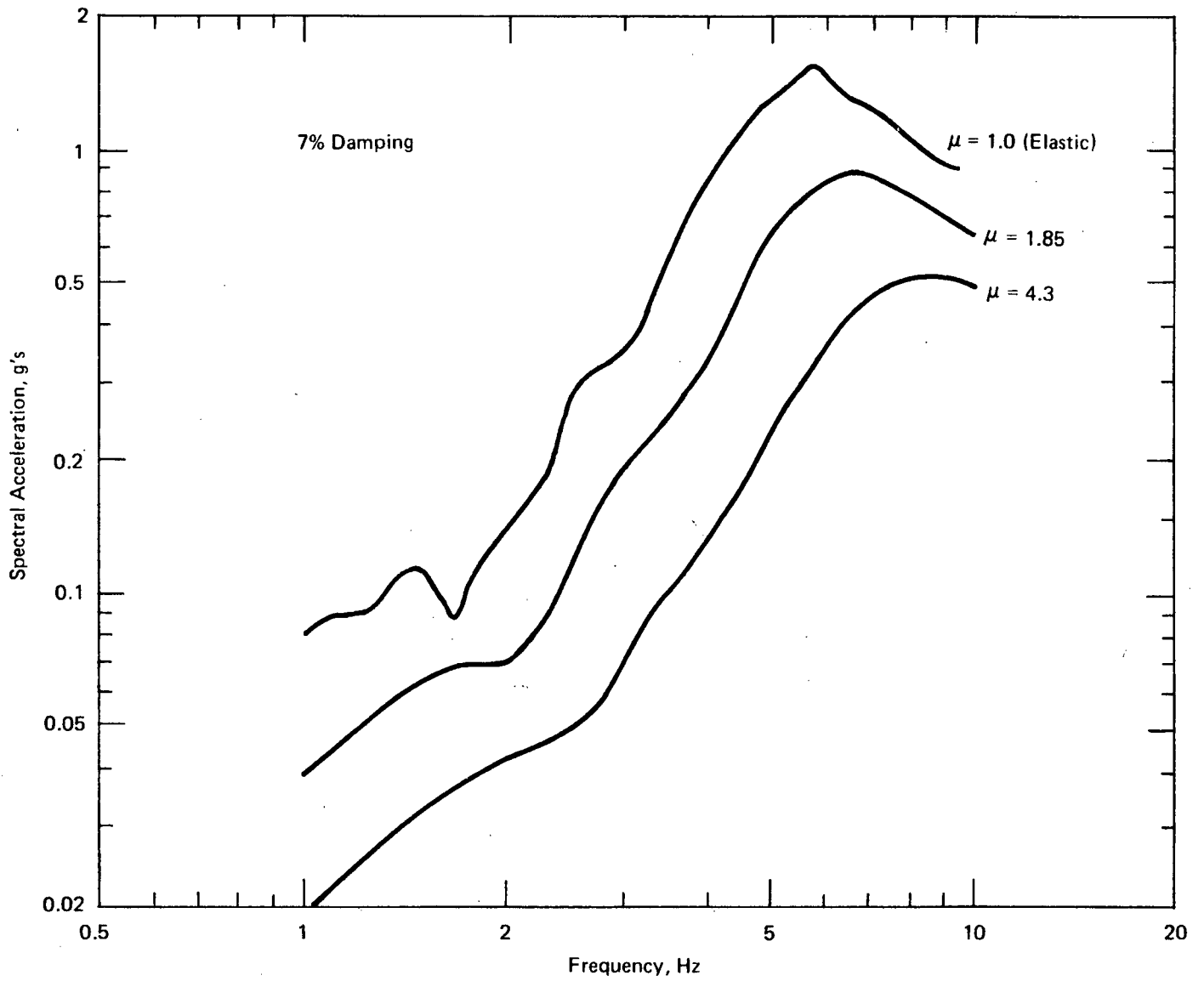
Based on Kennedy et al. (1984)
(Vol. 1 of NUREG/CR-3805)

Figure 2-4. Accelerogram Scale Factors Required to Attain Ductility of 4.3 versus Magnitude



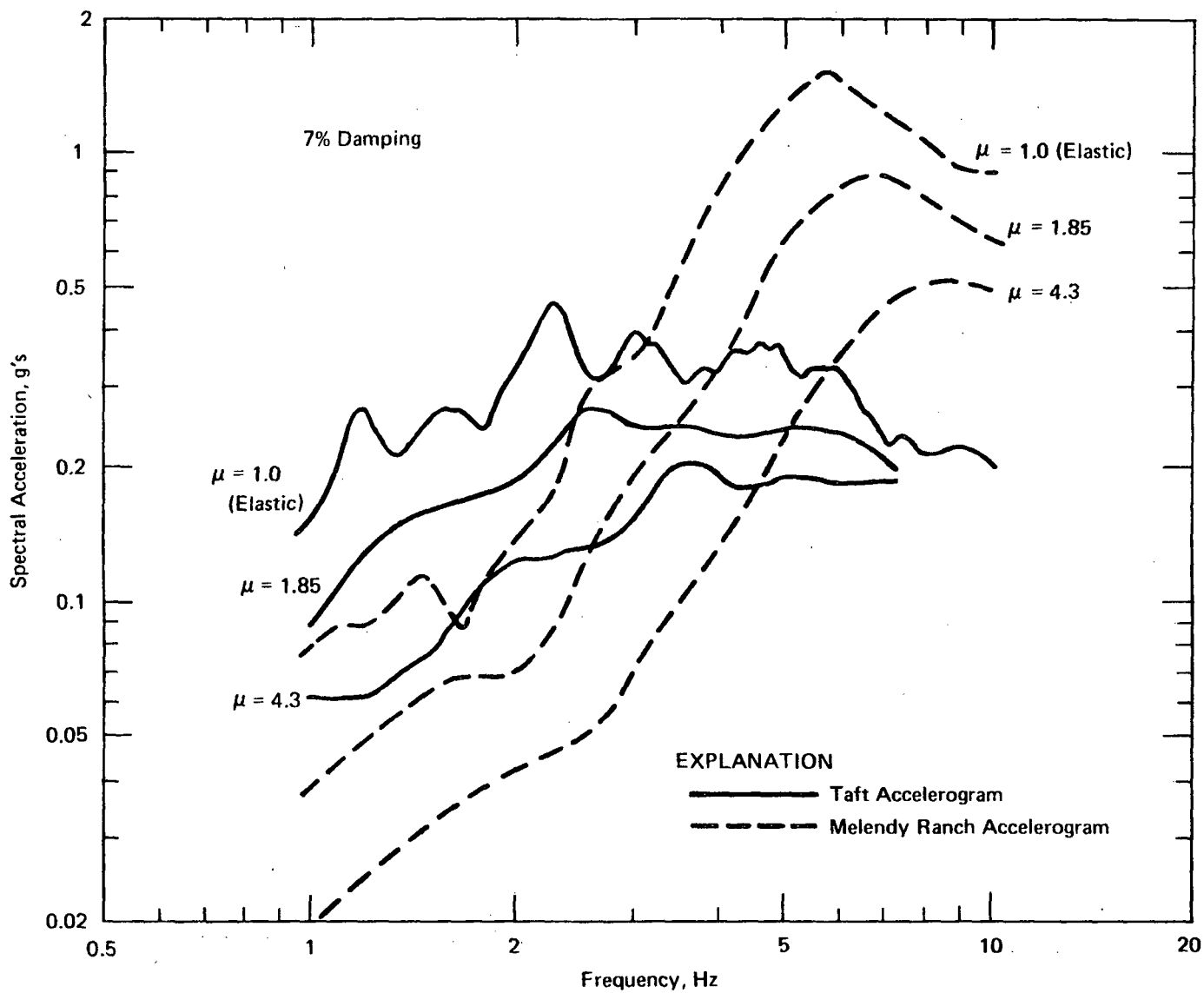
From Kennedy et al. (1984)
 (Vol. 1 of NUREG/CR-3805)

Figure 2-5. Inelastic Response Spectra Corresponding to Reg. Guide 1.60 Response Spectra



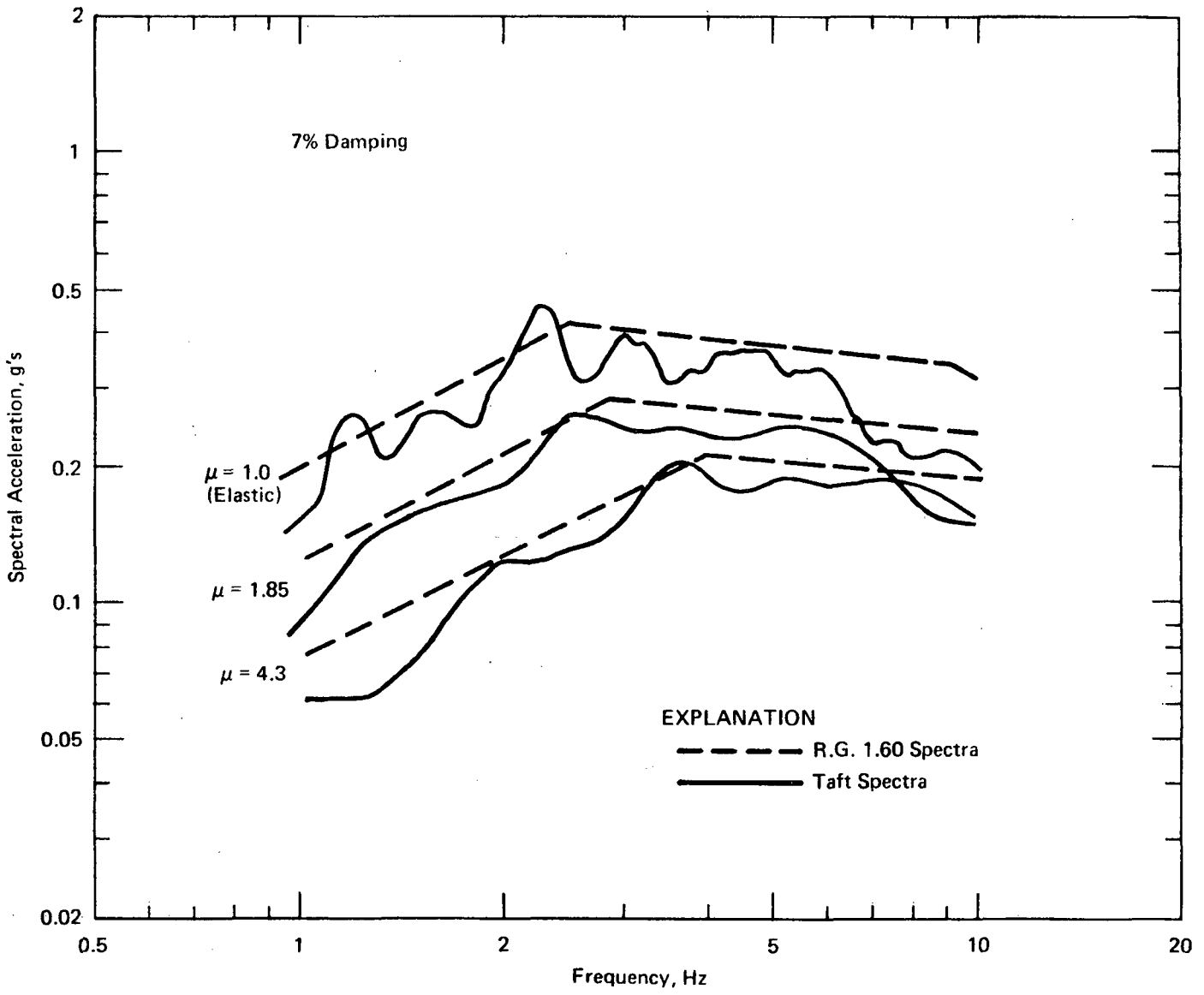
From Kennedy et al. (1984)
 (Vol. 1 of NUREG/CR-3805)

Figure 2-6. Inelastic Response Spectra for Melendy Ranch Accelerogram



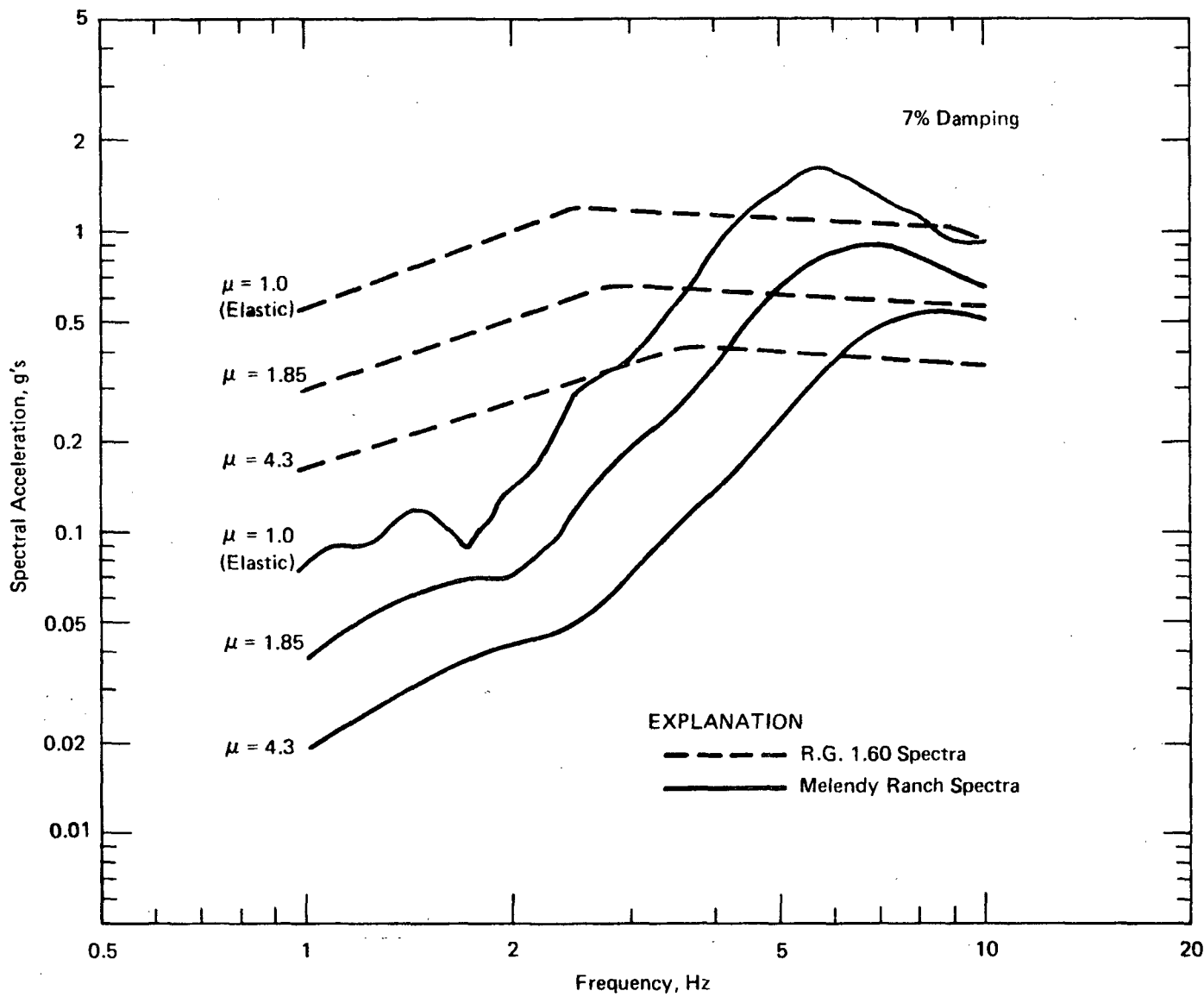
From Kennedy et al. (1984)
 (Vol. 1 of NUREG/CR-3805)

Figure 2-7. Comparison of Inelastic Response Spectra for Taft and Melendy Ranch Accelerograms



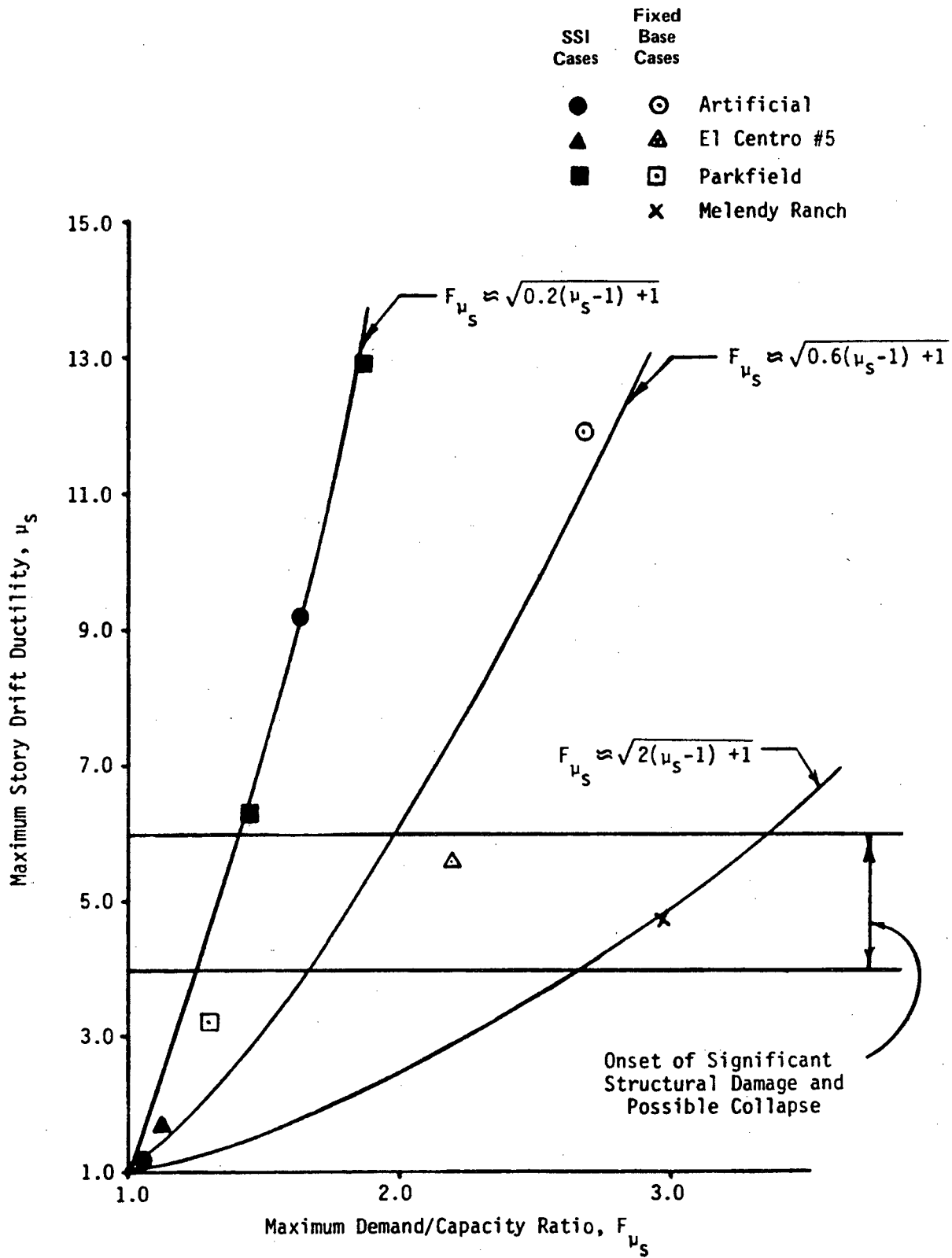
Based on Kennedy et al. (1984)
(Vol. 1 of NUREG/CR-3805)

Figure 2-8. Comparison of Taft Spectra with Reg. Guide 1.60 Spectra Anchored to "Effective" Design Acceleration



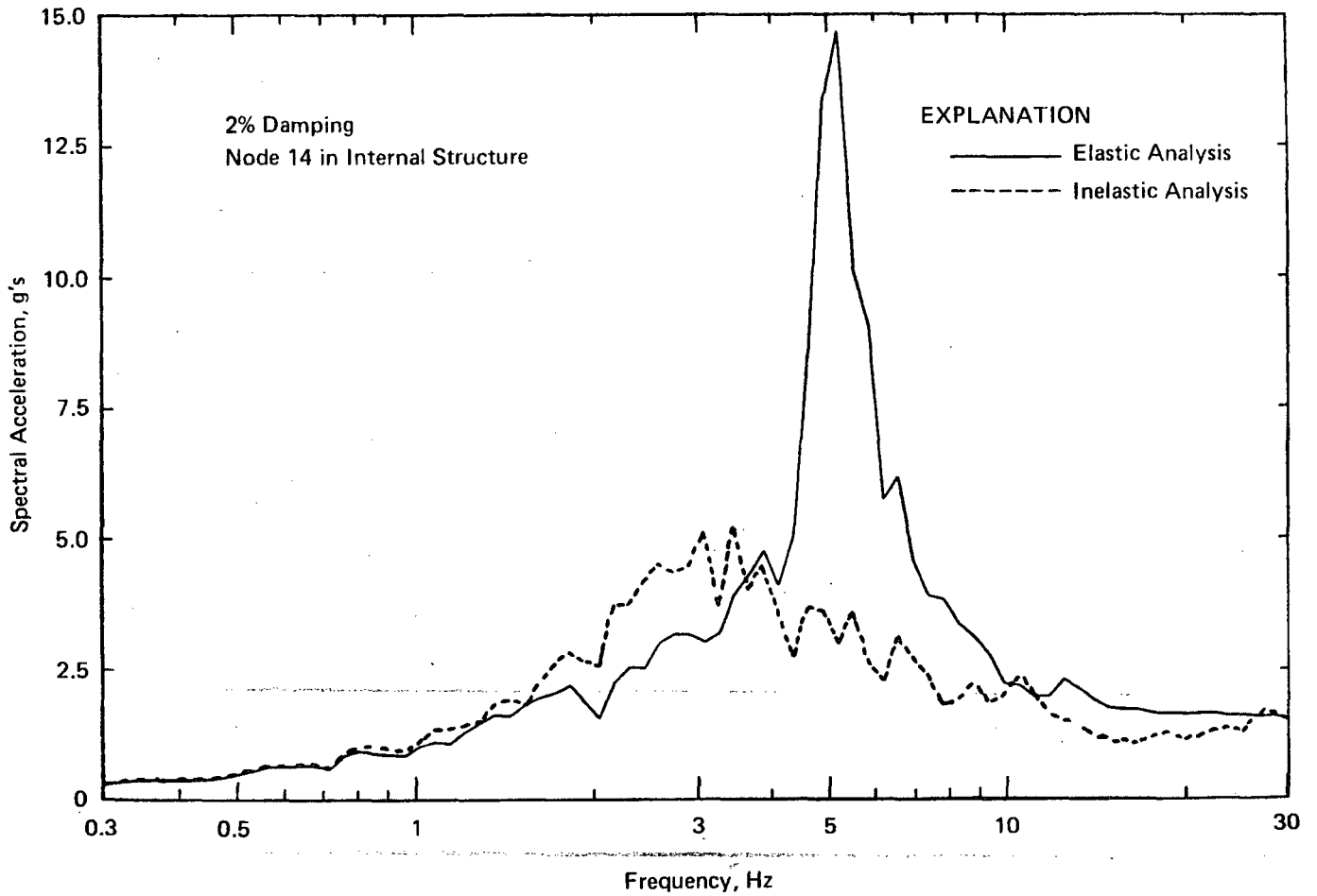
Based on Kennedy et al. (1984)
(Vol. 1 of NUREG/CR-3805)

Figure 2-9. Comparison of Melendy Ranch Spectra with Reg. Guide 1.60 Spectra Anchored to "Effective" Design Acceleration



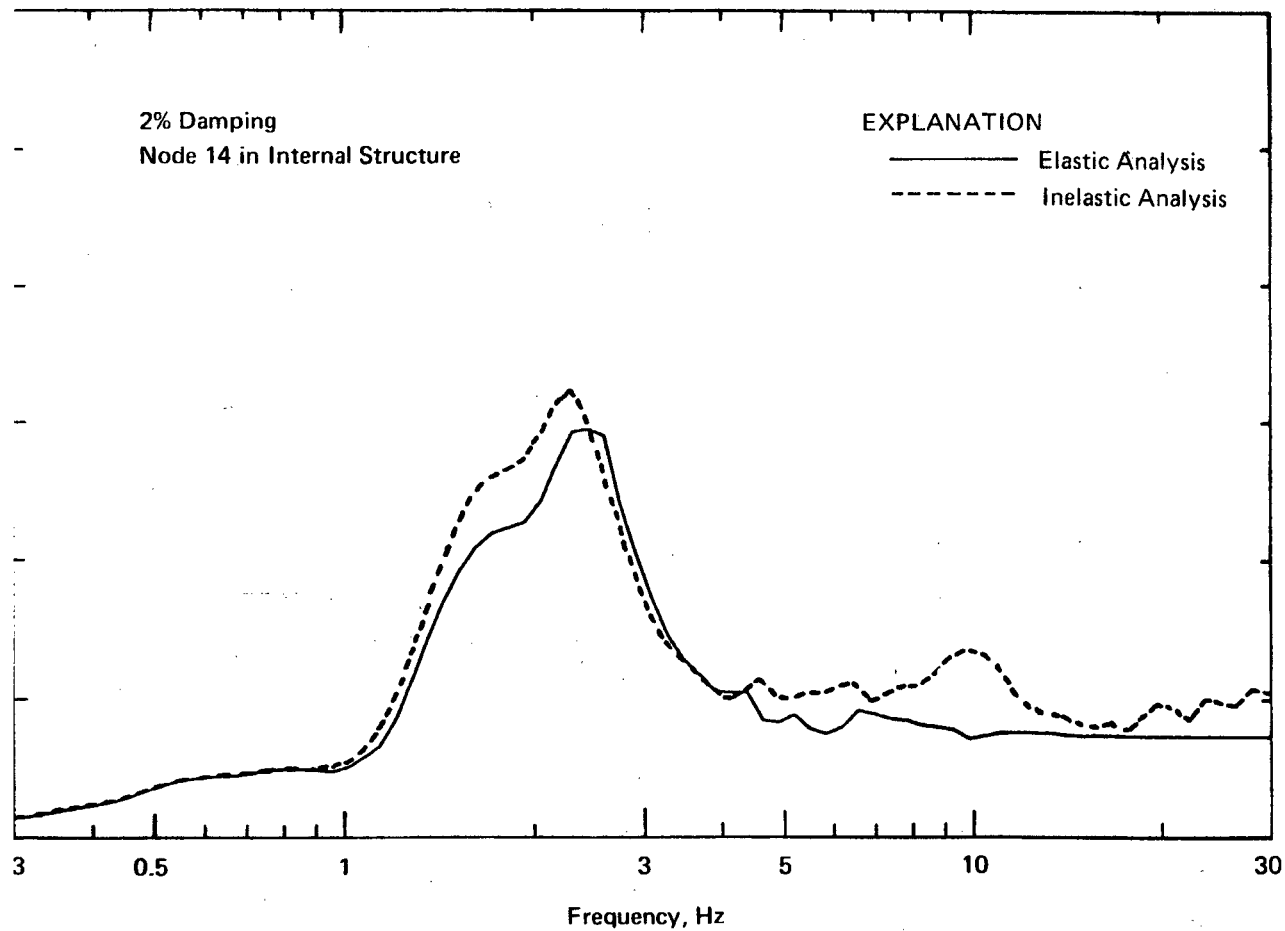
From Kennedy et al. (1985)
(Vol. 2 of NUREG/CR-3805)

Figure 2-10. Reactor Building Maximum Story Drift Ductility versus Maximum Demand/Capacity Ratio for Fixed-Base and Soil-Structure Interaction Cases



From Kennedy et al. (1985)
(Vol. 2 of NUREG/CR-3805)

Figure 2-11. Comparison of In-Structure Response Spectra from Elastic and Inelastic Analysis of Reactor Building – Fixed-Base Case, Artificial Accelerogram (0.5g) Input



From Kennedy et al. (1985)
(Vol. 2 of NUREG/CR-3805)

Figure 2-12. Comparison of In-Structure Response Spectra from Elastic and Inelastic Analysis of Reactor Building – Soil-Structure Interaction (Stiff Soil) Case, Parkfield Accelerogram (0.5g) Input

3. ENGINEERING CHARACTERIZATION OF GROUND MOTION AS RELATED TO SPATIAL VARIATIONS OF GROUND MOTION AND SOIL-STRUCTURE INTERACTION

This part of the study addressed the engineering characterization of earthquake ground motion as related to the spatial variations of ground motion and soil-structure interaction. The study included both a comprehensive series of parametric soil-structure interaction analyses (Luco et al., 1986) and a review of observational data pertaining to spatial variations of ground motion (Chang et al., 1986).

The parametric soil-structure interaction analyses covered a broad range of structure-foundation-excitation conditions. From these analyses, free-field ground motion characteristics affecting elastic structural response were examined. Based on these results as well as findings described in Section 2 on the ground motion characteristics affecting inelastic structural response, conclusions were arrived at regarding the characterization of the free-field control motion from the standpoint of adequately predicting structural response.

Given a characterization of the free-field control motion at the ground surface, other important considerations for characterizing ground motion for nuclear power plant structures include: variations of ground motion with depth (important because structures are typically embedded); and variations of ground motion in a horizontal plane (important because foundations typically cover a considerable horizontal extent). Conclusions regarding appropriate characterizations of variations of ground motion with depth and variations of ground motion horizontally were developed using both the results of the parametric soil-structure interaction analyses and the study of observational data on spatial variations of ground motion.

The following sections summarize the main findings and conclusions pertaining to characterization of the free-field control motion, characterization of variations of ground motion with depth, and characterization of variations of ground motion in a horizontal plane.

3.1 CHARACTERIZATION OF FREE-FIELD CONTROL MOTION

3.1.1 Effects of Soil-structure Interaction on Structural Response for Different Free-field Motions

The parametric soil-structure interaction analyses conducted in this study included analyses of a reactor building founded on four soil profiles for four sets of input excitations. The soil profiles varied substantially in stiffness, from relatively hard (profile I with shear wave velocity of 3,600 ft/sec) to relatively soft (profile IV with shear wave velocity of 1,000 ft/sec). The characteristics of the profiles are summarized in Table 3-1. Two different embedment depths for the reactor building (20 ft and 40 ft, corresponding to depth-to-diameter ratios of approximately 0.15 and 0.3) were used in these analyses.

The input motions used in the study consisted of four sets of three-component excitations defined at the free-field ground surface. These input motions correspond to the Parkfield 1966 Station No. 2 record, Imperial Valley 1979 El Centro Station No. 5 record, Bear Valley 1972 Melendy Ranch record, and artificial accelerograms consistent with Reg. Guide 1.60. For purposes of the study, all acceleration time histories were normalized to a peak acceleration of 0.5 g. The input motions are summarized in Table 3-2. Vertically propagating waves were assumed in the part of the study summarized in this section.

The three actual earthquake records (the Parkfield 1966 Station No. 2 record, Imperial Valley 1979 El Centro Station No. 5 record, and Bear Valley 1972 Melendy Ranch record) were obtained from sites underlain by different soil conditions. The characteristics of the records reflect the effects of the site conditions on ground motion as well as effects of the earthquake source characteristics and the source-to-site wave propagation. Ground motion data indicate large variability in frequency content and duration of individual ground motion records obtained at the same sites or sites with similar soil conditions. Thus, for the purposes

of parametrically evaluating the influence on response of variations in free-field ground motion characteristics, all three actual earthquake records and the non-site-specific artificial (Reg. Guide 1.60) accelerograms were considered to be applicable ground surface motions for all soil profiles analyzed in this study.

The soil-structure interaction analyses were made using a substructure analysis approach and the CLASSI computer program (Wong and Luco, 1980). Details of the modeling and analysis methods are given in Luco et al. (1986).

Structural response was examined in these analyses for a number of structural response parameters, including: peak translational and rotational accelerations at the top of the basemat, near the top and midpoint of the containment shell, and near the top and midpoint of the internal structure; floor response spectra at these same locations; and peak base forces and moments at the base of the containment shell and base of the internal structure. A few of the results of the analyses are presented here to illustrate effects of soil-structure interaction for different input excitations. The results are presented in detail in Luco et al. (1986).

The effects of soil-structure interaction on the containment shell base shear force for cases of 40-ft embedment are shown in Table 3-3 for the different input excitations and soil profiles. Effects were similar for containment shell peak base moment and peak acceleration near the top of the containment shell. The effects on base shear force shown in the table are expressed as the ratio of peak base shear force from soil-structure interaction analyses to peak base shear force from analysis for a rigid rock (fixed-base) condition. Table 3-3 indicates that soil-structure interaction effects on the base shear force can be very significant. Generally, the base shear force with soil-structure interaction was in the range of being moderately higher (ratio of about 1.25) to substantially lower (ratio of about 0.5) than the base shear

force for a rigid rock condition. However, in some cases, larger increases and decreases in base shear force response due to soil-structure interaction occurred. As shown in Table 3-3, for the Melendy Ranch input motion, soil-structure interaction decreased response by as much as a factor of 6 (ratio of 0.16); and for the Parkfield excitation, soil-structure interaction increased response by as much as a factor of 1.7.

The substantial variations in these ratios, including the large decreases and increases in response for Melendy Ranch and Parkfield, respectively, are due in large measure to differences in the frequency content of the input motions. For Melendy Ranch and Parkfield, this is illustrated in Figures 3-1 and 3-2 in which the response spectra of the free-field input control motions are shown along with the fundamental characteristic frequencies of the soil-structure systems for the different soil profiles and the rigid rock (fixed base) condition. Figure 3-1 illustrates that the large decreases in base shear force for softer soil profiles for the Melendy Ranch input motion are associated with the system frequency shifting from a highly amplified portion of the spectra of the input motion for the rigid rock case to a low-amplified portion of the spectra for the softer soil cases. The opposite occurs for Parkfield, where the substantial increases in base shear force for softer soil profiles correspond to system frequency shifting from a low-amplified portion of the spectra to a pronounced spectral peak (Figure 3-2). The predominant frequency of the base shear force response is approximately equal to the system frequency, which varies from 2 to 4.5 Hz for the four soil profiles and rigid rock (Figures 3-1 and 3-2). The results for base shear force presented here illustrate the importance of ground motion frequency content in determining whether and to what degree soil-structure interaction will increase or reduce structural response.

It should be noted that the artificial (Reg. Guide 1.60) input motion does not fit exactly the smooth spectral curves defined by Reg. Guide 1.60. At the fixed-base frequency of the structure (4.5 Hz), the

spectral amplitudes of the artificial input motion drop below (by about 20 percent) the smooth spectral curves for 2 and 5 percent damping and are about the same as the smooth spectral curve for 10 percent damping. Therefore, it can be expected that, if the artificial motion had enveloped the smooth Reg. Guide 1.60 spectra at this frequency, the ratios shown in Table 3-3 for the artificial (Reg. Guide 1.60) excitation would have been lower. For soil profiles I and II, the ratios would have been approximately equal to or less than 1 rather than the ratios of 1.23 and 1.15 shown in the table.

Typical effects of soil-structure interaction on floor response spectra are illustrated in Figure 3-3 for the artificial (Reg. Guide 1.60) excitation. For horizontal motion at the top of the basemat, the effect is a reduction in spectral values almost throughout the entire frequency range for all four soil profiles. However, at high levels of the containment shell and internal structure, spectral response increases in the vicinity of the system frequency. Effects of soil-structure interaction on floor spectra for all the input excitations are illustrated in Figures 3-4 and 3-5. In Figure 3-4, for soil profile II having a shear wave velocity of 1800 ft/sec, the ratios of horizontal floor response spectrum amplitude for a soil-structure interaction case to the amplitude for the rigid rock case are shown for locations at the top of the basemat and near the top of the containment shell. Similar ratios are shown in Figure 3-5 for soil profile IV having a shear wave velocity of 1000 ft/sec. The general reduction in spectral amplitudes at the top of the basemat is evident in these figures. Near the top of the containment shell, the increase in spectral amplitudes in the vicinity of the soil-structure system frequency (approximately 3 Hz for profile II and 2 Hz for profile IV) and reductions in spectral amplitudes at the fixed-base frequency of the containment shell (approximately 4.5 Hz) can be seen. Figures 3-4 and 3-5 indicate that soil-structure interaction has a generally similar effect on floor response spectra for the different input motions. However, the magnitude of the effect can be quite different for different excitations in some cases, as illustrated

by the substantial differences in the spectral ratios for some of the excitations in Figures 3-4 and 3-5. This again is indicative of the significance of the frequency content of the input motion on the effect of soil-structure interaction.

3.1.2 Effects of Free-field Motion on Structural Response for Given Foundation Conditions

The parametric soil-structure interaction analyses also permit direct examination of the differences in structural response associated with differences in the input excitation for a given foundation condition. The effect of the input motion on the peak base shear force in the containment shell is illustrated in Table 3-4. Effects were similar for containment shell peak base moment and peak acceleration near the top of the containment shell. The table shows ratios of the base shear force obtained for each of five input motions to the base shear force obtained using the artificial accelerogram input motions having spectra consistent with Reg. Guide 1.60. The ratios are presented for each of four soil profiles plus a rigid rock condition. Generally, the artificial (Reg. Guide 1.60) excitation leads to higher base shear forces than the other input motions (ratios less than 1.0). The smallest ratios were obtained for the Melendy Ranch excitation. For Melendy Ranch, for all soil profiles except the very stiff profile I, the base shear forces were a factor of 2.5 to 4 lower than those with the Reg. Guide 1.60 motion (i.e., ratios of 0.4 to 0.25). However, some control motions, in particular El Centro Sta. No. 5 (Comp. N230°E) excitation for profile III and El Centro Sta. No. 5 (Comp. N230°E) and Parkfield excitations for profile IV, resulted in substantially higher base shears than the Reg. Guide 1.60 motion (ratios of about 1.3 to 1.5 in these cases).

These results were found to closely relate to the frequency content of the input excitations. Figure 3-6 shows the response spectra for 2-, 5-, and 10-percent damping of each control motion along with the fundamental characteristic frequencies of the soil-structure systems for the rigid rock case and soil profiles I through IV. For the

soil-structure systems analyzed, an assessment of the overall effective system damping in the fundamental mode using a procedure described by Tsai (1974) indicated values slightly above the average structural damping of 6 percent for soil profiles I through III, increasing to about 15 percent for soil profile IV. The relative spectral amplitudes of the input motions for 15 percent damping are similar to those shown in Figure 3-6 for 5 and 10 percent damping. Figure 3-6 indicates that the cases of substantially higher base shear forces for Parkfield and El Centro Sta. No. 5 (Comp. N230°E) excitations relative to the Reg. Guide 1.60 excitation can be explained by higher spectral amplifications (for damping in the range of about 5 to 15 percent) of these input motions relative to the Reg. Guide 1.60 excitation at the fundamental characteristic frequencies of the soil-structure system.

To further examine these results in relation to the frequency content of the input excitations, ratios of response spectral amplitudes (for 2-, 5-, and 10-percent damping) of each input motion to the Reg. Guide 1.60 input motion were calculated. The ratios for the Parkfield excitation and the Melendy Ranch (N29°W) excitation are shown in Figures 3-7 and 3-8, respectively, along with the fundamental characteristic frequencies of the soil-structure systems and the ratios of base shear forces from Table 3-4. It can be seen that the ratios of response spectral amplitudes for the higher damped spectra (5- and 10-percent) show the same trend as the ratios of base shear forces. Although quantitative agreement of the response spectral ratios and the ratios of base shear forces would not be expected, the two sets of ratios do have values that are quite similar. This correlation of the base shear response to the response spectral characteristics of the input motion illustrates clearly the importance of frequency content of the free-field motion to structural response.

At the characteristic frequency of the soil-structure system for soil profile IV, the spectral amplitudes of the artificial (Reg. Guide 1.60) input motion drop slightly below (by about 10 percent) the smooth spectral curves for 5 and 10 percent damping that are defined by

Reg. Guide 1.60. If the artificial motion had enveloped the smooth Reg. Guide 1.60 spectra at this frequency, the ratios of base shear response of the recorded motions to the artificial motion would have been slightly lower (by about 10 percent) than the values shown in Table 3-4 for soil profile IV. Thus, the ratios for the El Centro Sta. No. 5 (Comp. N230°E) and Parkfield excitations would have been slightly lower than the values of 1.3 to 1.5 shown in Table 3-4.

In Figures 3-9, 3-10, and 3-11, floor response spectra (2-percent damping) for all of the input motions are compared for each soil profile for locations at the top of the basemat, near the top of the containment shell, and near the top of the internal structure. In general, the floor spectra for the Reg. Guide 1.60 input motion envelop those for the other input motions. The generally small exceedances of the floor spectra associated with the Reg. Guide 1.60 input motion appear to generally reflect the relative spectral amplitudes for 2-percent damping of the input motions as illustrated in Figure 3-6. For some input motion, larger exceedances of the floor spectra associated with the Reg. Guide 1.60 input motion can be observed in Figures 3-10 and 3-11 for frequencies higher than 5 Hz. These exceedances reflect higher floor peak accelerations resulting from a given input motion than from the Reg. Guide 1.60 input motion.

3.1.3 Free-field Ground Motion Characterization

Both the soil-structure interaction analyses and the structural inelastic response analyses conducted for this study have thus emphasized the importance of the frequency content of the ground motion in determining structural response. As was summarized in Section 2.1, structural inelastic response was importantly influenced by frequency content over the frequency range from the structural elastic frequency to a lower frequency corresponding to a certain amount of inelastic deformation. In the elastic soil-structure interaction analyses summarized in Sections 3.1.1 and 3.1.2, some response quantities, such as containment shell base shear force, were largely determined by frequency

content in the vicinity of the fundamental characteristic frequency of the soil-structure system, which is lower than the structural elastic fixed-base frequency. However, frequency content over a broad frequency range was important to floor response spectra. As summarized in Section 2.1, the duration of strong shaking was also found to be an important ground motion characteristic influencing structural inelastic response.

Ground motion frequency content as well as duration of strong shaking are strongly dependent on site-specific factors including earthquake source characteristics, source-to-site wave propagation characteristics, and local site conditions. Therefore, the results of this study are strongly supportive of the use of site-specific ground motion characterizations rather than standard non-site-specific characterizations such as Reg. Guide 1.60 spectral shapes. Because of limitations in knowledge of the tectonic environment at many sites, as well as limitations in the amount of recorded ground motion data and in knowledge of ground motion phenomena, it is often difficult to incorporate site-specific considerations. However, they should be incorporated to the extent possible.

Depending on site-specific factors, site-specific smooth response spectral shape may differ greatly from standard spectral shapes. For example, the effect of local soil conditions on spectral shapes was examined by Seed et al. (1976) and Mohraz (1976). Response spectral shapes from Seed et al. (1976) are compared with the spectral shape for Reg. Guide 1.60 in Figure 3-12. The comparison indicates that spectral shapes for different categories of soil conditions may differ significantly from each other and from the Reg. Guide 1.60 spectral shape.

An example of the effect of earthquake source characteristics on response spectral shapes is illustrated in Figure 3-13. In the figure, a response spectral shape obtained from statistical analysis of data from small-magnitude ($M_L \approx 4$) earthquakes is compared with a response spectral shape similarly obtained for a moderate-magnitude ($M_L \approx 6\frac{1}{2}$) earthquake. Both data sets represent recordings obtained on the ground floor of instrument shelters or other small buildings at firm alluvial

soil sites. The recordings were all within approximately 10 km of the ruptured fault. As shown, the spectral shape for the small magnitude events is very narrow-banded and high-frequency in comparison to the spectral shape for the moderate magnitude events. The very important effect of earthquake magnitude on response spectral shape is illustrated by this figure. As magnitude increases, spectrum broad-bandedness increases, due to increasing content of long-period motion with increasing magnitude.

In developing a site-specific ground motion characterization, it is essential to recognize and allow for the uncertainty in ground motion characteristics. Uncertainty in site-specific spectra is appropriately incorporated by specifying a smooth design response spectrum at a reasonably conservative level (typically 84th percentile level). The smooth spectrum is intended to cover a reasonable range of ground motion spectral characteristics, in terms of both the amplitudes and the frequencies of the spectral peaks, that could occur at a site for a given design earthquake. Such spectra may be developed based on statistical analysis of ground motion data recorded under similar conditions, supplemented as appropriate by analytical studies of site-specific factors (i.e., earthquake rupture, source-to-site wave propagation, and/or local site response). Having developed a smooth design response spectrum, acceleration time histories compatible with this spectrum and of realistic duration for the design event may be selected or developed. For a given design earthquake and component of motion, the time histories may consist of either a single artificial time history whose spectrum envelops the design spectrum, or multiple recorded time histories whose spectra differ individually but collectively envelop the design spectrum. For a realistic appraisal of nonlinear structural response, the use of recorded time histories is preferable to use of an artificial time history.

While the results of this study support the desirability of site-specific ground motion characterizations, they also indicate that

the standard Reg. Guide 1.60 spectral shapes provide a generally conservative design basis. This is to be expected because of the broad-banded nature of the Reg. Guide 1.60 spectra and the fact that spectral amplifications are set at the 84th percentile levels. Thus, for example, the soil-structure interaction analyses indicated a generally conservative base shear response and generally conservative floor response spectra associated with Reg. Guide 1.60. In some cases analyzed, the Reg. Guide 1.60 motion provided an overwhelmingly conservative response (as illustrated in Table 3-4 for the Melendy Ranch input motion for soil profiles II, III, and IV). However, in other cases, the Reg. Guide 1.60 input motion resulted in a moderately unconservative response (as illustrated in Table 3-4 for the El Centro Sta. No. 5 [Comp. N230°E] input motion for soil profiles III and IV and the Parkfield input motion for profile IV).

3.2 CHARACTERIZATION OF VARIATIONS OF GROUND MOTION WITH DEPTH

3.2.1 Analytical Predictions of Ground Motion Variations with Depth

Plane wave propagation models are used in current practice in conducting soil-structure interaction analyses for nuclear power plant structures. A wave field consisting of vertically propagating waves is typically assumed for these analyses. In this section, the nature of analytical predictions of ground motion variations with depth using current practice is illustrated. Subsequent sections present: a review of available empirical evidence on ground motion variations with depth; an analysis of the effects on structural response of neglecting these variations; and conclusions regarding ground motion characterization.

The following comparisons are for soil profile IV (Table 3-2) and the artificial (Reg. Guide 1.60) input motion used in the soil-structure interaction analyses conducted for this study. Figure 3-14 provides a comparison of the response spectrum of the horizontal input motion at the free-field ground surface (free-field control motion) with the response spectrum of the motion at a depth of 40 ft in the free field obtained

from deconvolution analysis. The spectrum of the motion at depth is significantly lower than the spectrum of the motion at the ground surface. The pronounced valley in the spectrum of the motion at depth occurs at the fundamental natural frequency of the overlying soil layer, which is approximately 6 Hz for this soil profile.

Also shown in Figure 3-14 are the horizontal and rocking foundation input motions for the soil-structure interaction analysis of the reactor building embedded at a depth of 40 ft in this soil profile. The foundation input motions are those resulting from kinematic interaction of a massless, rigid foundation with the free-field wave field. Due to kinematic interaction, the higher-frequency peaks and valleys of the foundation-level, free-field motion are smoothed out in the horizontal component of the foundation input motion and a rocking component of motion is introduced. The low spectral amplitudes of the horizontal component of the foundation input motion in the high frequency range relative to the free-field control motion and the introduction of a rocking component illustrate the potential significance of ground motion variations with depth.

Figure 3-15 provides comparisons similar to those in Figure 3-14 but for the vertical component of motion. The valley or dip in the free-field foundation level spectrum is not as pronounced for the vertical component as for the horizontal component because it occurs at a higher frequency (approximately 15 Hz for this soil profile), corresponding to compression wave propagation for the vertical component versus shear wave propagation for the horizontal component.

Figures 3-16 through 3-18 compare the foundation input motions (from Figures 3-14 and 3-15) with the actual foundation response motions that resulted from the complete soil-structure interaction analysis of the reactor building embedded at a depth of 40 ft. Figure 3-16 indicates that, for this case, for the horizontal component, the actual foundation motion is nearly the same as the foundation input motion. For the vertical component, comparison of Figures 3-15 and 3-17 indicates that

the actual foundation motion is more similar to the free-field foundation level motion than to the foundation input motion. Figures 3-16 and 3-17 further illustrate the potential significance of the variations of ground motion with depth. As shown in Figure 3-18, the actual foundation rocking response motion is greatly different from the rocking component of the foundation input motion. The rocking response mainly reflects response of the soil-structure system (which has a fundamental characteristic frequency of about 2 Hz in this case, as is evident in Figure 3-18), to the horizontal component of the foundation input motion.

3.2.2 Observational Data on Variations of Earthquake Ground Motion with Depth

A review of observational data on the variations of earthquake ground motion with depth was conducted during this study and is presented by Chang et al. (1986). The ground motion data most pertinent to evaluating free-field ground motion variations with depth are from downhole arrays. Data from the Narimasu and Waseda, Japan downhole arrays were acquired and analyzed during this study. In addition, published data from other downhole arrays in Japan and the U.S. were compiled and reviewed. These array data included data from the Earthquake Research Institute array, University of Tokyo array, Tokyo International Airport array, Ukishima Park array, Futtsu Cape array, Kannonzaki array, and Iwaki and Tomioka arrays in Japan; and the Richmond Field Station, California array, Menlo Park, California array, and Beatty, Nevada array in the U.S.

In addition to the downhole array data, sets of ground motion data from the basements of embedded structures and nearby non-embedded structures or free-field ground surface stations were compiled and reviewed. These data included motions recorded at a large LNG tank in Japan, the Hollywood Storage Building, California, the Humboldt Bay, California Power Plant, four groups of buildings during the 1971 San Fernando earthquake, and the Pleasant Valley, California pumping plant during the 1983 Coalinga earthquake.

A few of the observational data pertaining to variations of ground motion with depth are summarized below to illustrate the trends of the findings of the study. Results for the data evaluated are presented in detail by Chang et al. (1986).

Figures 3-19 through 3-23 illustrate results of the analyses of the Japanese downhole data from the Narimasu site. The variations with depth of peak ground acceleration of the NS and EW components recorded by the array are shown in Figure 3-19; the corresponding variations with depth of response spectra of the ground motions are shown in Figure 3-20. These figures illustrate the substantial reductions in the amplitudes of recorded peak accelerations and response spectra with depth below the ground surface.

Deconvolution analyses of the Narimasu array site were made using the recorded surface (-1m) motions as input motions. These analyses utilized the vertical plane-wave propagation technique that is typically used in practice (computer program SHAKE). The assumption of vertically incident waves is consistent with the predominant wave field estimated for the ground motion at the Narimasu site. At the depths at which motions were recorded (-5m, -8m, -22m, and -55m), motions were calculated from the deconvolution analyses. The calculated peak accelerations and response spectra are compared with the recorded ground motions in Figures 3-21 and 3-22. The calculated ground motions show reductions in amplitude and changes in frequency content with depth that are generally consistent with those of the recorded motions. The calculated ground motions are somewhat higher than the recorded motions with differences tending to increase at greater depths, indicating that the results of the deconvolution analyses are conservative. Similar results and observations were obtained for the Waseda data that were also acquired and analyzed in detail during this study (Chang et al., 1986). There are two possible reasons for the differences between the recorded and calculated ground motions. One reason for the calculated motions being

higher than the recorded motions is scattering of seismic waves in the near-surface soils. As a result of scattering, the near-surface motions may contain components of motion that would not be predicted by plane wave propagation theory for vertically propagating waves. When the near-surface motions containing these components of motion are deconvolved, the resulting calculated motions at depth would be higher than the recorded motions.

The other reason is that the high frequency motions may be over-damped in the theoretical calculation (Roesset, 1980). The motions are calculated based on the assumption of a constant soil damping throughout the duration of shaking, as required to be made in currently available frequency domain linear or equivalent linear techniques used for deconvolution and soil-structure interaction analysis. In reality, soil damping varies throughout the duration of shaking. The higher frequency motions during the shaking tend to be associated with smaller strains and thus with lower damping. Thus, when an average soil damping is used in calculations, high frequency motions may be overdamped, resulting in an overestimation of high-frequency ground motion at depth from a deconvolution analysis. It is expected that this effect would become more significant for high levels of excitation.

For either of the reasons outlined above, deconvolution analyses will tend to result in calculated motions at depth that are higher than the recorded motions, indicating that, in general, deconvolution analyses are likely to lead to conservative estimates of ground motion at depth.

Additional deconvolution analyses of the Narimasu and Waseda sites were made for parametric variations of soil shear modulus. Analyses for parametric variations in soil properties are commonly made in conducting ground response analyses to cover the uncertainties in the properties. Typically, such analyses are conducted for upper-bound and lower-bound variations from average or best-estimated low-strain shear wave velocities or shear moduli. In this study, upper-bound and lower-bound

shear moduli were obtained by multiplying and dividing the average low-strain shear moduli by a factor of 1.5. Nonlinear soil response in such analyses is typically incorporated in practice using the equivalent linear method (Seed and Idriss, 1969), in which shear modulus and damping values used in the response computation are selected to be compatible with the average shear strain induced during the motion using an iterative procedure. The equivalent linear method was used for these parametric analyses. Response spectra of the calculated motions at different depths from the analyses of the Narimasu site are compared with the recorded ground motions in Figure 3-23. The comparisons show that the response spectra of the calculated motions at depths envelop those of the recorded motions. Similar results were obtained for the Waseda site. These results indicate that the current practice of conducting deconvolution analyses for rather wide parametric variations in soil properties results in conservative estimates of ground motion at depth.

From the review and analyses of all the downhole array data examined during this study, it is concluded that both peak accelerations and response spectra decrease significantly with depth and that the observed trends of variations of ground motion with depth are generally consistent with those predicted by plane wave propagation models assuming vertically propagating shear waves. As noted above, there is some evidence, as well as reason to expect, that analytical predictions result in somewhat conservative estimates of ground motion variations with depth.

The ground motions recorded at the Humboldt Bay Power Plant during the 1975 Ferndale, California earthquake provide data on the motions at the base of a massive, deeply embedded structure relative to those at the ground surface in the free field. Figures 3-24 and 3-25 show the response spectra of the ground motions recorded at the base of the refueling building (deeply embedded at a depth of 84 feet) and at the free-field ground surface. The horizontal ground motions at the base of the embedded structure are significantly lower than the free-field ground surface motions as illustrated in Figure 3-24. However, the vertical

motion at the base of the structure is higher than the free-field motion as shown in Figure 3-25. The horizontal motions were analyzed in detail by Valera et al. (1975) and Tajirian et al. (1984). Their analyses, which incorporated wave propagation effects on the variation of ground motion with depth and soil-structure interaction effects, resulted in good agreement of the response spectra of the calculated motions and the recorded motions at the base of the refueling building, as shown in Figure 3-26.

Another example of data for embedded structures is provided by ground motion recordings obtained in nearby buildings with and without basements during the 1971 San Fernando, California earthquake. These data have been analyzed by Seed and Lysmer (1980), Tera Corp. (1980), and Chang et al. (1986). The data indicate that, in general, the foundation motions of the buildings with basements are significantly lower than the foundation motions in nearby buildings without basements. Response spectra comparisons for two nearby buildings with and without basements, showing reduction in lower-period (higher-frequency) motions for the basement motions, are shown in Figure 3-27. Analysis of this data pair (Chang et al., 1986; Kim, 1984) indicated that the reductions were larger than those that would be predicted considering variations in ground motion with depth and soil-structure interaction effects.

There are limitations in the available data base pertaining to evaluating variations of ground motion with depth. Available data from downhole arrays analyzed to date are of relatively low amplitude (highest peak accelerations equal to or less than about 0.1 g). It is desirable to have additional data to verify trends at higher acceleration levels including assessment of the influence of nonlinear soil behavior (nonlinear effects should be small for the low excitation levels of the currently available downhole data). Also, most of the downhole array data are for relatively soft soil conditions, and more data are needed for stiffer soils. Despite these limitations, there does exist an

impressive body of data from which to examine empirical trends and compare with results of analyses. From a review of these data, it is concluded that the empirically observed trends are generally consistent with predictions from plane wave propagation models as are typically used in practice in evaluating ground motion variations with depth and conducting soil-structure interaction analyses. It appears that the analysis methods tend to result in somewhat conservative estimates of the variations of ground motion with depth.

3.2.3 Effects on Structural Response of Neglecting Ground Motion Variations with Depth

In practice, soil-structure interaction analyses for embedded structures have sometimes been conducted using an approach that neglects embedment effects on the foundation input motion (i.e., that neglects or excludes the variations of ground motion with depth and kinematic interaction effects). In such analyses, the translational components of the foundation input motion have been taken directly as those of the control motion, and the rocking components of the foundation input motion have been neglected. To assess the effects of this practice of excluding variations of ground motion with depth and kinematic interaction on structural response, a series of comparative analyses was included in the parametric soil-structure interaction analyses of a reactor building conducted during this study (Luco et al., 1986). These comparative analyses were conducted for two embedment depths (20 ft and 40 ft), four soil profiles (I, II, III, and IV), and four seismic excitations (Reg. Guide 1.60 artificial time history, and Melendy Ranch, El Centro Station No. 5, and Parkfield Station No. 2 recorded time histories). Structural responses from the analyses that excluded effects of ground motion variations with depth and kinematic interaction (referred to subsequently herein as "analyses excluding kinematic interaction") were compared with analyses in which these effects were included. The structural responses examined included all the parameters mentioned in Section 3.1.1 including

base shear forces and moments and peak accelerations and floor response spectra at various locations in the containment shell and internal structure.

Complete results of these analyses are presented in Luco et al. (1986). It was found that for all parameters for all cases analyzed, excluding kinematic interaction increased the response. The effects of excluding kinematic interaction on the peak base shear force in the containment shell for the 40 ft-embedment-depth cases are summarized in Table 3-5 in terms of the ratio of the peak base shear force excluding kinematic interaction to that including kinematic interaction. The effects increase as the profile stiffness decreases, and they are largest for high-frequency excitations such as the Melendy Ranch record. Thus, for the Melendy Ranch excitation, the ratio of peak base shear force excluding kinematic interaction to that including kinematic interaction increased from a value less than 1.1 for a very stiff (rocklike) soil profile (profile I with shear wave velocity of 3,600 ft/sec) to as much as 1.7 to 1.8 for softer soil profiles (profiles III and IV with shear wave velocity of 1,000 ft/sec in the upper 40 ft). Figure 3-28 illustrates the large reduction due to kinematic interaction in the foundation input motion relative to the free-field ground surface control motion for the Melendy Ranch excitation and soil profile IV.

On the other hand, excluding kinematic interaction had a relatively small effect for the Parkfield excitation, which has a low content of high frequency motion. As shown in Table 3-5, the base shear force ratios for Parkfield ranged from slightly above 1 for profile I to a maximum less than 1.2 for profile III. For the Parkfield excitation, the reduction in the foundation input motion due to kinematic interaction is much less than the reduction for the Melendy Ranch excitation. This can be seen by comparing the effects of kinematic interaction on the foundation input motion for Parkfield in Figure 3-29 with those for Melendy Ranch shown in Figure 3-28.

As expected, effects of excluding kinematic interaction decreased with decreasing embedment depth, and thus were smaller for 20-ft embedment than for 40-ft embedment in every case analyzed.

Effects of excluding kinematic interaction on floor response spectra are illustrated in Figure 3-30 for the case of the artificial (Reg. Guide 1.60) excitation, soil profile III, and 40-ft embedment. It can be seen that substantial increases in floor response spectra occurred when kinematic interaction was excluded from the analysis.

The results obtained from these analyses indicate that the practice of excluding kinematic interaction can lead to significant overestimation of structural responses. The overestimation increases with decreasing soil stiffness, increasing high-frequency content of the free-field control motion, and increasing embedment depth. These results emphasize the importance of incorporating variations of ground motion with depth on characterizing foundation motions and conducting soil-structure interaction analyses.

It should be noted that the analytical effects of not including variations of ground motion with depth examined in this section pertain to the substructure method of carrying out soil-structure interaction analyses. In these analyses, the control motion was specified directly as the input motion to soil-structure systems excluding kinematic interaction effects. The effects would not be the same if the procedure for prescribing the control motion is not the same. For example, using the finite element method, an approach that has been employed to exclude reductions of ground motion with depth is to input the control motion at the foundation level in the free field rather than at the finished grade. With such a practice, wave propagation analysis leads to motions at the finished grade that are generally greatly amplified above the control motion specified for the site. Furthermore, induced foundation rotations due to kinematic interaction are automatically included in finite element analyses. (As a result of ground motion amplifications

above the foundation level, the induced foundation rotations are further amplified.) Because of these two effects, it may be expected that the approach to excluding ground motion reductions with depth by specifying the control motion at the foundation level in the free field in finite element soil-structure interaction analyses will overestimate response to an even greater degree than in the analyses conducted in this study.

3.2.4 Ground Motion Characterization

On the basis of the evaluations described in the previous sections, it is concluded that appropriate variations of ground motion with depth should be incorporated in characterizing foundation input motions and conducting soil-structure interaction analyses for embedded structures. It is also concluded that current wave propagation analysis procedures for characterizing these variations provide reasonable and apparently somewhat conservative estimates of ground motions at depth.

It is desirable to incorporate uncertainty in the characterization of ground motion with depth. A reasonable way to accomplish this is by varying the soil properties. The primary reason for varying the soil properties is to incorporate uncertainty in the properties in a soil-structure interaction analysis. However, in addition to the effects of soil property variations on the soil impedances and inertial interaction, such variations affect the foundation input motion resulting from the variations of ground motion with depth and kinematic interaction.

The effects of soil property variations on variations of ground motion with depth were illustrated in Section 3.2.2 in connection with analysis of the Narimasu downhole data from Japan. It was shown therein that upward and downward variations in low-strain shear moduli by a factor of 1.5 resulted in conservatively enveloping the variations of recorded ground motion with depth. Soil property variations of this order would typically exceed the uncertainty associated with soil property measurements, but such variations are considered reasonable at

present to cover other uncertainties associated with a soil-structure interaction analysis, including uncertainties in ground motion variations with depth.

The effects on structural response of variations in soil properties of the order of magnitude discussed above was examined from results obtained in the soil-structure interaction analyses of a reactor building conducted during the study (Luco et al., 1986). A series of analyses was carried out for soil profiles V and VI having properties summarized in Table 3-6. The stiffer profile (V) had shear moduli that were approximately 1.25 times those of the softer profile (VI) in the upper 12.5 ft, 1.45 times those of the softer profile between 12.5 ft and the foundation embedment depth of 40 ft, and 1.5 to 1.55 times those of the softer profile at greater depths. Soil damping ratios for S-waves were in the range of approximately 0.02 to 0.03 for profile V, increasing to 0.04 to 0.07 for profile VI. The effects of the property variations are summarized in Table 3-7 for a number of response parameters for four input excitations. It can be seen that the soil property variations resulted in significant effects on response. Effects on floor spectra, presented in Luco et al. (1986), were similarly significant. These results emphasize the need for incorporating soil property variations in soil-structure interaction analyses. As stated previously, such variations directly affect inertial interaction as well as the input motion in soil-structure interaction analyses.

3.3 CHARACTERIZATION OF VARIATIONS OF GROUND MOTION IN A HORIZONTAL PLANE

For purposes of this study, variations of ground motion in a horizontal plane have been considered in two categories. The first is phase differences in ground motion. For variations in this category, acceleration time histories of ground motion are identical at different points in a horizontal plane in the free field but are shifted in time. The second category is incoherence. Variations in this category are differences in the acceleration time histories (and thus in the ground motion amplitudes and frequency content) horizontally from point to point. The findings of the study regarding ground motion characterization for phase variations of ground motion and incoherence in a horizontal plane are summarized in the following subsections.

3.3.1 Phase Differences in Ground Motion in a Horizontal Plane

Phase differences in ground motion in a horizontal plane depend on the apparent horizontal velocity of the seismic waves. For vertically propagating waves, the apparent horizontal velocity is infinite and there are no phase differences in ground motion in a horizontal plane. For other wave fields (inclined-incident body waves or surface waves), phase differences in ground motion occur. Non-vertically incident body waves have an apparent horizontal propagation velocity related to the wave incidence angle. The phase differences increase as the angle of incidence from vertical of the waves increases and the apparent horizontal velocity correspondingly decreases. The issue with regard to phase differences of ground motion horizontally is whether these differences can be expected to significantly affect structural response or whether the typical assumption of vertically propagating waves is adequate for defining the free-field seismic wave field and conducting soil-structure interaction analysis.

3.3.1.1 Apparent Horizontal Wave Propagation Velocity

The effects of phase differences of ground motion in a horizontal plane on foundation and structural response, sometimes called "wave

passage effects", are clearly related to the apparent horizontal propagation velocity of the waves. The slower the apparent velocity, the greater will be the difference in response relative to that for vertically propagating waves.

The presently available empirical observations on apparent wave speeds are quite limited. The data consist of observations from several earthquakes in Japan at two sites, the 1979 Imperial Valley, California earthquake, and earthquakes recorded at the SMART 1 array in Taiwan. The available data were reviewed by O'Rourke et al. (1982) and are summarized by Chang et al. (1986). One of the array sites in Japan is located at the Tokyo International Airport at Haneda, Tokyo. At this site, the array consists of six surface accelerometers spaced at an interval of 500 meters with a total length of the array equal to 2,500 meters. Acceleration time histories from three earthquakes were used by Tsuchida et al. (1977 and 1980) to calculate their cross-correlation functions. Based on these data, Tsuchida et al. computed the time-shift for the maximum correlation between two sets of recordings at two accelerometers separated by a distance of 2,500 meters. Assuming that the waves propagated directly from the epicenters to the array site, Tsuchida et al. calculated the velocities of the wave propagation to be in a range of 2.6 to 5.3 km/sec for the three earthquakes.

Another array in Japan consisted of six accelerometers placed at 100 m intervals. Recordings from two earthquakes were used by Tamura et al. (1977) to calculate the apparent propagation velocity using cross-correlation techniques similar to those of Tsuchida et al. The values of the apparent propagation velocity for two earthquakes calculated by Tamura et al. were 2.6 and 2.9 km/sec.

O'Rourke et al. (1982) calculated the apparent propagation velocity of the initial shear wave using the recordings along a radial line from the epicenter from the 1979 Imperial Valley earthquake. The apparent propagation velocity calculated over a wide range of epicentral distances

was 3.7 km/sec for this event. The Taiwan SMART 1 array data indicate that the predominant energy of the most intense motion propagated at approximately 3 km/sec across the array (Bolt et al., 1982).

Table 3-8 summarizes the apparent horizontal propagation velocities inferred from empirical data. As shown in Table 3-8 and discussed above, the apparent velocities range from about 2.5 to 5.5 km/sec.

Apparent horizontal propagation velocities of ground motion have also been estimated from analytical studies of fault rupture and wave propagation in layered earth models. Studies conducted by Luco and Sotiropoulos (1980), Bouchon and Aki (1982), and Campillo and Bouchon (1983) indicate that the apparent horizontal propagation velocities are controlled by the shear wave velocity in the deeper rocks in which fault rupture occurs rather than by the lower shear wave velocity of near-surface sediments. For sites close to faults, the apparent horizontal propagation velocities can also be controlled by the velocity of propagation of the fault rupture. The apparent velocities calculated in these analytical studies generally exceeded 2 km/sec.

In summary, both the limited recorded data and analytical studies are indicative of high apparent horizontal propagation velocities of seismic waves. Velocities inferred from these data and studies generally exceed 2.5 km/sec.

3.3.1.2 Effects on Structural Response of Non-vertically Incident Waves

The effects of non-vertically-incident waves propagating at some apparent horizontal velocity on the response of a reactor building and an auxiliary building were analyzed in the parametric soil-structure interaction analyses conducted during this study (Luco et al., 1986). Three combinations of apparent horizontal velocities were analyzed for. In the first case (designated Case c) infinite velocities were assumed, i.e., vertically propagating waves. In the second case (designated Case b), transverse ground motions (i.e., transverse to the direction of wave

propagation) were assumed to propagate at 3 km/sec and to be associated with SH-waves, and longitudinal ground motions (i.e., in the direction of wave propagation) and vertical ground motions were assumed to propagate at 4.5 km/sec and to be associated with P-SV waves. In the third case (designated Case a and used only for the reactor building analysis), these velocities were reduced to 1.5 km/sec and 2.25 km/sec. Three-component, free-field control motions at the ground surface consisted of both the artificial (Reg. Guide 1.60) accelerograms and the Melendy Ranch record (Table 3-1). The reactor building model used in the study had a diameter of approximately 125 ft and was embedded at a depth of 40 ft. The auxiliary building model had a length of 270 ft in the direction of wave propagation and a width of 100 ft in the transverse direction and was assumed unembedded. Soil profiles II, III, and IV (Table 3-2) were used in analyses for the reactor building, and soil profile III was used in analyses for the auxiliary building. The structural responses examined included peak translational and rotational accelerations and response spectra at the top-of-foundation and higher levels of the structures and base shear forces and moments.

Effects on Translational and Rocking Responses - Non-vertically incident wave effects on translational and rocking responses are summarized in this section, and effects on torsional responses are discussed in the following section. For response components transverse to the direction of wave propagation, it was found that the filtering or scattering effect of the foundation on the non-vertically incident waves reduced responses in comparison to those for vertically propagating waves. Designating the x, y, and z directions as the longitudinal, transverse, and vertical directions, respectively, non-vertically incident waves resulted in reduced response for translational y-components of motion (\ddot{u}_y), for rocking components about the x-axis ($\ddot{\phi}_x$), for the y-component of base shear (F_y), and the base moment about the x-axis (M_x). Similarly, vertical responses (\ddot{u}_z and F_z) were reduced. However, these reductions in transverse and vertical responses were small. For the

reactor building, they were generally less than 5 percent even for the case of the slower wave speeds (Case a). The effects tended to be larger for the auxiliary building, having the larger foundation, than for the reactor building, but were still less than 5 percent for the case analyzed (Case b).

For responses in the longitudinal direction, the effects of non-vertically incident waves tended to reduce response due to scattering. However, at the same time, non-vertically incident wave effects tended to increase response due to increased rocking of the foundation caused by the phase differences of the motion across the foundation. The net effect was a decrease in response for some response parameters and an increase in response for others, without any consistent trend. Both increases and decreases were generally small. Except for rocking about the y-axis ($\ddot{\phi}_y$), changes in response were generally less than about 10 percent for either the reactor building or auxiliary building for Case b and less than about 20 percent for the reactor building for Case a. Larger increases in high-frequency (greater than 10Hz) rocking response ($\ddot{\phi}_y$) were obtained, particularly for the Melendy Ranch input excitation. The effect of increased rocking response is to increase the vertical response toward the perimeter of the structures and the horizontal response at higher levels of the structures.

In a study of the response of the Hollywood Storage building during the San Fernando earthquake (summarized in this study in Chang et al., 1986), Newmark et al. (1977) associated large reductions in the translational foundation response relative to the free-field response to wave passage effects. Apart from the fact that the observed effects at the Hollywood Storage building may have reflected embedment and soil-structure interaction effects rather than wave passage effects (see Chang et al., 1986), the apparent horizontal propagation velocities used by Newmark et al. (1977) to match the observed reductions (approximately 0.5 km/sec) were much lower than those used in the present study.

Luco and Wong (1982), in soil-structure interaction analyses of a reactor building, found generally higher reductions in translational response due to non-vertically incident SH waves than the reductions obtained in the present study. However, low horizontal propagation velocities of approximately 0.6 to 0.85 km/sec were used in their analyses. In analyses of a reactor building for non-vertically incident waves having propagation velocities of 2 to 4 km/sec for SH waves and 3 to 6 km/sec for P-SV waves, Wong and Luco (1981) found effects of non-vertical wave incidence on translational and rocking responses to be less than 10 percent, similar to the effects found in the present study.

Based on both the available data and studies pertaining to apparent horizontal propagation velocities of seismic waves and the results of soil-structure interaction analyses summarized above, it appears that non-vertically incident wave effects on translational response and probably on rocking response are small enough to be neglected in most cases.

Effects on Torsional Response - The transverse component of non-vertically incident waves induces a torsional response of a structure due to the transverse motions being out of phase across the foundation. The torsional response is approximately inversely proportional to the apparent wave speed and is zero for vertically propagating waves input to a symmetric structure.

Torsional responses due to non-vertically incident waves may potentially increase horizontal motions toward the perimeter of a structure relative to the motions due to vertically incident waves. In the soil-structure interaction analyses conducted using the artificial (Reg. Guide 1.60) accelerogram input motions, the torsional effects on perimeter motions were generally small. The effects were larger for the auxiliary building than for the reactor building; effects on floor spectra of perimeter motions for the auxiliary building are illustrated in Figure 3-31.

Torsional effects on perimeter motions were larger for the Melendy Ranch input motion than for the artificial (Reg. Guide 1.60) accelerogram input motion for both the reactor building and the auxiliary building. The small effects on floor spectra of perimeter motions for the reactor building due to the Melendy Ranch input are illustrated in Figure 3-32. For the auxiliary building, the Melendy Ranch input resulted in a substantial increase in perimeter motions as illustrated by the floor response spectra in Figure 3-33. The relatively large effect of the Melendy Ranch input compared to the artificial (Reg. Guide 1.60) accelerogram input can be seen by comparing Figures 3-31 and 3-33. Two factors account for the larger torsional effects for the Melendy Ranch input than for the artificial (Reg. Guide 1.60) accelerogram input. The first is that both input motions caused a strong torsional response in the non-vertically incident wave analyses, reflecting a relatively rich content of high-frequency motion for both inputs. The second is that the horizontal translational response along the axis or center of mass of the structures was substantially larger for the Reg. Guide 1.60 input than for the Melendy Ranch input. (The reason for this second factor is that the Reg. Guide 1.60 input has a much higher content of motion than the Melendy Ranch input at the fundamental characteristic frequencies of the soil-structure systems for the cases analyzed; refer to Section 3.1.2). As a result of these two factors, the torsional response resulted in a larger increase of the perimeter motions relative to the motions along the structure axis or center of mass for the Melendy Ranch input than for the Reg. Guide 1.60 input.

Another measure of the torsional effects induced by non-vertically incident waves is the ratio of the induced peak base torque (torsional base moment about the z-axis, M_z) from non-vertically incident wave cases divided by the product of the peak base shear force, F_y , from vertically incident wave cases and the structure base length or diameter in the direction of wave propagation, $2L$ (where L is the half-length or radius) i.e., $M_z/F_y(2L)$. This ratio represents a measure of the "accidental eccentricity" (normalized by the base length, $2L$) that would

be required to be assumed in an analysis for vertically propagating waves to induce the same peak torque obtained in an analysis for non-vertically incident waves. However, because of differences in the time at which the peak base shear force and the peak torque may occur, this ratio may overestimate the accidental eccentricity.

The trends for accidental eccentricity obtained from the soil-structure interaction analyses were similar to those for effects on perimeter motions as summarized above. Accidental eccentricities were larger for the auxiliary building than for the reactor building and larger for the Melendy Ranch input than for the Reg. Guide 1.60 input. For the Reg. Guide 1.60 input to the reactor building, accidental eccentricities were equal to or less than 3 percent for cases of faster apparent wave propagation velocity (Case b) and equal to or less than 6 percent for cases of slower apparent wave propagation velocity (Case a). The accidental eccentricity for the auxiliary building for Case b was 6 percent.

For the Melendy Ranch input to the reactor building, accidental eccentricities were equal to or less than 10 percent and 20 percent for Cases b and a, respectively. The value for the auxiliary building for Case b was 19 percent. The reasons for the larger accidental eccentricities for the Melendy Ranch input than for the Reg. Guide 1.60 input are similar to those just mentioned to explain the larger effect on perimeter motions for the Melendy Ranch input, namely strong torsional response (M_z) for both inputs but much stronger translational response (F_y) for the Reg. Guide 1.60 input.

Limited analyses were also made to examine the effect of phasing of the time histories of torque and base shear on the apparent accidental eccentricity. These analyses are described in Appendix A. For cases using the Reg. Guide 1.60 input, it was found that the accidental eccentricity decreased considerably, to values less than 1 percent for the cases examined, due to maximum torque and base shear occurring at different times. Figure 3-34 illustrates the out-of-phasesness of the

torque and base shear time histories of responses for the auxiliary building analysis using the Reg. Guide 1.60 input. However, for the narrow-banded, short-duration Melendy Ranch input, peak torque and shear responses were out of phase in some cases and nearly in phase in other cases examined. Even with consideration of phasing, the accidental eccentricity for the case of the Melendy Ranch input to the auxiliary building was approximately 15 percent.

The torsional response of a reactor building due to non-vertically incident waves was also examined by Wong and Luco (1981) using apparent horizontal wave propagation velocities similar to those used in the present study (2 to 4 km/sec for SH waves). They found that torsion induced by non-vertically incident waves increased peak perimeter accelerations at the base by 10 percent and 20 percent above that for vertically incident waves for apparent wave velocities of 4 km/sec and 2 km/sec, respectively. The accidental eccentricity they obtained for the slower apparent wave velocity was 5 to 6 percent. An artificial accelerogram having pronounced peaks at three frequencies (3, 8, and 14 Hz) was the input free-field control motion in this analysis.

In practice, an accidental eccentricity of 5 percent has often been assumed to incorporate possible effects of non-vertically incident waves. The analyses discussed above indicate that such a value of accidental eccentricity would generally cover response for cases in which the free-field input motion has a broad-banded response spectrum, such as Reg. Guide 1.60. Due to differences in phasing of the torsional and translational response, the 5 percent provision may be quite conservative in many cases. The analyses are also indicative of sufficiently small effects of non-vertically incident waves on perimeter response motions for this type of input motion that these effects could be neglected in most cases.

It also appears, however, that more significant torsional effects due to non-vertically incident waves may occur with some other types of free

field motions. Specifically, the study indicates that a significant torsional effect may be associated with narrow-banded, high-frequency, short-duration input motions, such as Melendy Ranch, that produce a strong torsional response but a weak translational response due to the spectral peak of the motion occurring at frequencies significantly higher than the fundamental characteristic frequency of the soil-structure system. In such cases, it appears that the accidental eccentricity can substantially exceed 5 percent and that effects on perimeter motions may be significant. Further studies are desirable to better define the range of practical conditions for which non-vertically incident wave effects on torsional response should be considered.

The above discussion pertains only to response for non-vertically incident waves versus response for vertically incident waves for given free-field input motions. The results should not be interpreted as indicating that torsional responses would necessarily require consideration of a Melendy-Ranch-type input motion and non-vertically incident wave fields. Even with the more pronounced torsional effects, the low translational response associated with a Melendy-Ranch-type input motion may still result in a low overall structural response relative to that for other input motions. The relative effects of different input motions on response in a soil-structure system are discussed in Section 3.1.3.

3.3.2 Incoherence of Ground Motion

Available ground motion data for examining variations in frequency content of ground motions over short horizontal distances are quite limited. Only data from differential arrays with closely spaced stations are useful for examining the coherence of ground motions over distances typical of the foundation dimensions of nuclear power plant structures. The data reviewed in this study (Chang et al., 1986) are from the El Centro, California Differential Array, the Chusal Differential Array in the USSR, and the Taiwan SMART 1 Array.

The presently available data that are considered most applicable to examining coherence of ground motions are the data recorded at the El Centro differential array during the 1979 Imperial Valley, California earthquake (M_L 6.6, M_S 6.9). The array is located 5 km from the closest point of the fault rupture. Five stations in the array, with station-to-station spacings varying from 18 to 85 m over a distance of 213 m, recorded intense ground motions from the earthquake. The acceleration time histories for the East-West components recorded by the array are shown in Figure 3-35. Although common time was lost for the data set, it appears that a reasonable coherence analysis of the data could be made. The data were analyzed by Smith et al. (1982) and King and Tucker (1982). Part of the analysis consisted of a "base-averaging" analysis. In this analysis, a spectral ratio or base averaging factor was computed that is the ratio (frequency by frequency) of the spectrum of the average of the individual time histories to the average of the spectra of the individual time histories. The average time history provides an estimate of the translational motion that a rigid, surface foundation with length equal to the length between array stations utilized, would experience due to the free-field surface motions recorded over that length. Thus, the computed spectral ratio can be viewed as a ratio of the translational motion of a rigid, surface foundation to the free-field ground motion. If the motions recorded at different stations are shifted in time to eliminate phase differences in the motions due to wave propagation, then the spectral ratios are a measure of the effects of incoherence on the foundation motions relative to the free-field motions.

The results of the base-averaging or spectral ratio analysis conducted by Smith et al. (1982) are illustrated in Figure 3-36 for horizontal motions between Stations 1 and 3 spaced 55 m apart and between stations 1 and 5 spaced 214 m apart. The curves labeled "clock time lineup" incorporate the effects due to some phase differences in the motions due to seismic wave propagation time across the array; whereas those labeled "arrival time lineup" represent results after attempting to shift the time histories to eliminate phase differences (i.e.,

incorporating only effects of incoherence). The results illustrated in Figure 3-36 utilized response spectra of the motions. Similar results were obtained by King and Tucker (1982) using smoothed Fourier spectra. The results illustrate that the spectral ratio or base averaging factor decreases with increasing frequency and with increasing array dimension. As shown, the results were not sensitive to whether or not the motions were time shifted for phase differences. For an array or foundation dimension of 55 m, these results indicate reductions in response spectral acceleration of horizontal motion due to incoherence of approximately 20 percent at frequencies between 20 and 30 Hz, 10 to 15 percent at frequencies between 10 and 20 Hz, 5 percent at frequencies between 5 and 10 Hz, and a negligible amount at frequencies below about 5 Hz. The reductions were smaller for vertical motions than for horizontal motions.

The Chusal Differential Array data analyzed by King and Tucker (1982) indicated substantially greater incoherence of ground motions than the data from the El Centro Differential Array. King and Tucker estimated reductions due to base averaging at the Chusal array (using Fourier spectra) in the 12 to 30 Hz frequency range of about 30 to 55 percent for a 55 m rigid foundation, compared to their estimate of 15 to 35 percent for the same foundation dimension at the El Centro Differential Array location. However, because of the effect of the steep bedrock surface underlying the soils at the Chusal site, a significant part of the incoherence likely resulted from differences in site response between individual stations.

Data from the SMART 1 array reported to date (Bolt et al., 1982) do not provide much information on coherence of ground motions over close distances as the data were for a minimum station spacing of 200 m. Correlation coefficients for this distance calculated by Bolt et al. (1982) for the whole wave forms of four pairs of records from one earthquake were approximately 0.6 to 0.7 for horizontal components and 0.5 for vertical components. For this earthquake, based on comparisons of seismograms and wave-number spectral plots, it was concluded that

coherent energy was present throughout the 20 second duration of strong shaking, at least for frequencies in the range 0.5 to 2 Hz for ground motions within a large area having a radius of 2 km. At high frequencies (greater than 6 Hz), the degree of coherence was small over the large area.

In summary, due to lack of coherence of free-field ground motions over horizontal distances, it appears that due to kinematic interaction a large foundation would experience average motions that are reduced from the free-field motions ("base-averaging" effect). The limited available data indicate that the effects for a 50 m wide foundation on a reasonably uniform soil condition might be to reduce the horizontal spectral acceleration by about 20 percent at frequencies between 20 and 30 Hz, by 10 to 15 percent at frequencies between 10 and 20 Hz, by 5 percent at frequencies between 5 and 10 Hz, and by a negligible amount at frequencies below about 5 Hz. The effects increase with frequency and foundation size and appear to be smaller for vertical motions than for horizontal motions. The base averaging effect may also depend on the relative rigidity of the foundation and the underlying soil deposit, increasing as the relative rigidity increases.

Incoherence could also introduce rotational components of motion in the foundation input motions. However, data are not presently available to assess potential rotational motions.

3.3.3 Ground Motion Characterization

With regard to phase differences of ground motions in a horizontal plane associated with non-vertically incident waves, the effects or significance of these differences to structural response clearly depend on the apparent horizontal propagation velocity of the seismic waves. The available data indicate that the apparent horizontal propagation velocities typically exceed 2.5 km/sec. For these high velocities, it appears that non-vertically incident wave effects on translational

response and probably on rocking response are small enough to be neglected in most cases. Torsional effects are also induced by non-vertically incident waves. Again considering the high apparent horizontal propagation velocities of the seismic waves, if the free-field ground motion has a broad-banded response spectrum, such as Reg. Guide 1.60, it appears that torsional effects would be adequately incorporated by providing a 5 percent accidental eccentricity. Thus, for such input free-field motions, it would generally be satisfactory to analyze assuming vertically propagating waves and incorporate non-vertically incident wave effects by using a nominal 5 percent accidental eccentricity provision.

However, more significant torsional effects due to non-vertically incident waves may be associated with some high-frequency, narrow-banded, short-duration input motions (such as the Melendy Ranch record) that excite a strong torsional response but a weak translational response for a structure on a soil site. For such a case, the weak translational response would tend to reduce the significance of the torsional response. It is desirable to conduct additional parametric studies to better define the range of practical conditions for which non-vertically incident wave effects on torsional responses should be considered.

Although this study is indicative that non-vertically incident wave effects generally do not need to be explicitly modeled in ground motion characterizations and soil-structure interaction analyses, the results should not be interpreted as meaning that assessments of the nature of the seismic wave field at a site are not required. It is believed that at least a qualitative assessment of the wave field associated with the design ground motion is desirable in any case. If such an assessment were to indicate, for some reason, a substantially slower apparent horizontal wave propagation velocity than the velocities indicated by current data and studies, or a significant contribution of Rayleigh waves to the ground motions, then the assumption of vertically propagating

waves may not be appropriate. Previous analyses (e.g., Luco and Wong, 1982) have shown the importance to structural response of such wave fields, but the assumptions of low wave velocity and wave fields due entirely to low velocity Rayleigh waves were unrealistic. It should also be noted that if foundation dimensions are substantially larger than those considered in this study, then effects of non-vertically incident waves on response could become more significant.

With regard to variations in the frequency content of ground motion in a horizontal plane due to incoherence, it appears that effects on foundation input motions could be incorporated as a frequency-dependent reduction in translational foundation input motions. The amount of the reduction is not well quantified at present due to limited data. The reductions for relatively uniform soil sites that are inferred from available data are summarized at the end of the preceding section. Incoherence could also introduce rotational components of motion in the foundation input motions. Data are not presently available to assess potential rotational motions.

Table 3-1

CHARACTERISTICS OF SOIL PROFILES I THROUGH IV

Layer No.	Depth Range (ft)	V _s (ft/sec)	V _p (ft/sec)	Q _s	Q _p	Density (pcf)	Poisson's Ratio	Damping Ratio	
								S-wave	P-wave
<u>SOIL PROFILE I</u>									
1	0-∞	3600	6735	25.0	40.	140.	0.30	0.02	0.01
<u>SOIL PROFILE II</u>									
1	0-40	1800	4409	16.7	50.	125.	0.40	0.05	0.01
2	40-250	1800	5970	16.7	50.	125.	0.45	0.03	0.01
3	250-∞	3600	6735	25.0	50.	140.	0.30	0.02	0.01
<u>SOIL PROFILE III</u>									
1	0-40	1000	2449	10.0	50.	125.	0.40	0.05	0.01
2	40-250	1800	5970	16.7	50.	125.	0.45	0.03	0.01
3	250-∞	3600	6735	25.0	50.	140.	0.30	0.02	0.01
<u>SOIL PROFILE IV</u>									
1	0-40	1000	2449	10.0	50.	125.	0.40	0.05	0.01
2	40-250	1000	5099	10.0	50.	125.	0.48	0.05	0.01
3	250-∞	3600	6735	25.0	50.	140.	0.30	0.02	0.01

From Luco et al. (1986) (Vol. 4 of NUREG/CR-3805)

Table 3-2

ACCELEROGRAMS USED IN SOIL-STRUCTURE INTERACTION ANALYSES

Accelerograms/ Earthquake	Magnitudes		Fault Distance (km)	Recorded Peak Acceleration (g)			Time Step (sec)	Cut-off Freq. (Hz)
	M _L	M _S		H.1	H.2	V		
Artificial/ NRC R.G.1.60*	--	--	--	.500	.500	.500	0.01	30
El Centro Array No. 5/ 1979 Imperial Valley	6.6	6.9	1	.374	.527	.441	0.01	30
Cholame-Shandon Sta. No. 2/1966 Parkfield*	5.6	6.4	<1	.489	.489	.206	0.02	25
Melendy Ranch/ 1972 Bear Valley	4.7	4.3	6	.516	.480	.174	0.02	25

* The two horizontal components for the Artificial and Parkfield records were assumed to be equal.

From Luco et al. (1986) (Vol. 4 of NUREG/CR-3805)

Table 3-3

EFFECTS OF SOIL-STRUCTURE INTERACTION ON BASE SHEAR FORCE
IN CONTAINMENT SHELL

Ratio of Peak Base Shear Force in Containment Shell
from Soil-structure Interaction Analysis to Peak Base
Shear Force from Fixed Base Analysis*

<u>Input (Control)</u> <u>Motion</u>	<u>Soil Profile</u> <u>I</u>	<u>Soil Profile</u> <u>II</u>	<u>Soil Profile</u> <u>III</u>	<u>Soil Profile</u> <u>IV</u>
R.G.1.60 Artificial	1.23	1.15	0.93	0.62
Melendy Ranch Comp. N61°E	0.82	0.47	0.30	0.16
Comp. N29°W	0.90	0.40	0.26	0.20
El Centro Sta. No. 5 Comp. N140°E	0.93	0.91	0.81	0.54
Comp. N230°E	0.97	1.64	1.61	1.06
Parkfield Sta. No. 2 Comp. N65°E	0.95	1.28	1.66	1.52

*From soil-structure interaction analyses for a reactor building embedded at a depth of 40 ft (Luco et al., 1986, Vol. 4 of NUREG/CR-3805)

Table 3-4

EFFECTS OF INPUT MOTION ON BASE SHEAR FORCE IN
CONTAINMENT SHELL FROM SOIL-STRUCTURE INTERACTION ANALYSIS

Ratio of Peak Base Shear Force in
Containment Shell for a Given Input Motion
to Peak Base Shear Force for R.G.1.60
Artificial Accelerogram Input Motion*

<u>Soil Profile</u>	<u>Melendy Ranch</u>		<u>E1 Centro Sta. No. 5</u>		<u>Parkfield</u>
	<u>Comp. N61°E</u>	<u>Comp. N29°W</u>	<u>Comp. N140°E</u>	<u>Comp. N230°E</u>	<u>Sta. No. 2 Comp. N65°E</u>
Rigid (Fixed Base)	0.97	0.94	0.85	0.77	0.63
I	0.65	0.69	0.64	0.61	0.48
II	0.40	0.33	0.67	1.11	0.70
III	0.31	0.27	0.74	1.34	1.12
IV	0.25	0.30	0.74	1.31	1.53

*From soil-structure interaction analyses for a reactor building embedded at a depth of 40 ft (Luco et al., 1986, Vol. 4 of NUREG/CR-3805)

Table 3-5

EFFECT OF EXCLUDING KINEMATIC INTERACTION ON BASE SHEAR FORCE
IN CONTAINMENT SHELL

Input (Control) Motion	Ratio of Peak Base Shear Force in Containment Shell without Kinematic Interaction to Peak Base Shear Force with Kinematic Interaction*			
	Soil Profile I	Soil Profile II	Soil Profile III	Soil Profile IV
R.G.1.60 Artificial	1.03	1.07	1.22	1.08
Melendy Ranch Comp. N61°E	1.07	1.11	1.67	1.79
Comp. N29°W	1.07	1.20	1.54	1.23
El Centro Sta. No. 5 Comp. N140°E	1.05	1.12	1.32	1.07
Comp. N230°E	1.04	1.08	1.18	1.10
Parkfield Sta. No. 2 Comp. N65°E	1.02	1.06	1.17	1.09

*From soil-structure interaction analyses for a reactor building embedded at a depth of 40 ft (Luco et al., 1986, Vol. 4 of NUREG/CR-3805)

Table 3-6

CHARACTERISTICS OF SOIL PROFILES V and VI

Layer No.	Depth Range (ft)	V _s (ft/sec)	V _p (ft/sec)	Q _s	Q _p	Density (pcf)	Poisson's Ratio	Damping Ratio	
								S-wave	P-wave
<u>SOIL PROFILE V</u>									
1	0-12.5	1000	2449	22.7	25.	125.	0.40	0.022	0.02
2	12.5-40	1025	2511	16.1	25.	125.	0.40	0.031	0.02
3	40-100	1075	5481	18.5	50.	125.	0.48	0.027	0.01
4	100-175	1150	5864	20.8	50.	125.	0.48	0.024	0.01
5	175-250	1200	6119	19.2	50.	125.	0.48	0.026	0.01
6	250-∞	3600	6735	50.0	50.	140.	0.30	0.010	0.01
<u>SOIL PROFILE VI</u>									
1	0-12.5	900	2205	11.6	25.	125.	0.40	0.043	0.02
2	12.5-40	850	2080	8.2	25.	125.	0.40	0.061	0.02
3	40-100	875	4462	7.9	50.	125.	0.48	0.063	0.01
4	100-175	925	4717	7.9	50.	125.	0.48	0.063	0.01
5	175-250	975	4972	7.2	50.	125.	0.48	0.069	0.01
6	250-∞	3600	6735	25.0	50.	140.	0.30	0.020	0.01

From Luco et al. (1986) (Vol. 4 of NUREG/CR-3805)

Table 3-7

EFFECTS OF RELATIVELY SMALL VARIATIONS IN SOIL PROPERTIES
ON STRUCTURAL RESPONSE FROM SOIL-STRUCTURE INTERACTION ANALYSIS

Ratio of Response of Reactor Building
 for Soil Profile V (Stiffer Profile)
 to Response for Soil Profile VI (Softer Profile)*

Response Parameter	R.G.1.60 Artificial	Melendy Ranch		El Centro Sta. No. 5		Parkfield Sta. No. 2 Comp. N65°E
		Comp. N61°E	Comp. N29°W	Comp. N140°E	Comp. N230°E	
Foundation:						
Peak Horizontal Acceleration	1.01	1.14	1.16	1.16	1.01	1.01
Peak Rotational Acceleration	1.20	1.16	1.14	1.20	1.08	1.12
Containment Shell:						
Peak Base Force	1.28	1.67	1.33	1.30	1.54	1.27
Peak Base Moment	1.32	1.29	1.27	1.28	1.64	1.28
Peak Horizontal Acceleration Near Top	1.32	1.27	1.31	1.28	1.62	1.27
Internal Structure:						
Peak Base Force	1.28	1.28	1.17	1.40	1.27	1.31
Peak Base Moment	1.45	1.24	1.19	1.53	1.40	1.32
Peak Horizontal Acceleration Near Top	1.43	1.24	1.19	1.53	1.39	1.32

*From soil-structure interaction analyses for a reactor building embedded at a depth of 40 ft (Luco et al., 1986, Vol. 4 of NUREG/CR-3805)

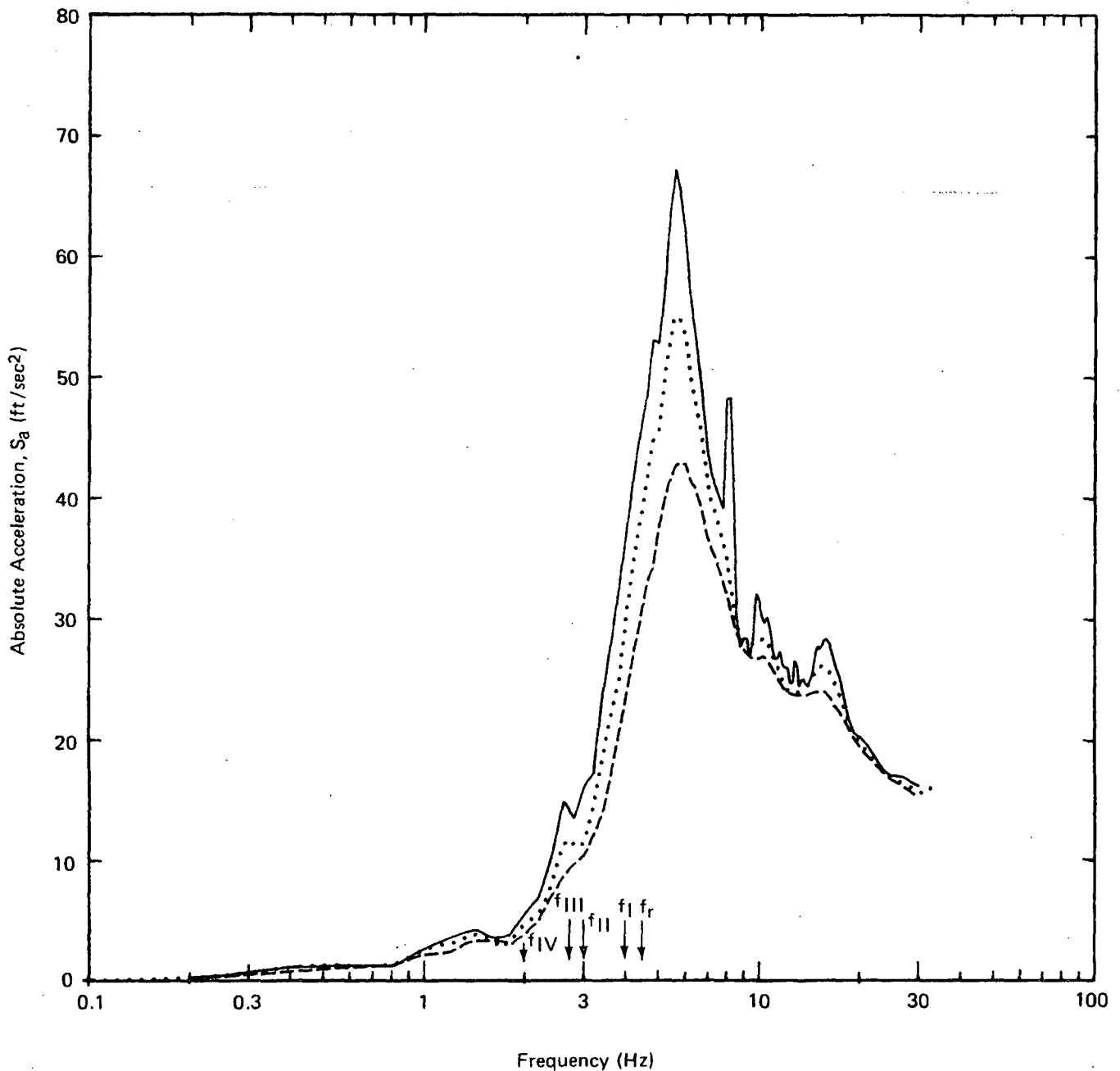
Table 3-8

SUMMARY OF APPARENT HORIZONTAL PROPAGATION VELOCITIES

(Adapted from O'Rourke et al., 1982)

Event	Site conditions	Focal depth (km)	Epicentral distance (km)	Apparent Horizontal Velocity C (km/s)	Method for calculating C
Japan 1/23/68	60 m soft alluvium	80	54	2.9	Cross-correlation array with common time
Japan 7/1/68	60 m soft alluvium	50	30	2.6	Cross-correlation array with common time
Japan 5/9/74	70 m of silty clay, sand and silty sand	10	140	5.3	Cross-correlation array with common time
Japan 7/8/74	70 m of silty clay, sand and silty sand	40	161	2.6	Cross-correlation array with common time
Japan 8/4/74	70 m of silty clay, sand and silty sand	50	54	4.4	Cross-correlation array with common time
Imperial Valley 10/15/79	> 300 m Alluvium	8	6 to 93	3.7	Epicentral distance vs. initial S-wave travel time
SMART I 1/29/81	Alluvium	11	30	3.0	Frequency-wave-number analysis

From Chang et al. (1986) (Vol. 3 of NUREG/CR-3805)

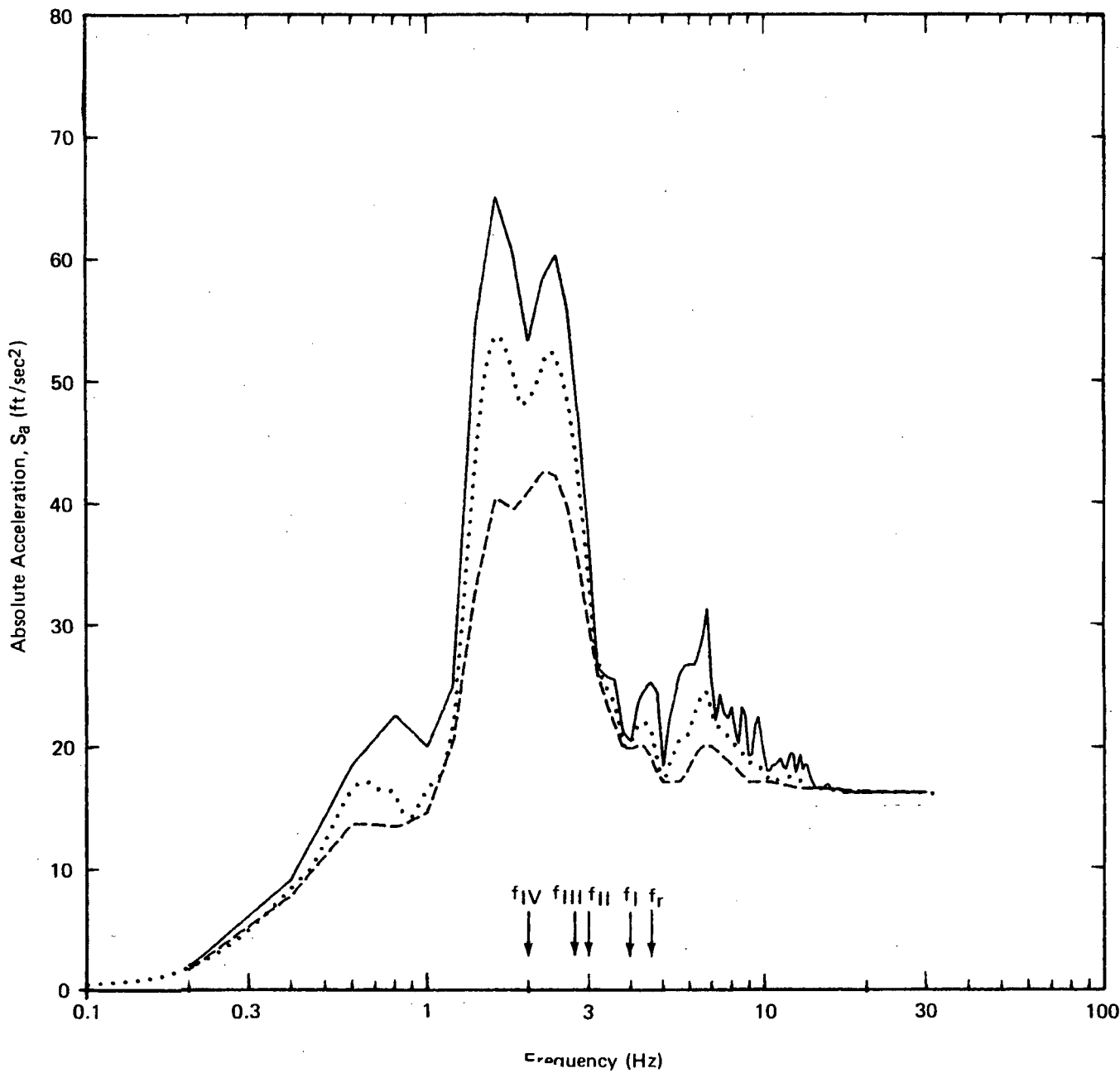


EXPLANATION

- Damping Ratio = 0.02
- Damping Ratio = 0.05
- Damping Ratio = 0.10

f = Fundamental characteristic frequencies of soil-structure systems for soil profiles I-IV (f_I , f_{II} , f_{III} , and f_{IV}) and rigid rock (f_r)

Figure 3-1. Frequency Content of Melendy Ranch (N29W) Input Motion in Relation to Characteristic Frequency of Soil-Structure Systems (Reactor Building, 40 ft Embedment, Vertically Incident Waves)

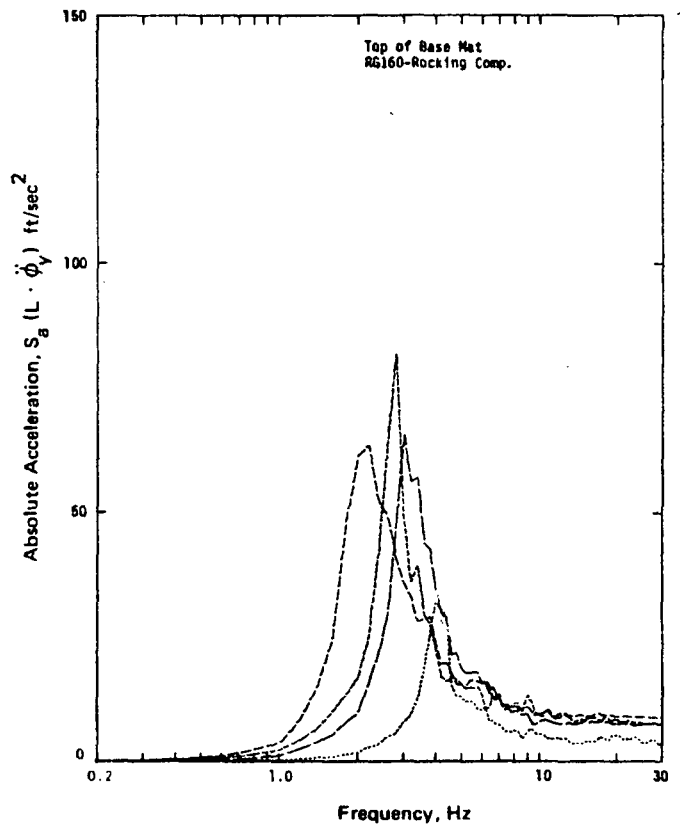
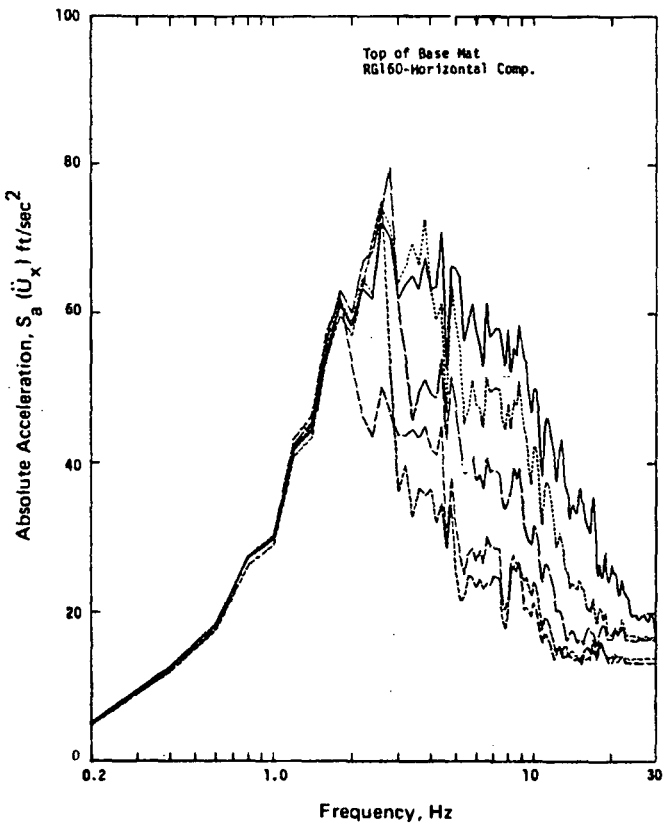
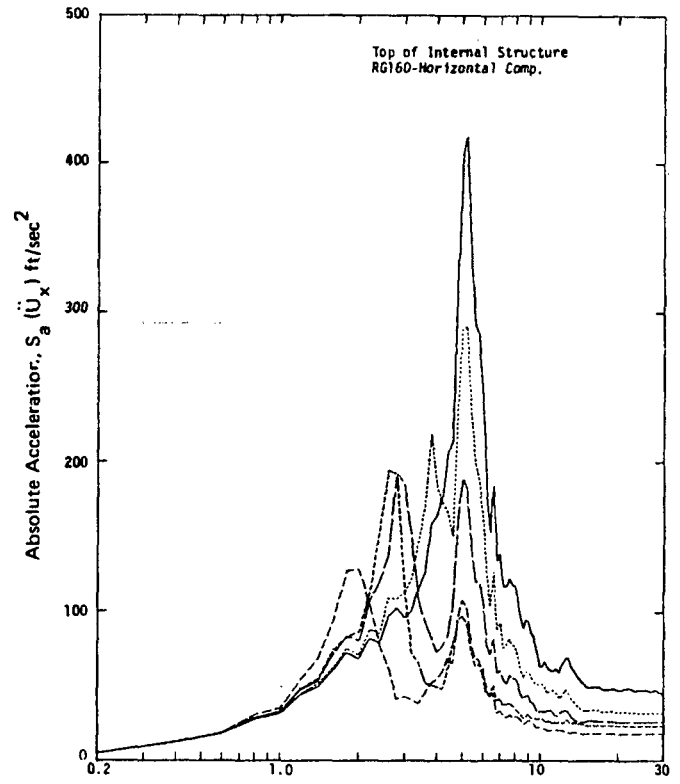
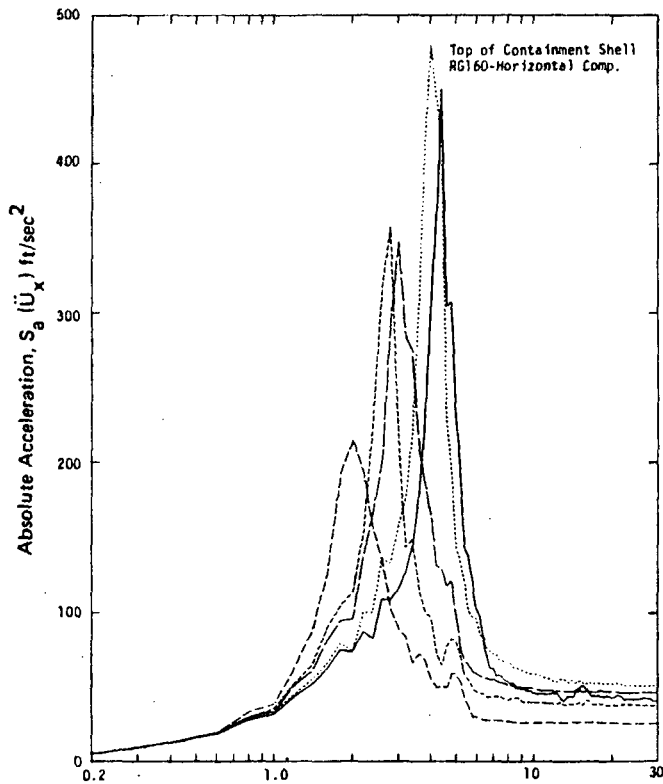


EXPLANATION

- Damping Ratio = 0.02
- Damping Ratio = 0.05
- Damping Ratio = 0.10

f = Fundamental characteristic frequencies of soil-structure system for soil profiles I-IV (f_I , f_{II} , f_{III} , and f_{IV}) and rigid rock (f_r)

Figure 3-2. Frequency Content of Parkfield Input Motion in Relation to Characteristic Frequencies of Soil-Structure Systems (Reactor Building, 40 ft Embedment, Vertically Incident Waves)

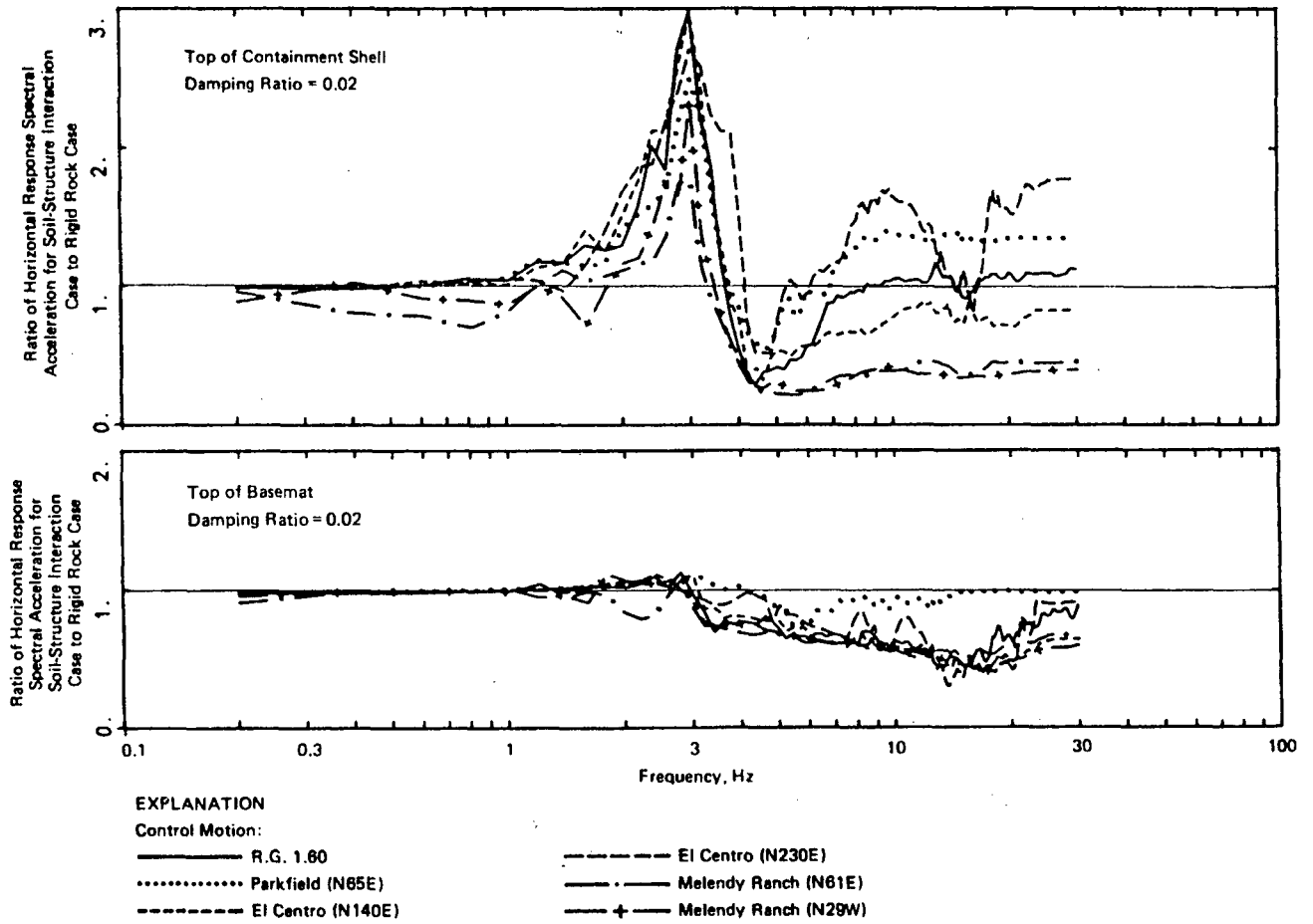


EXPLANATION

- | | |
|------------------|----------------------|
| ————— Rigid Soil | ----- Profile III |
| Profile I | ----- Profile IV |
| ----- Profile II | Damping Ratio = 0.02 |

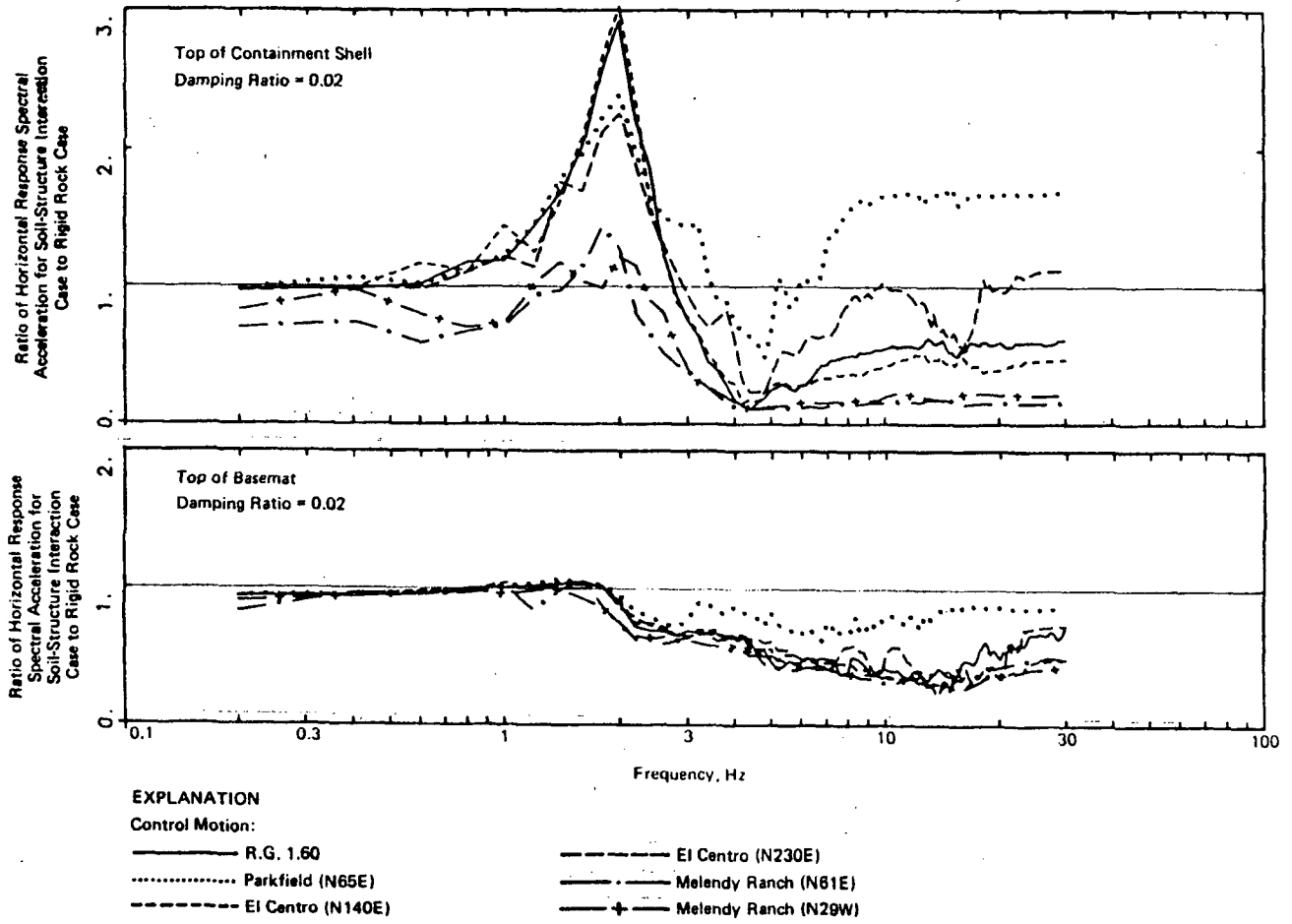
From Luco et al. (1986)
(Vol. 4 of NUREG/CR-3805)

Figure 3-3. Comparison of Floor Response Spectra of Reactor Building for Rigid Soil, Soil Profiles I, II, III and IV Using Artificial R.G. 1.60 Motion as Control Motion (Vertical Incidence, 40 ft Embedment)



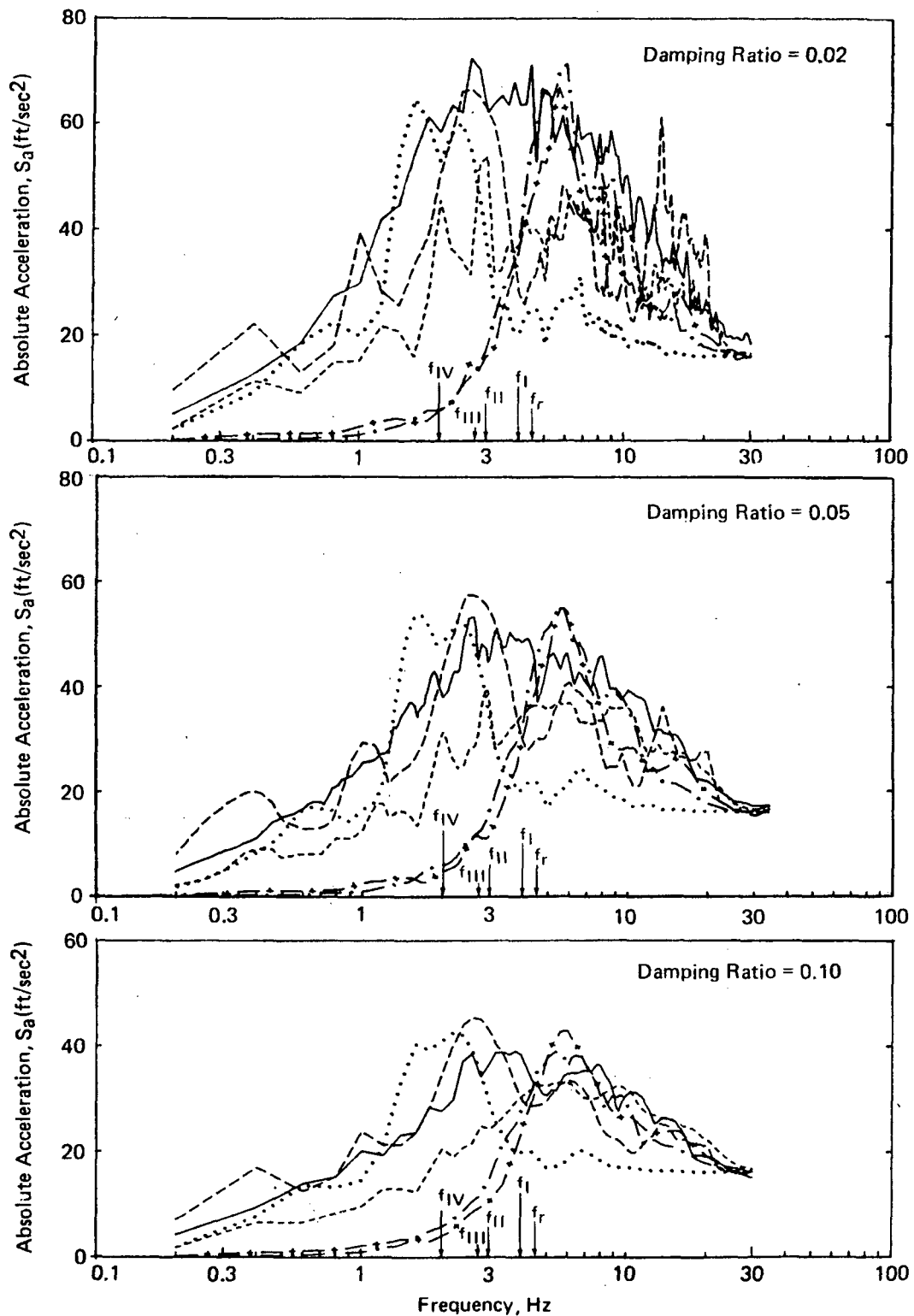
Based on Luco et al. (1986)
(Vol. 4 of NUREG/CR-3805)

Figure 3-4. Effects of Soil-Structure Interaction on Floor Response Spectra (Reactor Building, 40 ft Embedment, Soil Profile II, Vertically Incident Waves)



Based on Luco et al. (1986)
(Vol. 4 of NUREG/CR-3805)

Figure 3-5. Effects of Soil-Structure Interaction on Floor Response Spectra (Reactor Building, 40 ft Embedment, Soil Profile IV, Vertically Incident Waves)



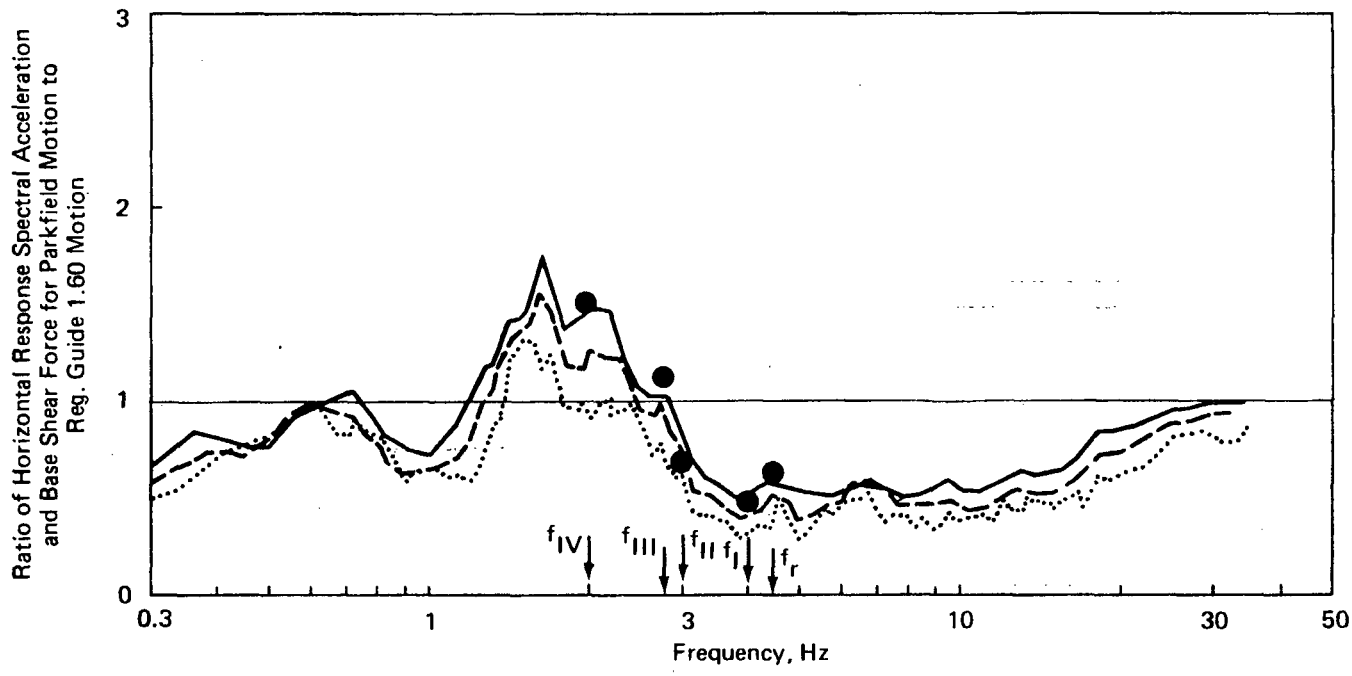
From Luco et al. (1986)
(Vol. 4 of NUREG/CR-3805)

EXPLANATION

- | | | | |
|-------|------------------------|-----------|----------------------|
| ————— | R.G. 1.60 (Horizontal) | ----- | El Centro (N230E) |
| | Parkfield (Horizontal) | ----- | Melendy Ranch (N61E) |
| ----- | El Centro (N140E) | + + + + + | Melendy Ranch (N29W) |

f = Fundamental Characteristic Frequencies of Soil-Structure Systems for Soil Profiles I-IV ($f_I, f_{II}, f_{III}, f_{IV}$) and Rigid Rock (f_R)

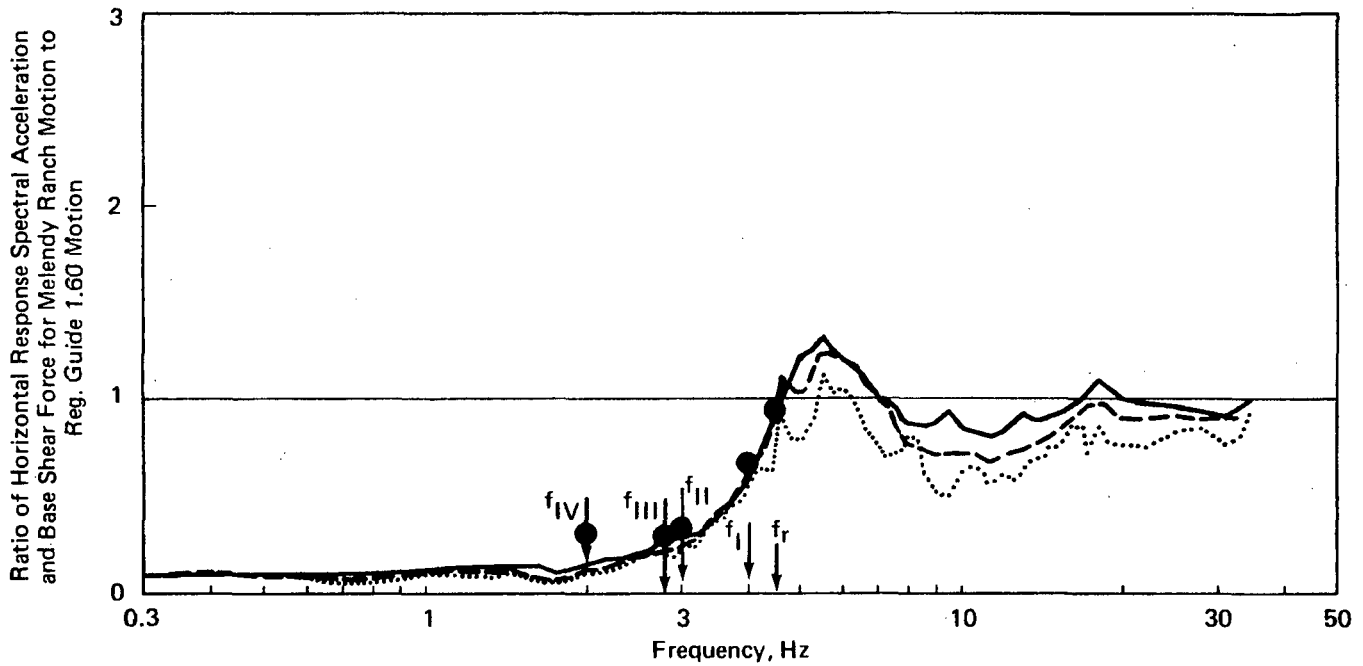
Figure 3-6. Comparison of Response Spectra of Different Control Motions Used in the Soil-structure Interaction Analyses



Based on Luco et al. (1986)
(Vol. 4 of NUREG/CR-3805)

- EXPLANATION**
- Damping Ratio = 0.02
 - Damping Ratio = 0.05
 - Damping Ratio = 0.10
- } Ratios of response spectra
- f_r = Fundamental natural frequency of fixed base model (4.5 Hz)
- $f_I, f_{II}, f_{III}, f_{IV}$ = Fundamental characteristic frequencies of soil-structure systems for soil profiles I, II, III, and IV (4, 3, 2.8, and 2 Hz)
- Ratios of base shear forces (from Table 3-4)

Figure 3-7. Relative Frequency Content of Parkfield and Reg. Guide 1.60 Input Motions in Relation to Characteristic Frequencies of Soil-Structure Systems and Base Shear Response (Reactor Building, 40 ft Embedment, Vertically Incident Waves)



Based on Luco et al. (1986)
(Vol. 4 of NUREG/CR-3805)

EXPLANATION

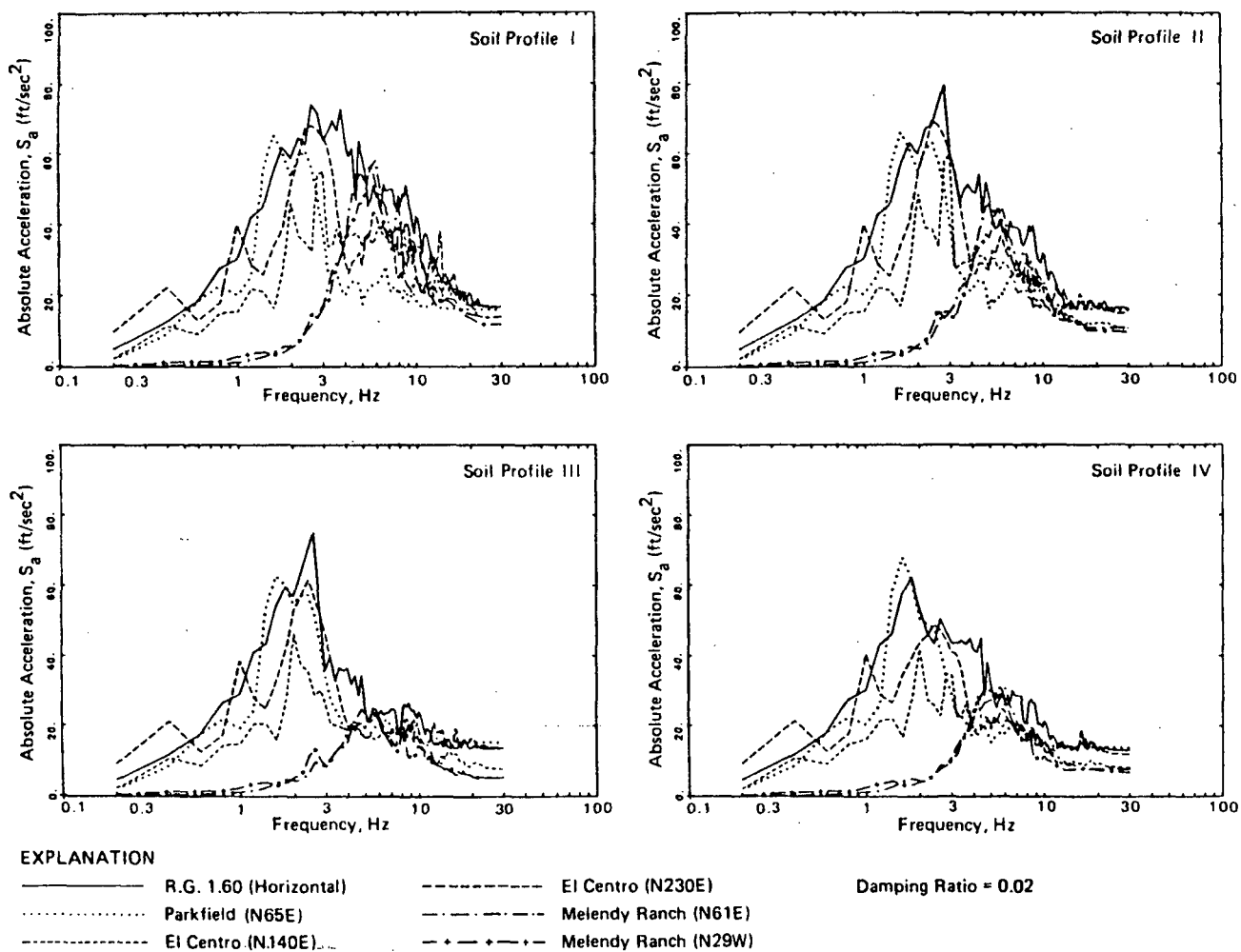
- Damping Ratio = 0.02
 - - - - - Damping Ratio = 0.05
 - Damping Ratio = 0.10
- } Ratios of response spectra

f_r = Fundamental natural frequency of fixed base model (4.5 Hz)

$f_I, f_{II}, f_{III}, f_{IV}$ = Fundamental characteristic frequencies of soil-structure systems for soil profiles I, II, III, and IV (4, 3, 2.8, and 2 Hz)

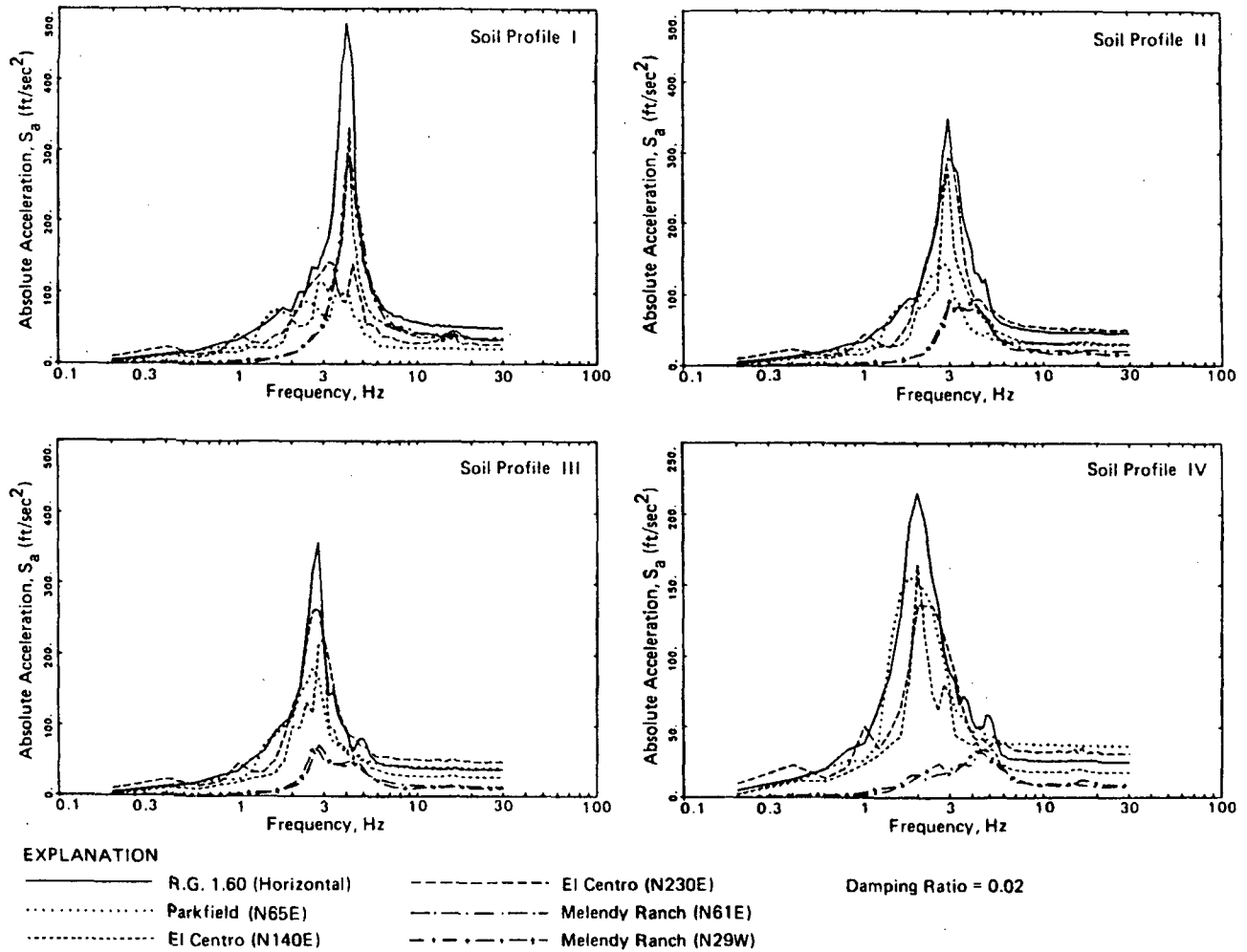
● Ratios of base shear forces (from Table 3-4)

Figure 3-8. Relative Frequency Content of Melendy Ranch (N29W) and Reg. Guide 1.60 Input Motions in Relation to Characteristic Frequencies of Soil-Structure Systems and Base Shear Response (Reactor Building, 40 ft Embedment, Vertically Incident Waves)



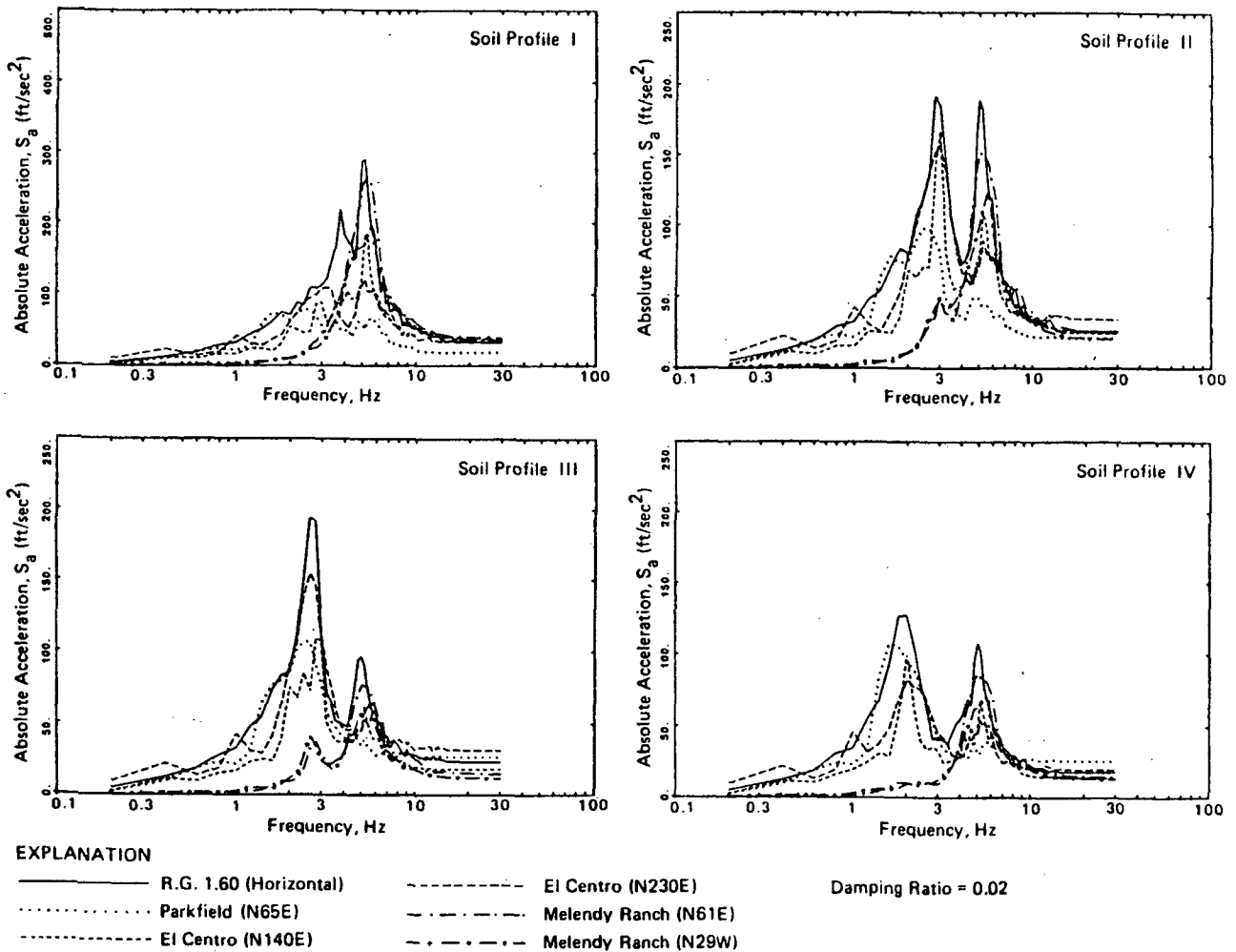
From Luco et al. (1986)
(Vol. 4 of NUREG/CR-3805)

Figure 3-9. Comparison of Floor Response Spectra at Top of Basemat of Reactor Building for Different Control Motions, (Vertical Incidence, 40 ft Embedment)



From Luco et al. (1986)
 (Vol. 4 of NUREG/CR-3805)

Figure 3-10. Comparison of Floor Response Spectra at Top of Containment Shell of Reactor Building for Different Control Motions, (Vertical Incidence, 40 ft Embedment)



From Luco et al. (1986)
 (Vol. 4 of NUREG/CR-3805)

Figure 3-11. Comparison of Floor Response Spectra at Top of Internal Structure of Reactor Building for Different Control Motions, (Vertical Incidence, 40 ft Embedment)

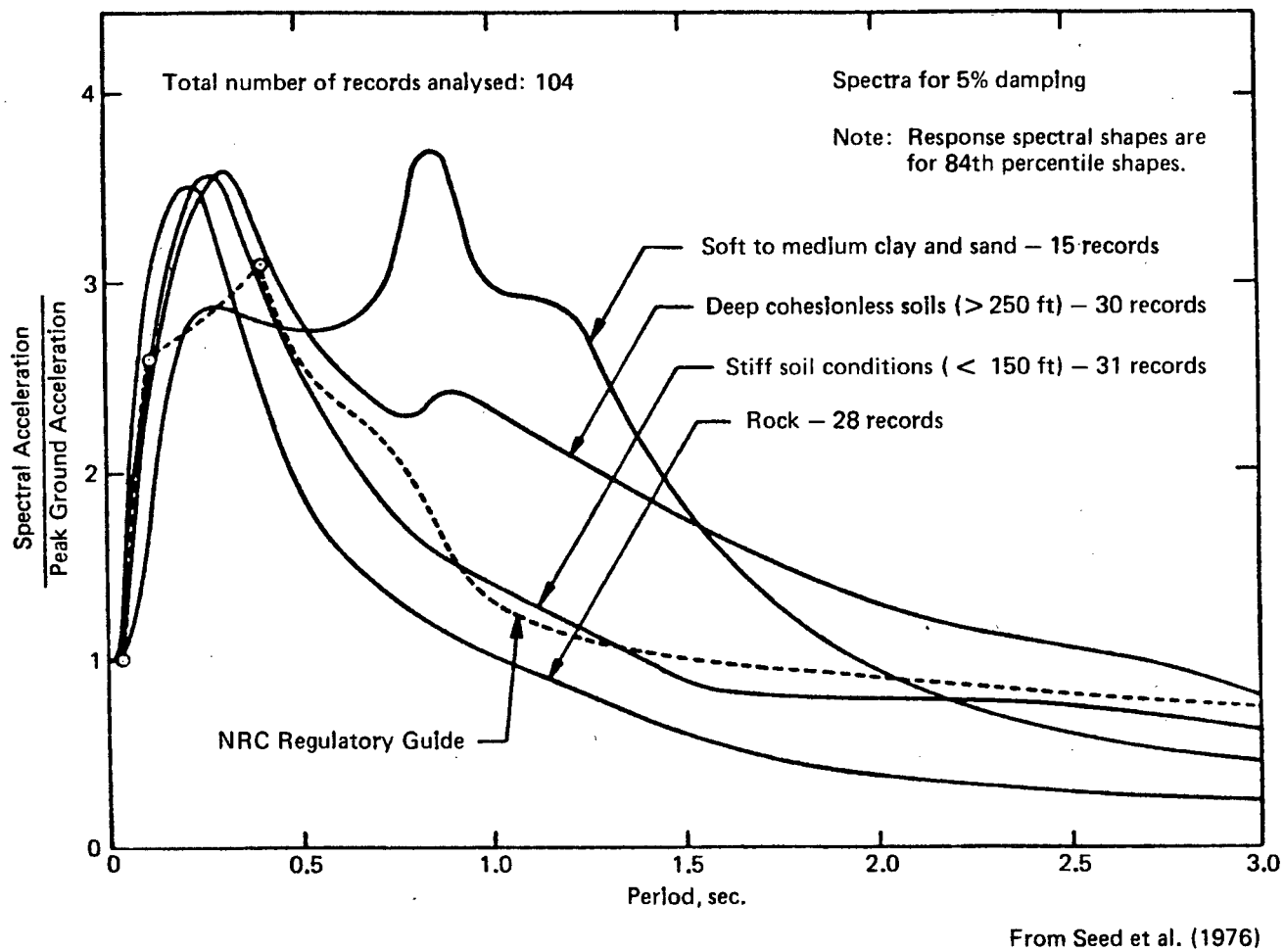
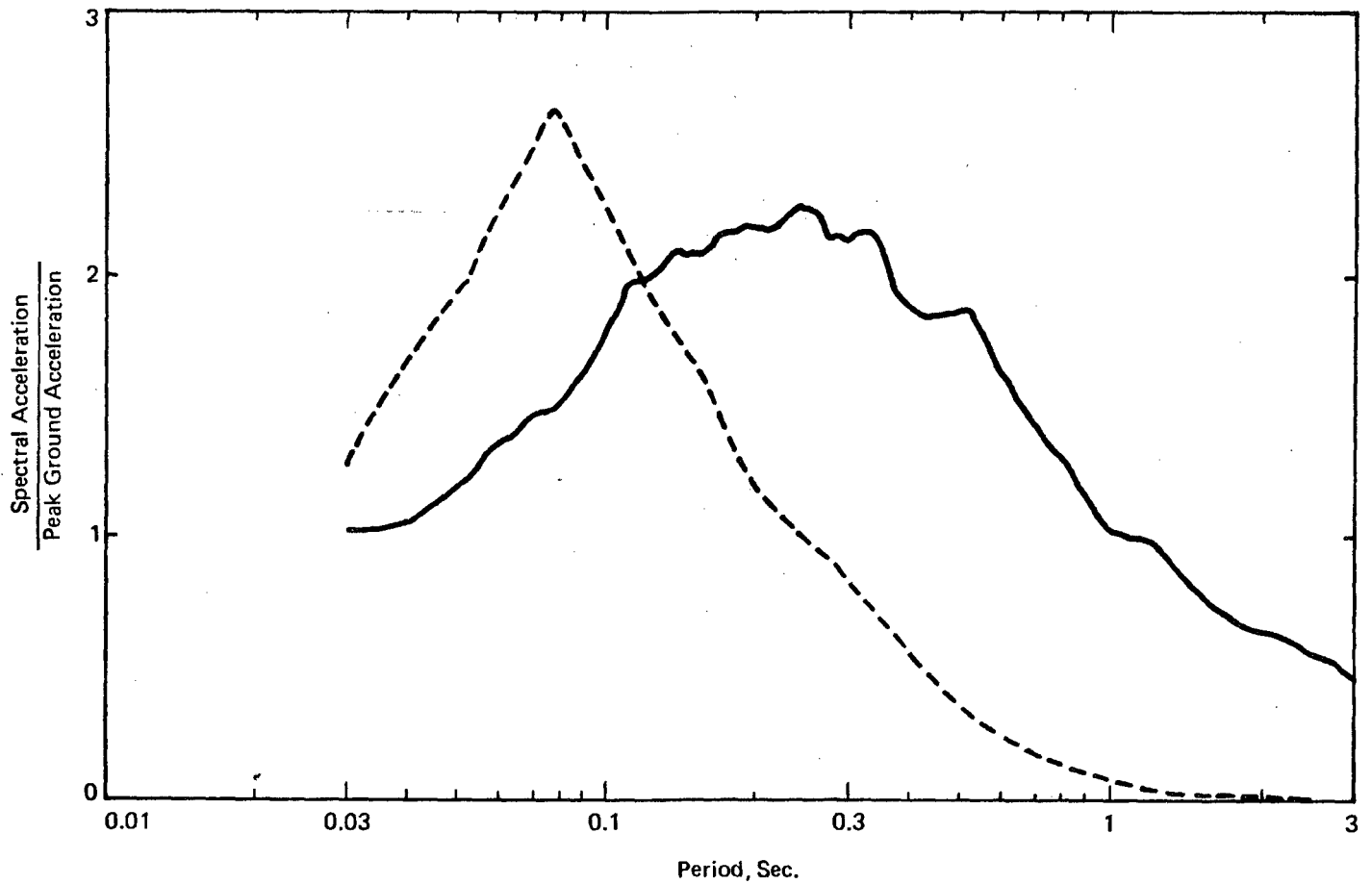


Figure 3-12. Illustration of Effect of Local Soil Conditions on Response Spectral Shapes from Statistical Analysis

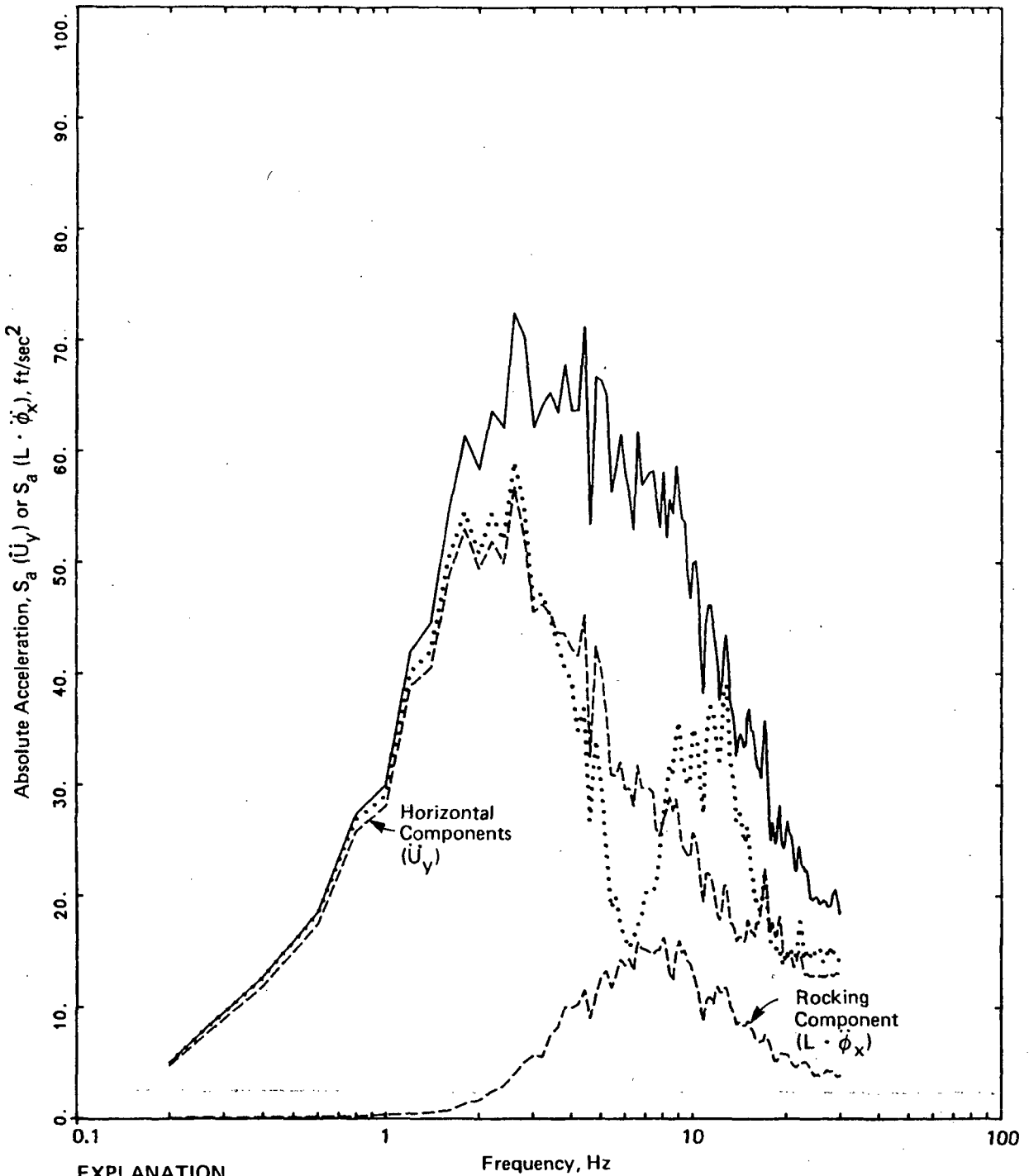


EXPLANATION

- 1979 Imperial Valley California Earthquake (M_L 6.6),
30 accelerograms
 - - - 1975 Oroville, California Earthquake Aftershocks, and
1980 Mammoth Lakes, California Earthquake Sequence
(Records from Earthquakes with M_L 4.0 ± 0.2), 74 accelerograms
- Damping Ratio = 0.05

Note: Response spectral shapes are median shapes

Figure 3-13. Illustration of Effect of Earthquake Magnitude on Response Spectral Shape from Statistical Analysis



EXPLANATION

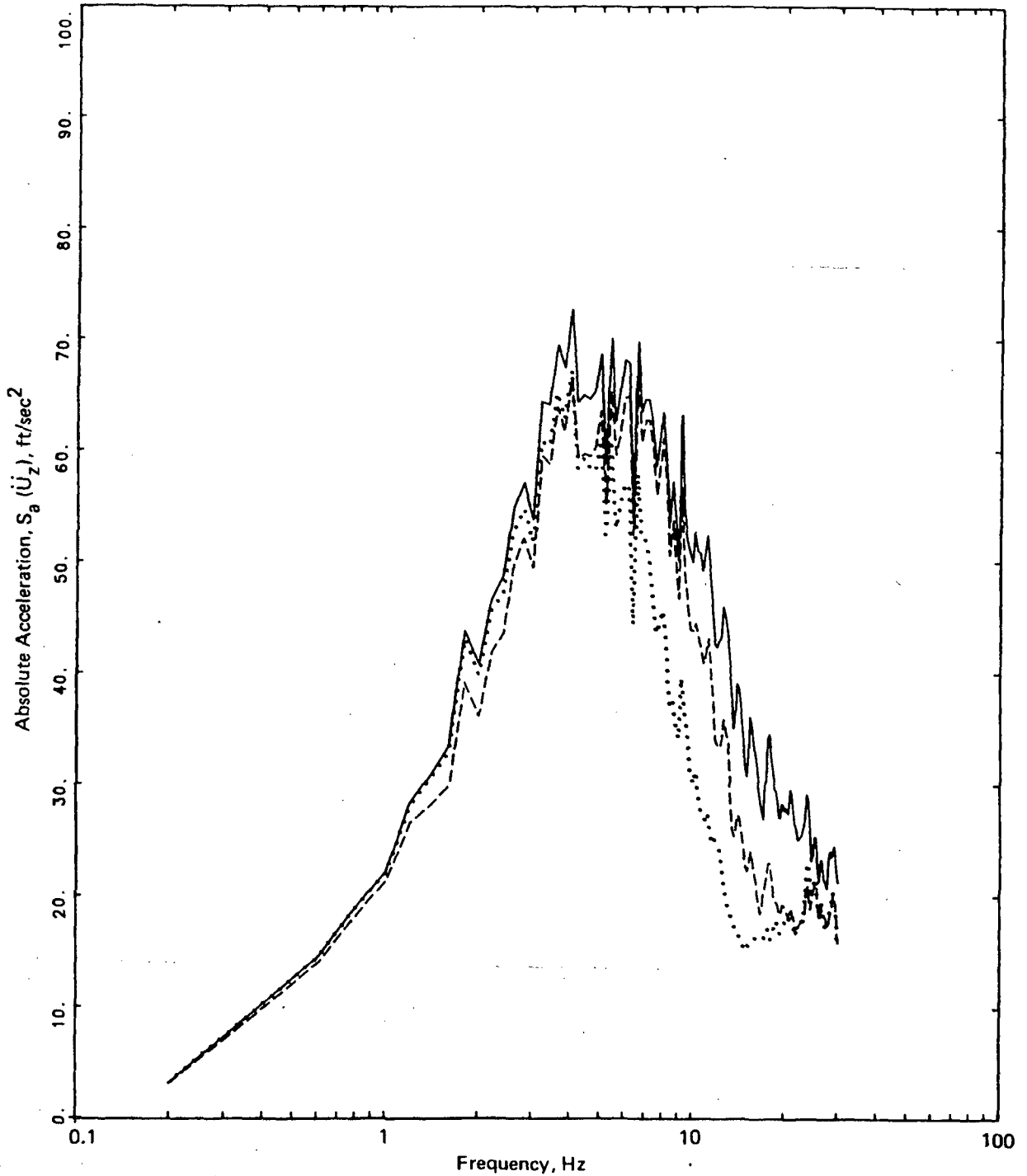
- R.G. 1.60 horizontal control motion
- Horizontal free-field foundation-level motion
- - - - Horizontal and rocking foundation input motions

Based on Luco et al. (1986)
(Vol. 4 of NUREG/CR-3805)

Damping Ratio = 0.02

L = 63.6 ft

Figure 3-14. Comparison of Response Spectra of Reg. Guide 1.60 Horizontal Control Motion, Horizontal Free-Field Foundation-Level Motion, and Foundation Input Motions, (Reactor Building, 40 ft Embedment, Soil Profile IV, Vertically Incident Waves)



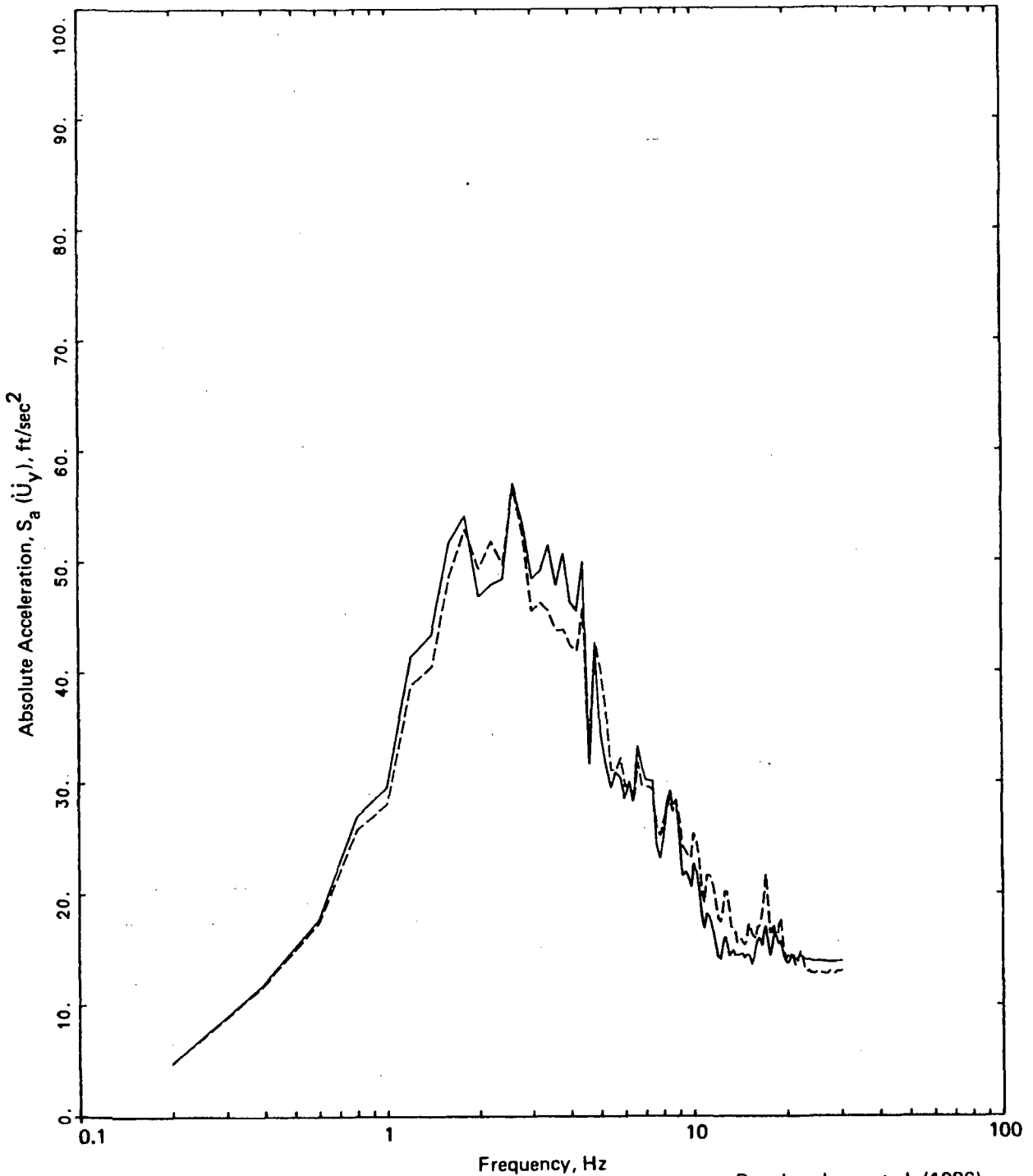
EXPLANATION

- R.G. 1.60 vertical control motion
- Vertical free-field foundation-level motion
- Vertical foundation input motion

Damping Ratio = 0.02

Based on Luco et al. (1986)
(Vol. 4 of NUREG/CR-3805)

Figure 3-15. Comparison of Response Spectra of Reg. Guide 1.60 Vertical Control Motion, Vertical Free-Field Foundation-Level Motion, and Vertical Foundation Input Motion, (Reactor Building, 40 ft Embedment, Soil Profile IV, Vertically Incident Waves)



Based on Luco et al. (1986)
(Vol. 4 of NUREG/CR-3805)

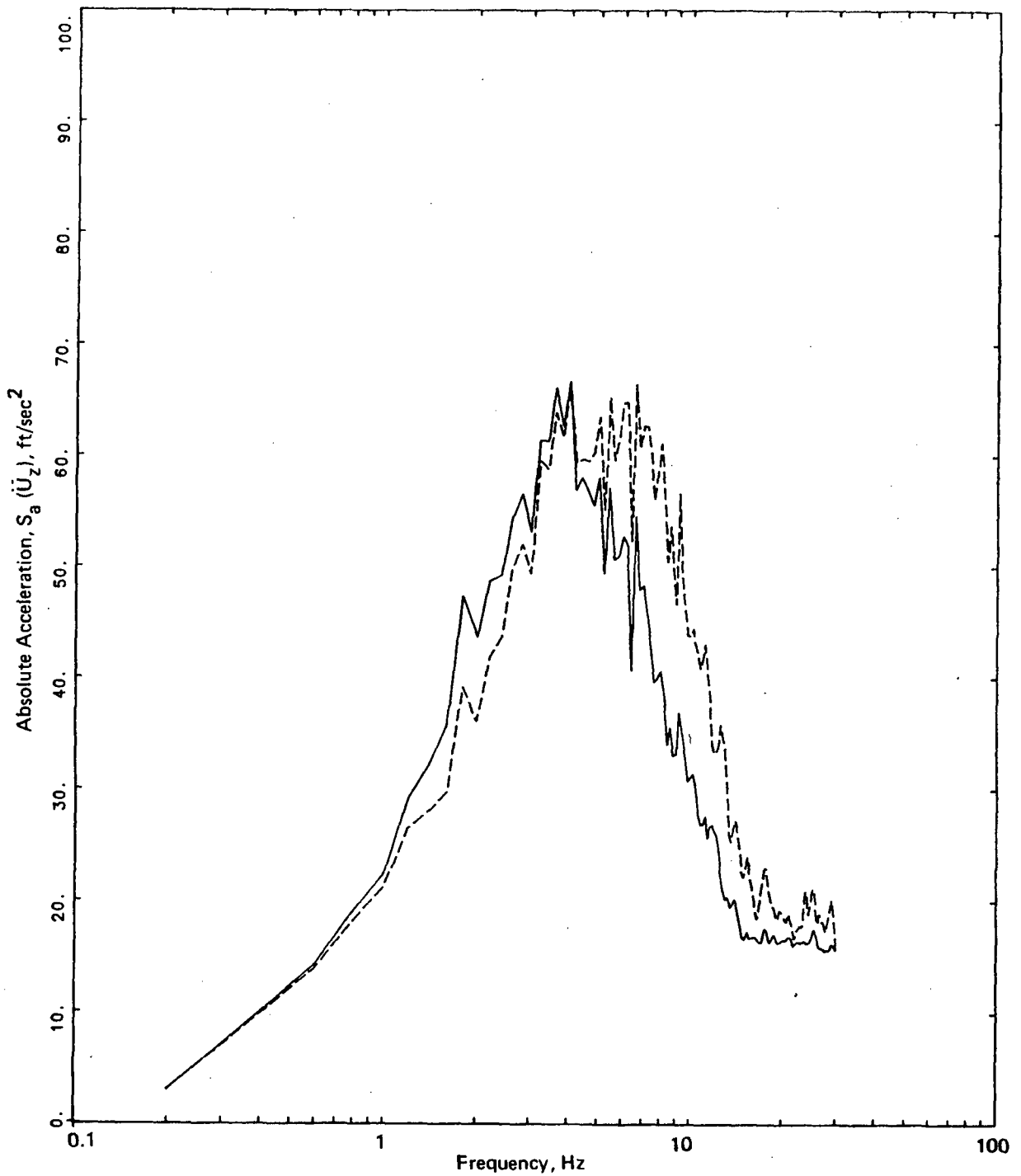
EXPLANATION

———— Horizontal foundation motion from complete SSI analysis

- - - - - Horizontal foundation input motion

Damping Ratio = 0.02

Figure 3-16. Comparison of Response Spectra of Horizontal Foundation Input Motion with Horizontal Foundation Motion from Complete Soil-Structure Interaction Analysis (Reactor Building, 40 ft Embedment, Soil Profile IV, Reg. Guide 1.60 Control Motion, Vertically Incident Waves)



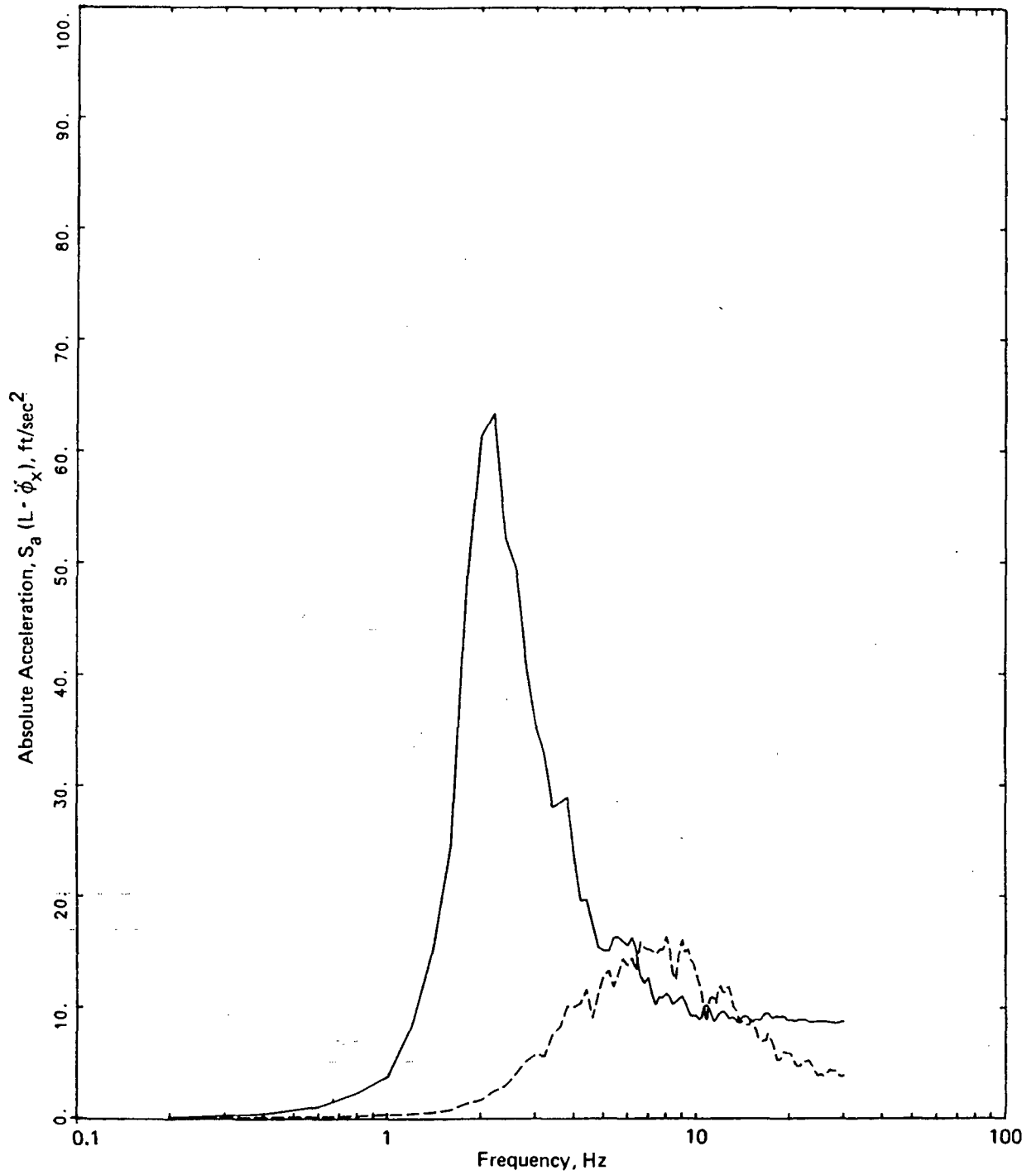
EXPLANATION

- Vertical foundation motion from complete SSI analysis
- - - Vertical foundation input motion

Damping Ratio = 0.02

Based on Luco et al. (1986)
(Vol. 4 of NUREG/CR-3805)

Figure 3-17. Comparison of Response Spectra of Vertical Foundation Input Motion with Vertical Foundation Motion from Complete Soil-Structure Interaction Analysis (Reactor Building, 40 ft Embedment, Soil Profile IV, Reg. Guide 1.60 Control Motion, Vertically Incident Waves)



Based on Luco et al. (1986)
(Vol. 4 of NUREG/CR-3805)

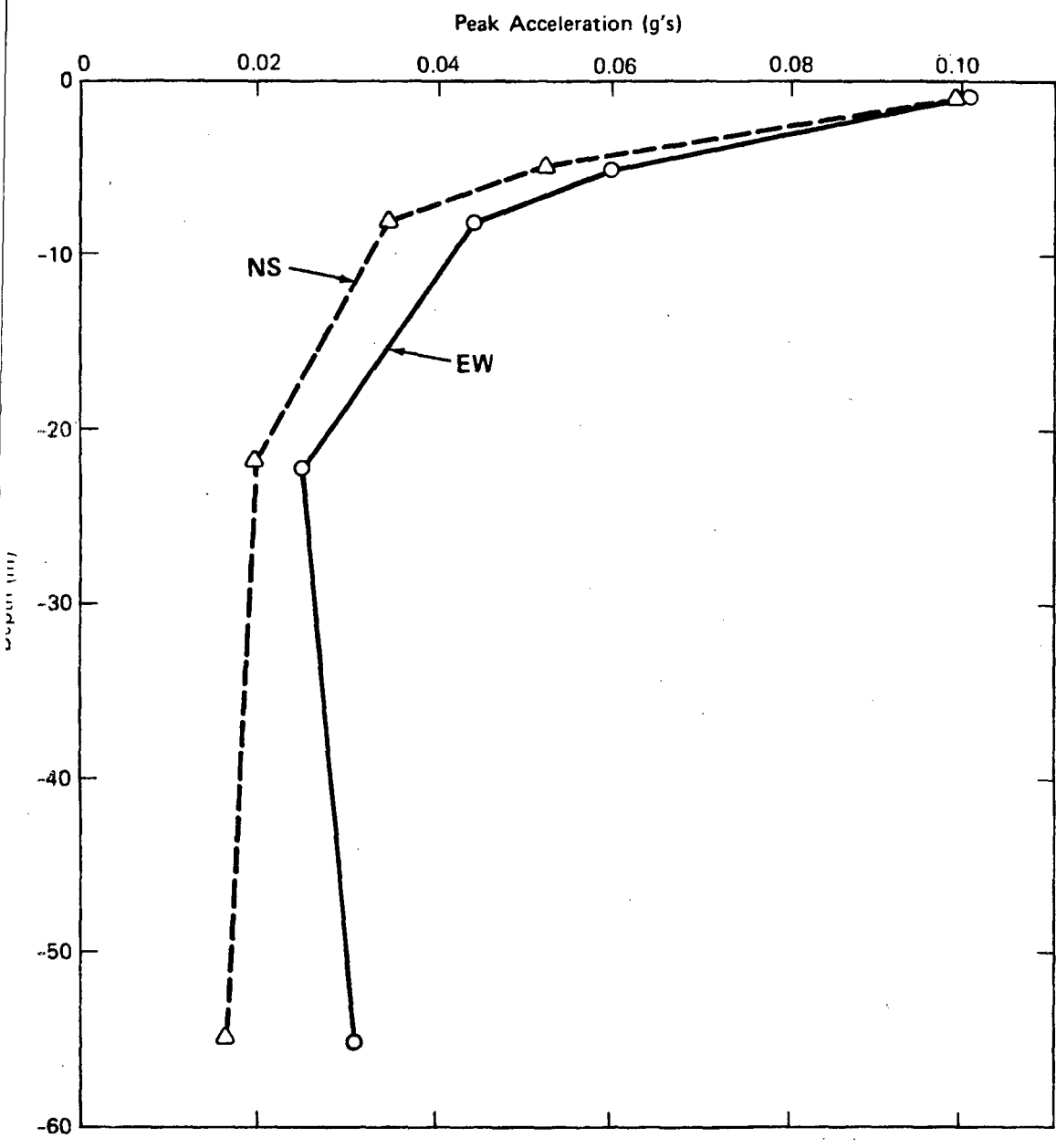
EXPLANATION

- Rocking foundation motion from complete SSI analysis
- Rocking foundation input motion

Damping Ratio = 0.02

L = 63.6 ft

Figure 3-18. Comparison of Response Spectra of Rocking Foundation Input Motion with Rocking Foundation Motion from Complete Soil-Structure Interaction Analysis (Reactor Building, 40 ft Embedment, Soil Profile IV, Reg. Guide 1.60 Control Motion, Vertically Incident Waves)



From Chang et al. (1986)
 (Vol. 3 of NUREG/CR-3805)

Figure 3-19. Variations of Recorded Peak Acceleration with Depth — Narimasu Downhole Array Data

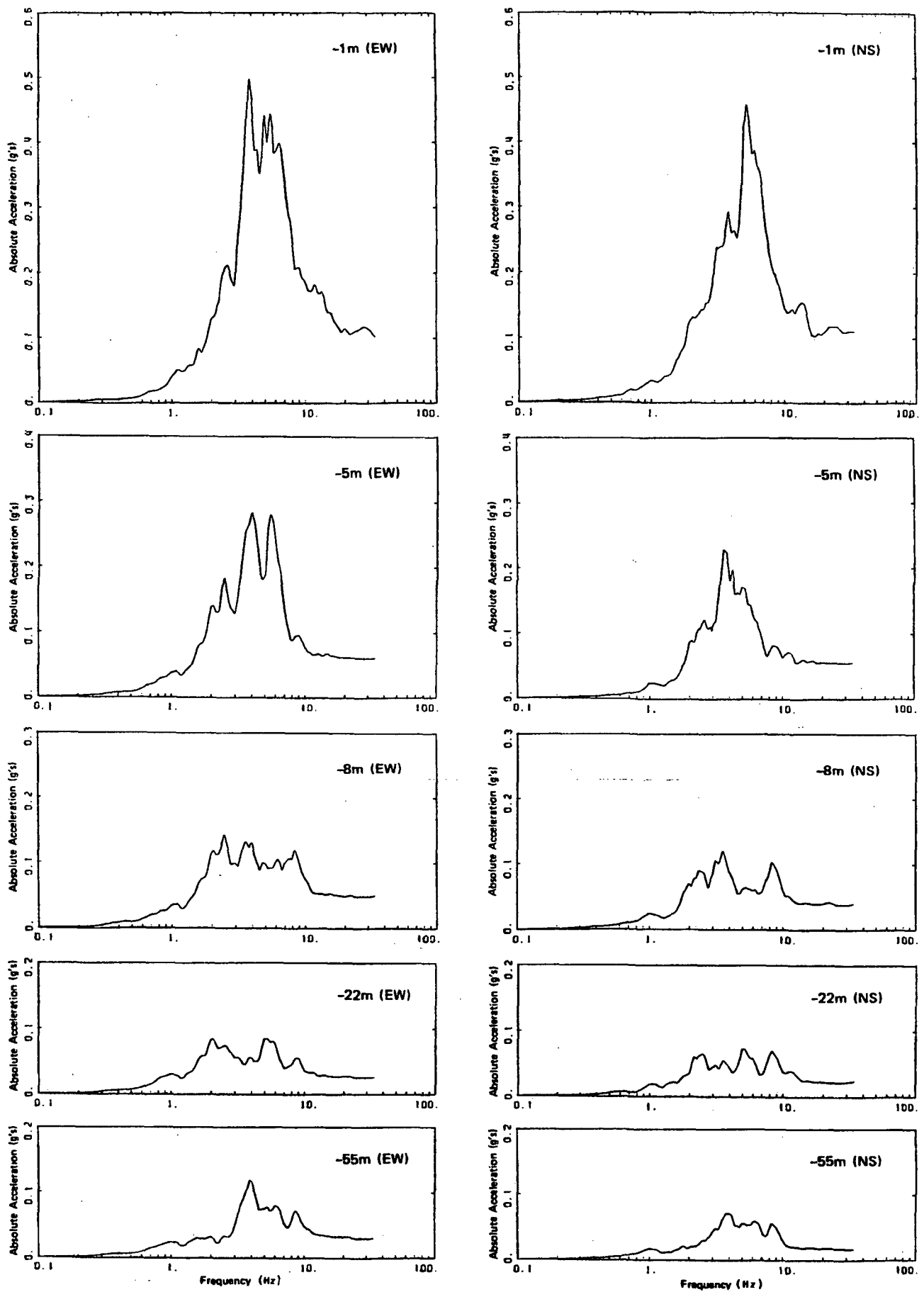
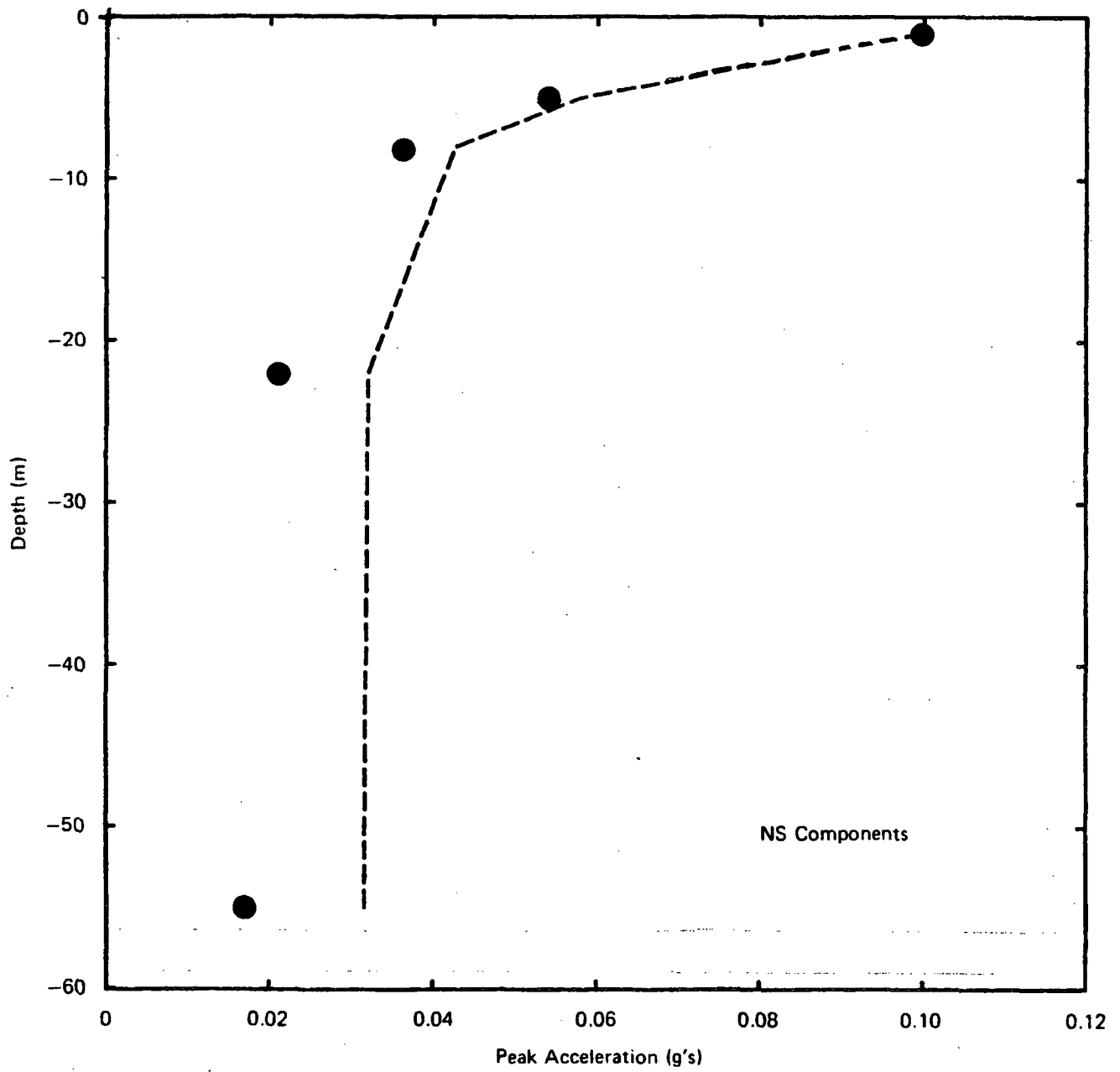


Figure 3-20. Response Spectra of Recorded Motions – Narimasu Downhole Array Data (Damping=0.05)

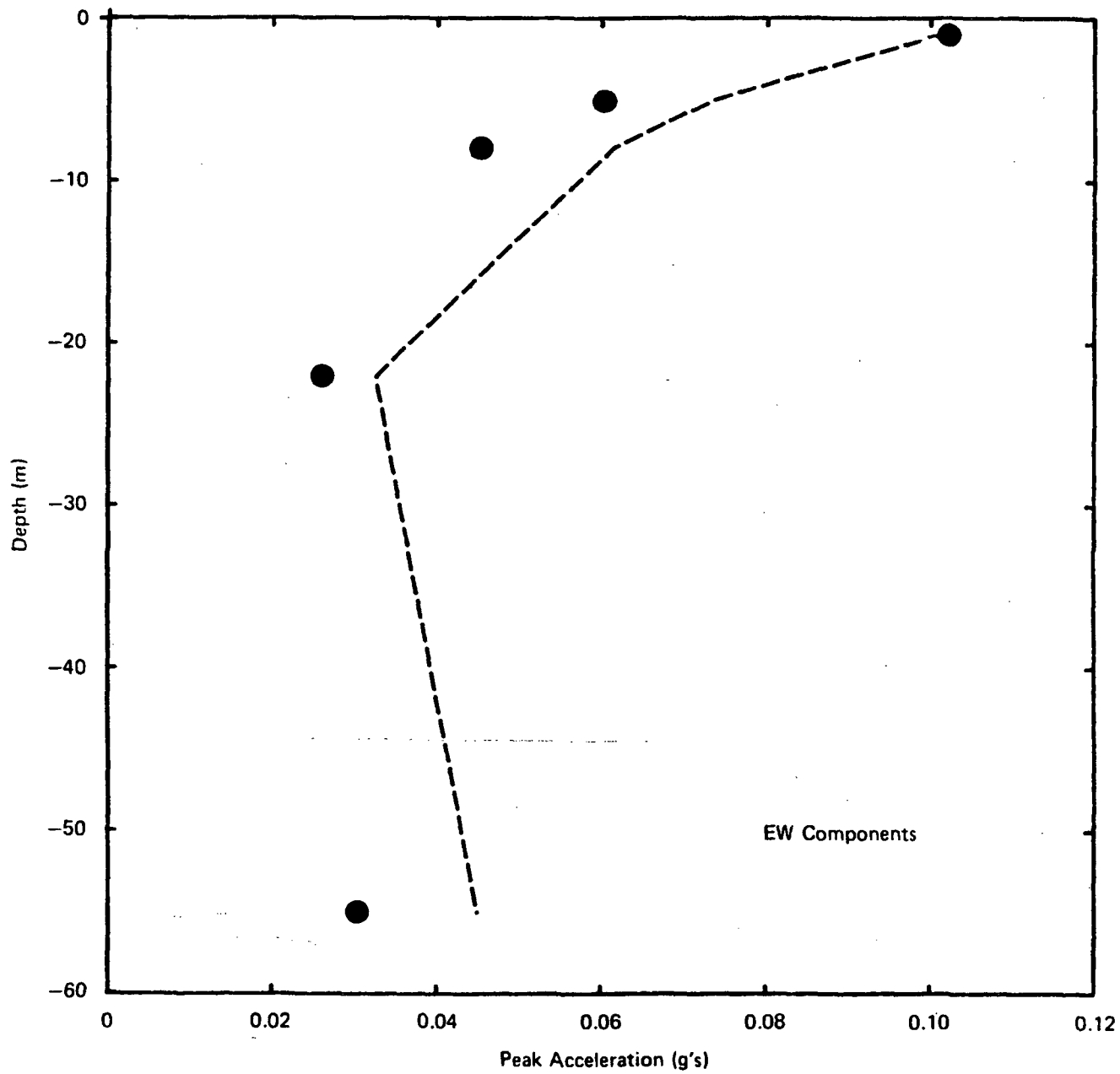
From Chang et al. (1986)
 (Vol. 3 of NUREG/CR-3805)



EXPLANATION
 ● Recorded
 - - - Computed

From Chang et al. (1986)
 (Vol. 3 of NUREG/CR-3805)

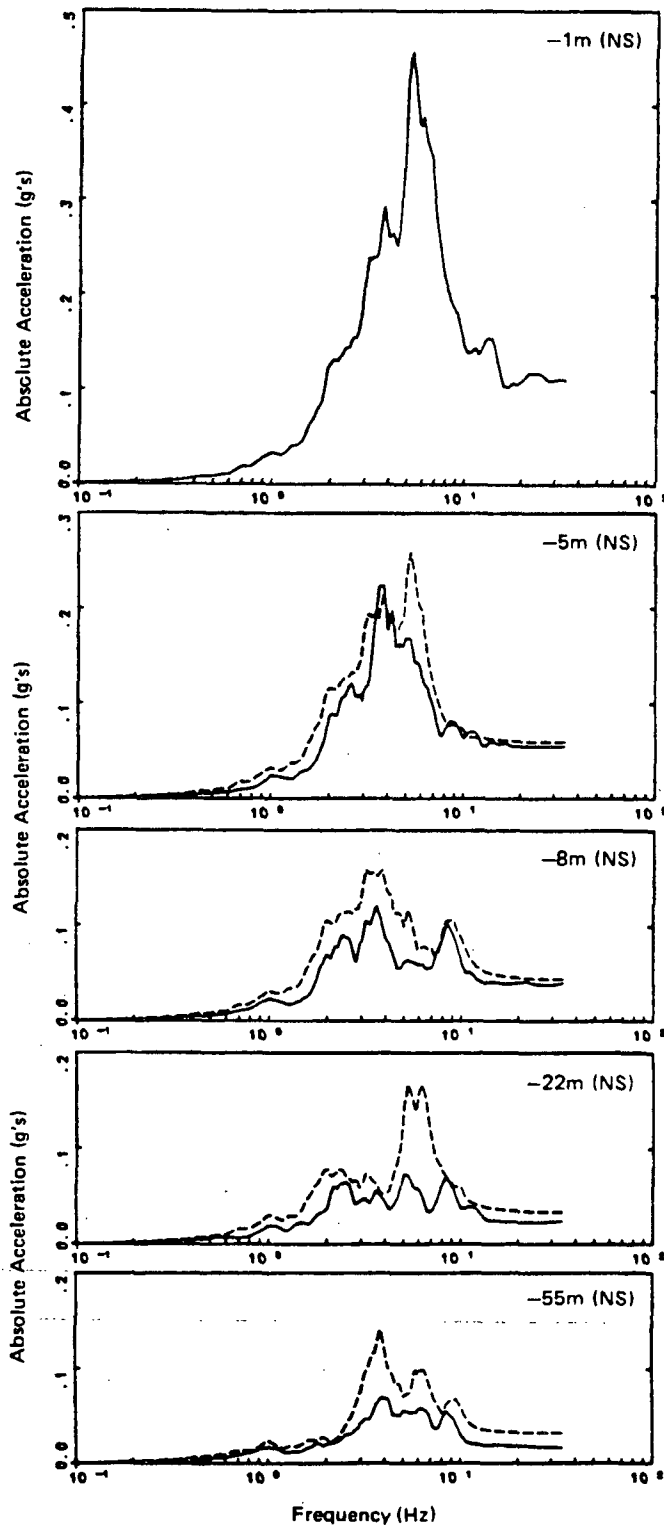
Figure 3-21a. Comparison of Calculated and Recorded Variations of Peak Acceleration with Depth, Deconvolution Analysis, NS Components, Narimasu Site



EXPLANATION
 ● Recorded
 - - - Computed

From Chang et al. (1986)
 (Vol. 3 of NUREG/CR-3805)

Figure 3-21b. Comparison of Calculated and Recorded Variations of Peak Acceleration with Depth, Deconvolution Analysis, EW Components, Narimasu Site

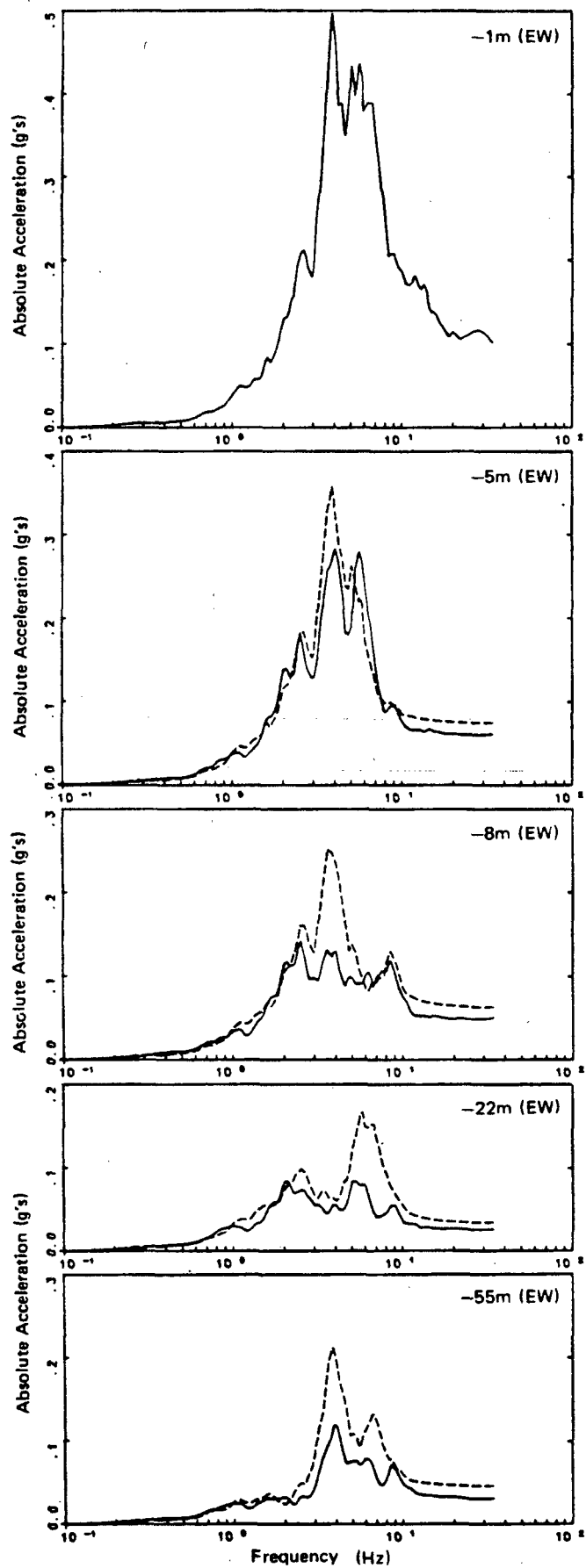


EXPLANATION

- Recorded
 - Computed from deconvolution analysis
- Damping = 0.05

From Chang et al. (1986)
 (Vol. 3 of NUREG/CR-3805)

Figure 3-22a. Comparison of Response Spectra of Recorded and Computed Motions, Deconvolution Analysis, NS Components, Narimasu Site

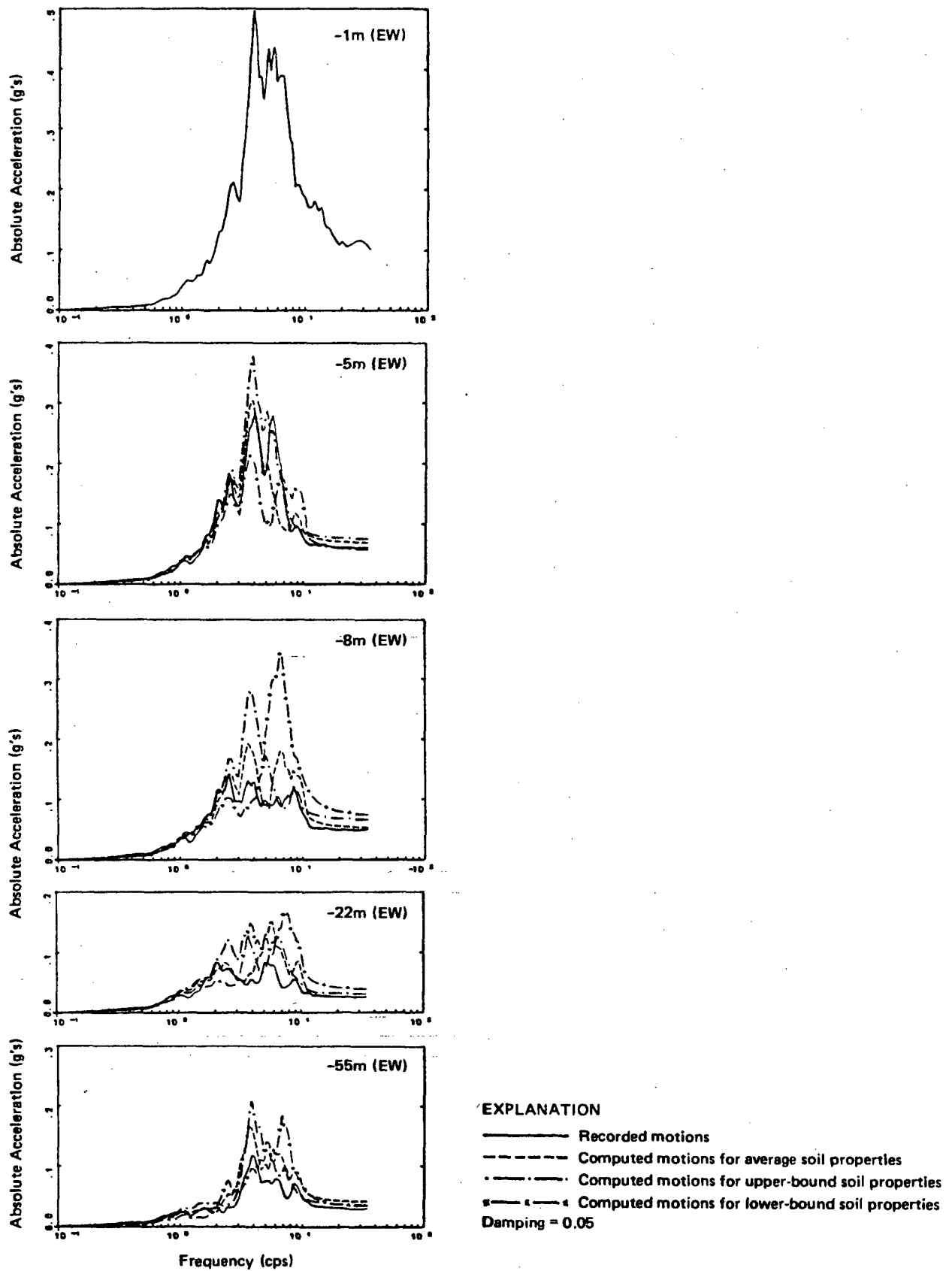


EXPLANATION

- Recorded
- - - - - Computed from deconvolution analysis
- Damping = 0.05

From Chang et al. (1986)
 (Vol. 3 of NUREG/CR-3805)

Figure 3-22b. Comparison of Response Spectra of Recorded and Computed Motions, Deconvolution Analysis, EW Components, Narimasu Site



From Chang et al. (1986)
 (Vol. 3 of NUREG/CR-3805)

Figure 3-23. Comparison of Response Spectra of Recorded and Computed Motions, Deconvolution Analysis with Parametric Variation in Soil Properties, EW Components, Narimasu Site

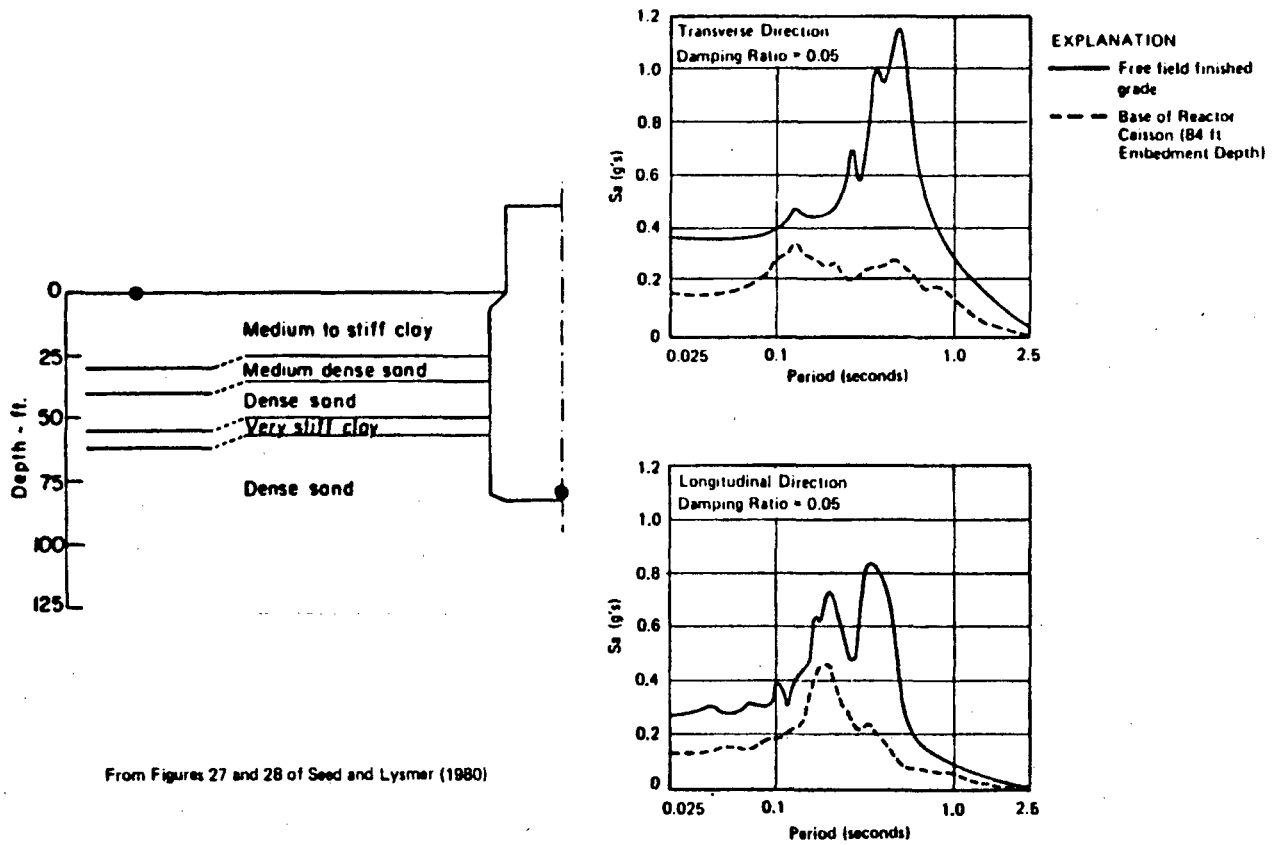
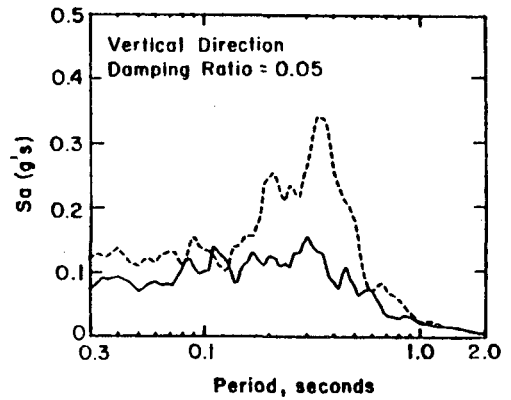
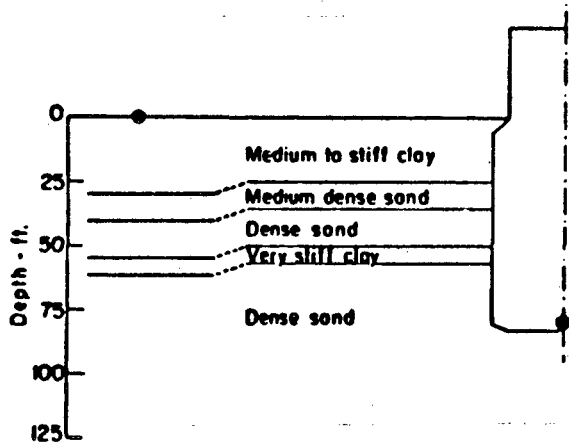


Figure 3-24. Comparison of Response Spectra of Accelerograms Recorded at Finished Grade in the Free Field and at the Base of the Reactor Caisson at the Humboldt Bay Plant During the June 6, 1975, Ferndale, California Earthquake (Horizontal Components)



EXPLANATION

- Free field finished grade
- - - - - Base of Reactor Caisson
(84 ft Embedment Depth)

From Chang et al. (1986)
(Vol. 3 of NUREG/CR-3805)

Figure 3-25. Comparison of Response Spectra of Accelerograms Recorded at Finished Grade in the Free Field and at the Base of the Reactor Caisson at the Humboldt Bay Plant During the June 6, 1975, Ferndale, California Earthquake (Vertical Component)

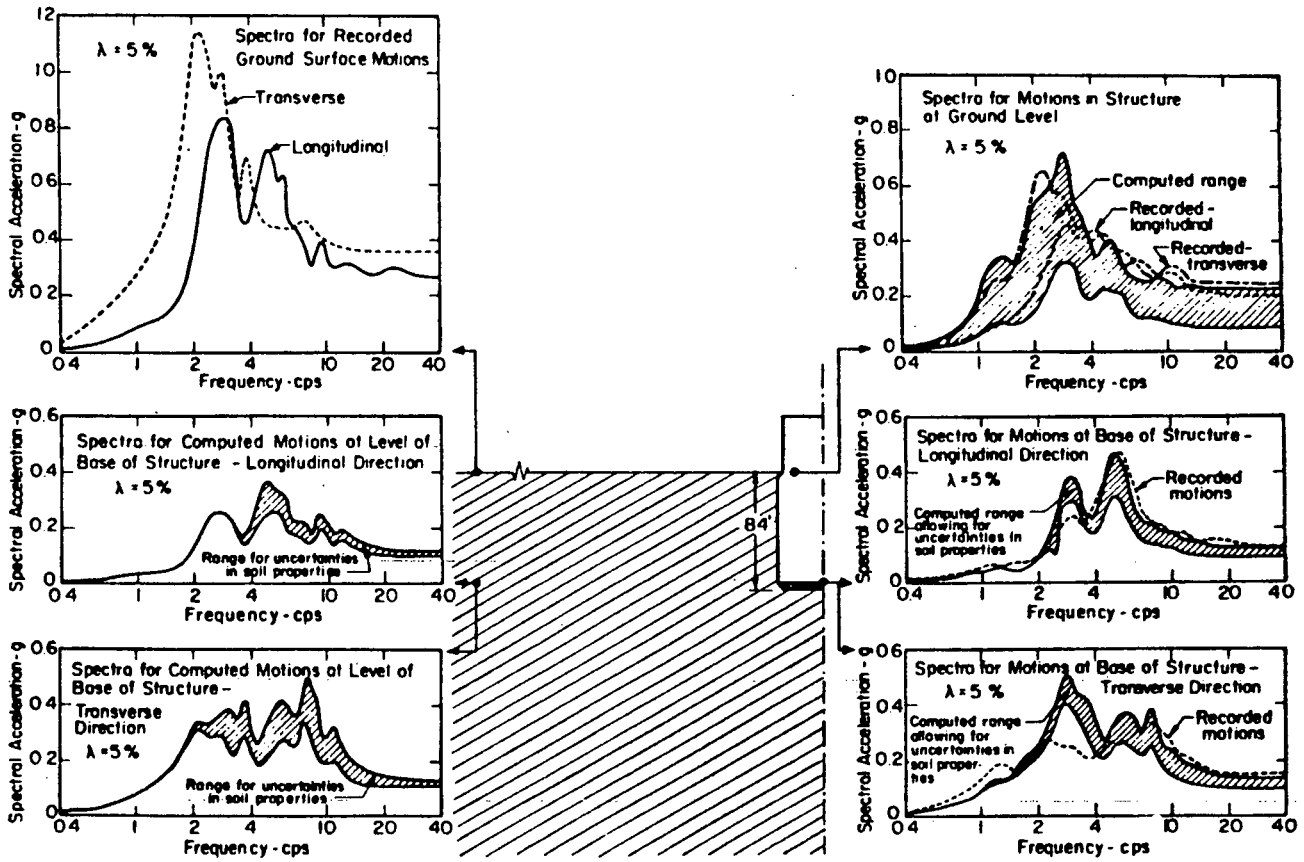
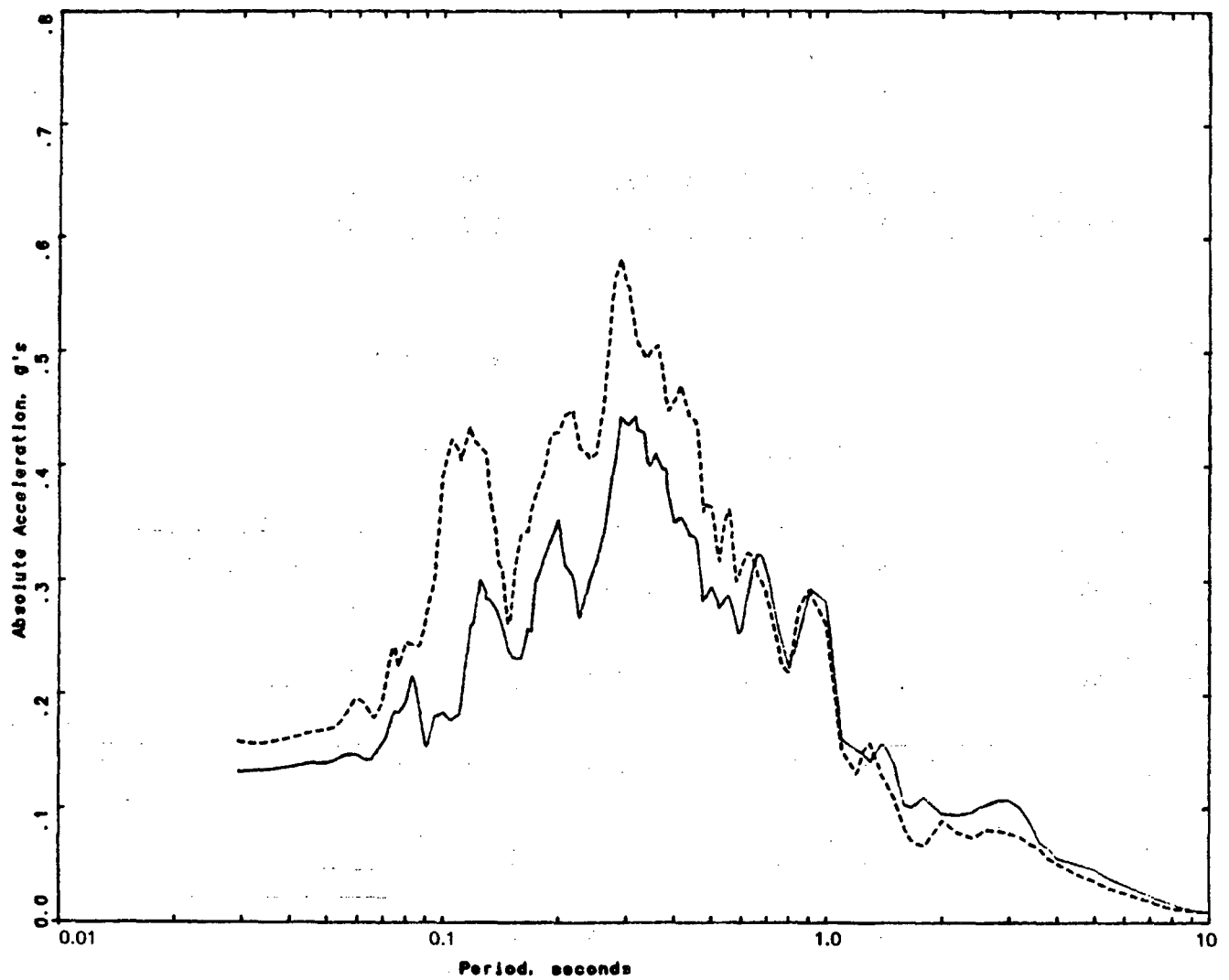


Figure 3-26. Comparison of Recorded and Computed Spectra in Refueling Building, Humboldt Bay Power Plant (after Valera et al., 1977)

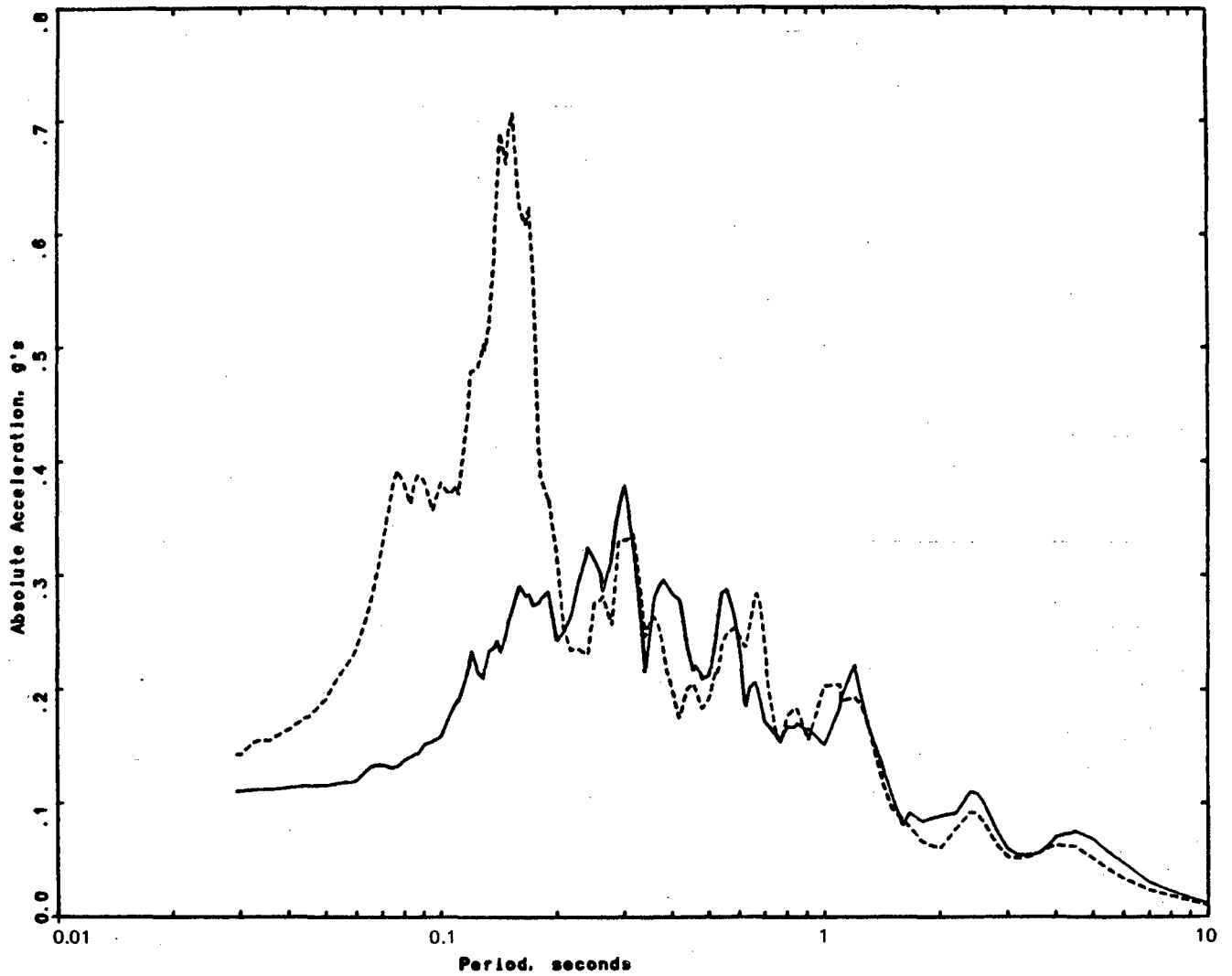


EXPLANATION

- Without basement : ST. 199(E083) - S00W
 - With basement : ST. 208(E075) - N00E
- 5% Damping

From Chang et al. (1986)
(Vol. 3 of NUREG/CR-3805)

Figure 3-27a. Comparison of Response Spectra of Motions Recorded at Stations 199 (without basement) and 208 (with basement) During the 1971 San Fernando Earthquake



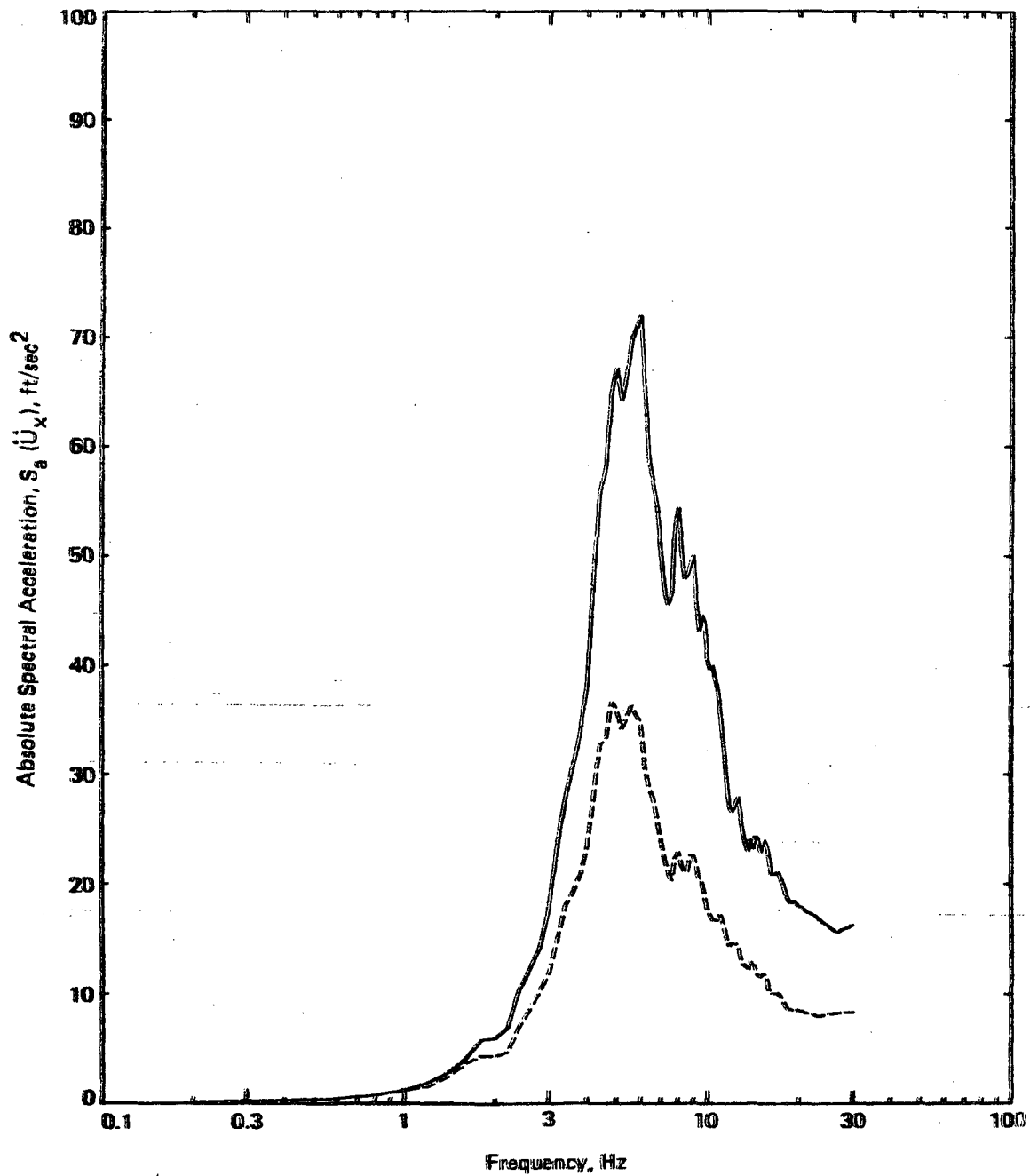
EXPLANATION

----- Without basement : ST. 199 (E083) - N90E
 ————— With basement : ST. 208 (E075) - S90W

5% Damping

From Chang et al. (1986)
 (Vol. 3 of NUREG/CR-3805)

Figure 3-27b. Comparison of Response Spectra of Motions Recorded at Stations 199 (without basement) and 208 (with basement) During the 1971 San Fernando Earthquake

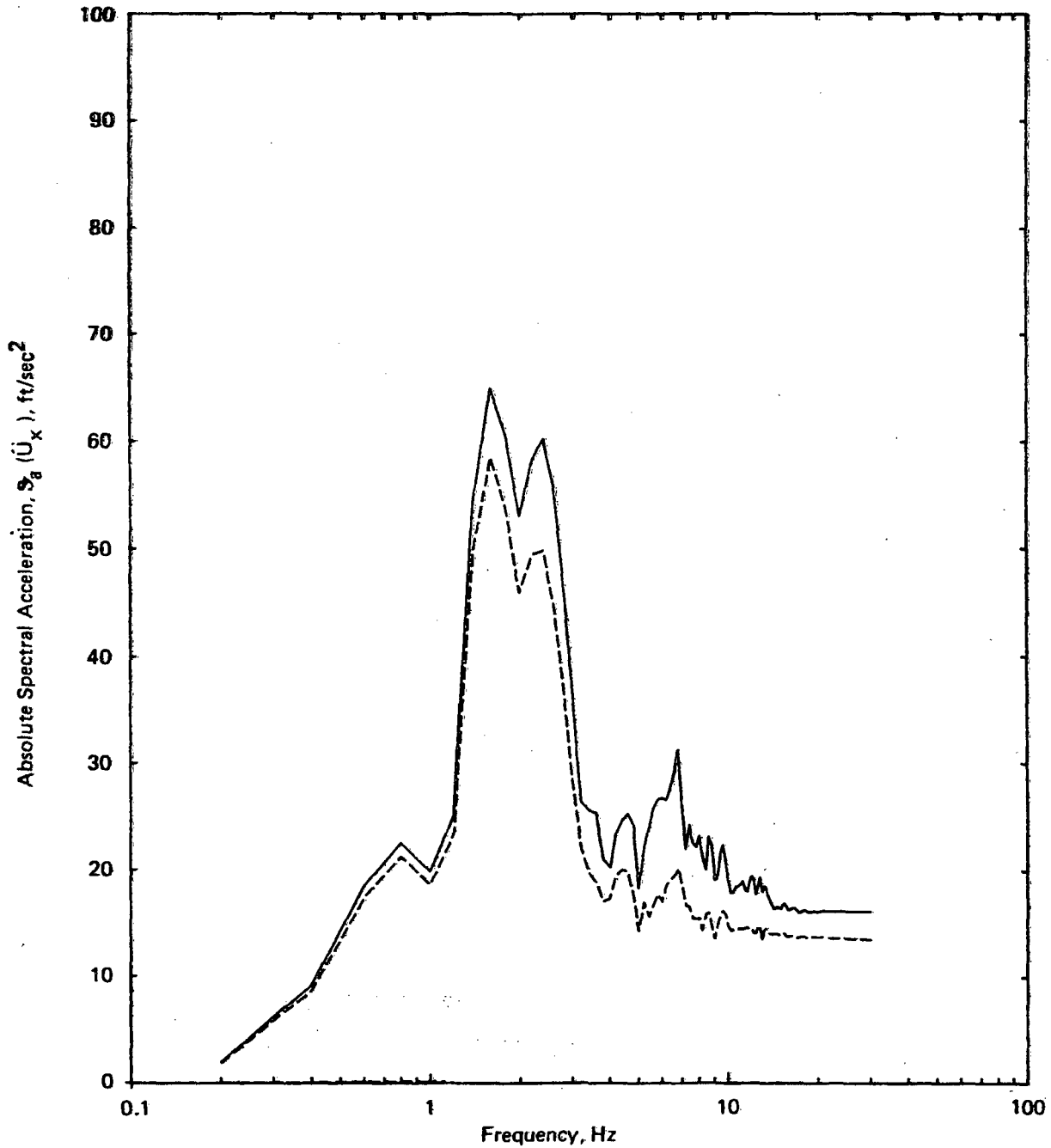


EXPLANATION

- Melendy Ranch horizontal control motion (N61E)
 - Horizontal foundation input motion for soil profile IV
- Damping Ratio = 0.02

Based on Luco et al. (1986)
(Vol. 4 of NUREG/CR-3805)

Figure 3-28. Comparison of Response Spectra of Melendy Ranch Control Motion and Corresponding Foundation Input Motion (Reactor Building, Soil Profile IV, 40ft Embedment, Vertically Incident Waves)



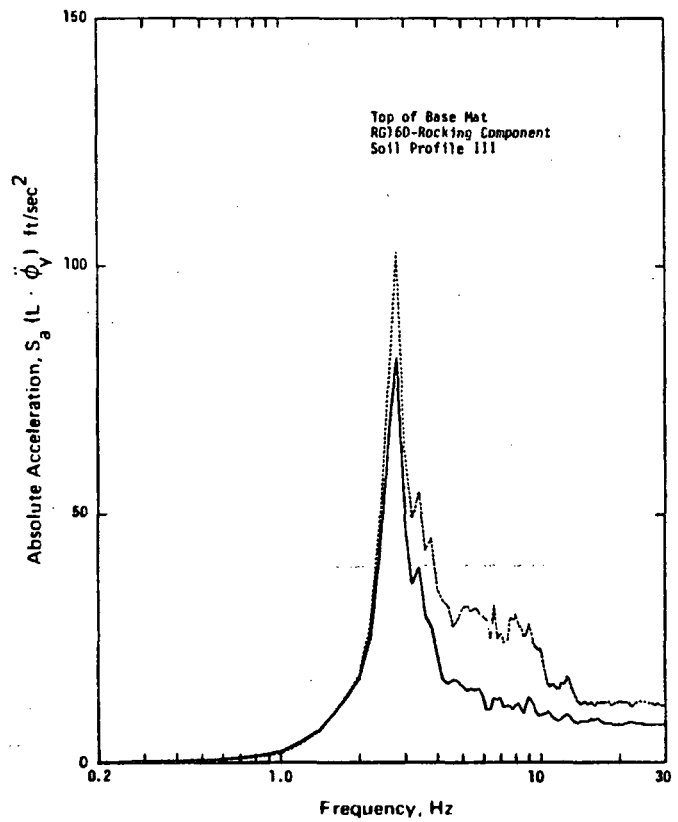
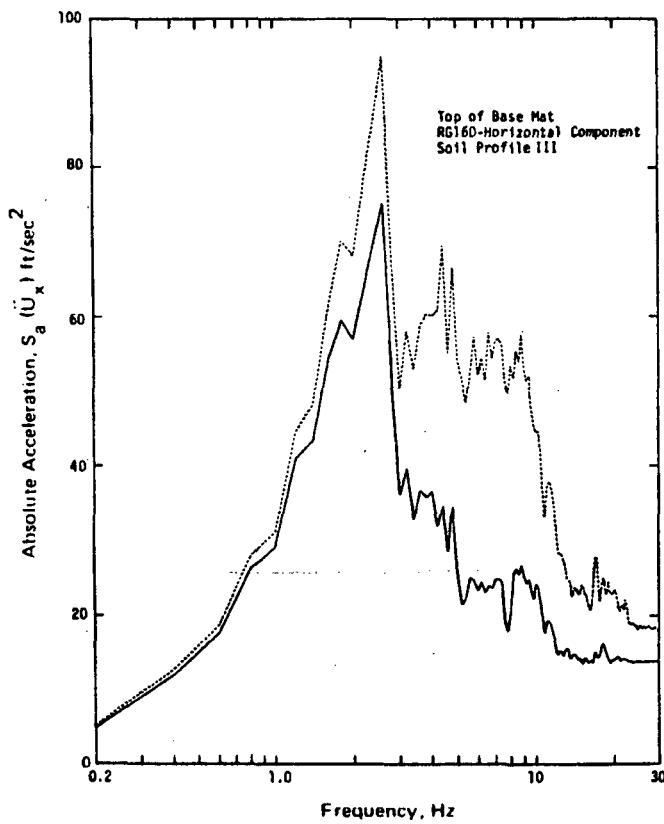
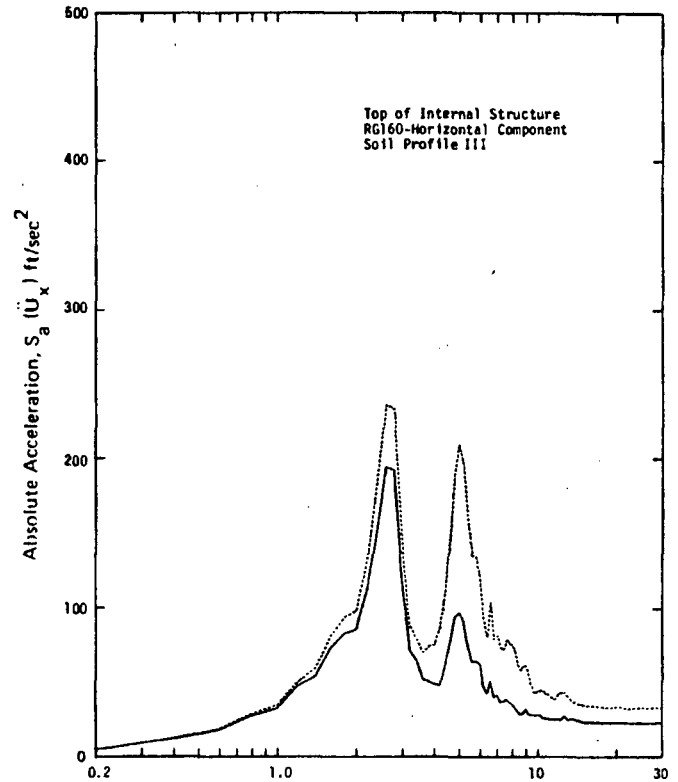
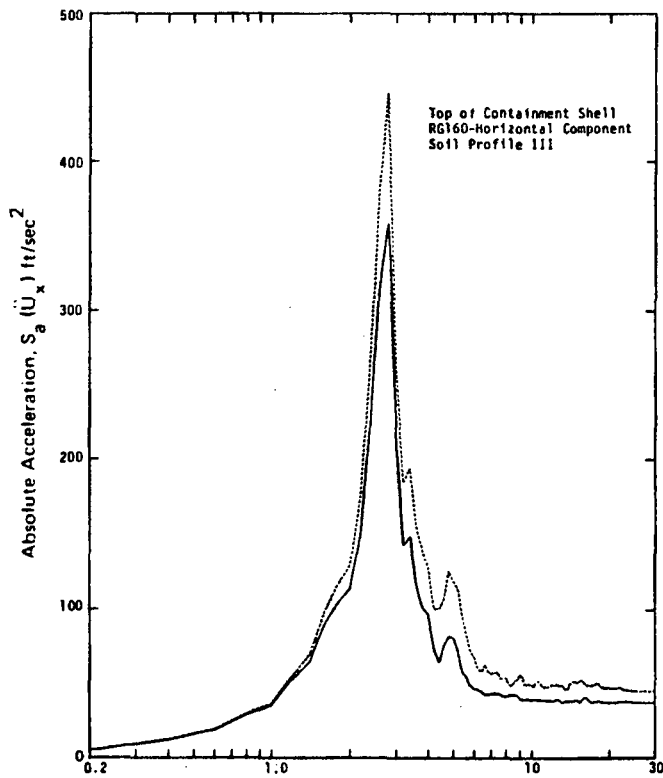
EXPLANATION

- Parkfield horizontal control motion (N65E)
- - - Horizontal foundation input motion for soil profile IV

Damping Ratio = 0.02

Based on Luco et al. (1986)
(Vol. 4 of NUREG/CR-3805)

Figure 3-29. Comparison of Response Spectra of Parkfield Control Motion and Corresponding Foundation Input Motion (Reactor Building, Soil Profile IV, 40 ft Embedment, Vertically Incident Waves)



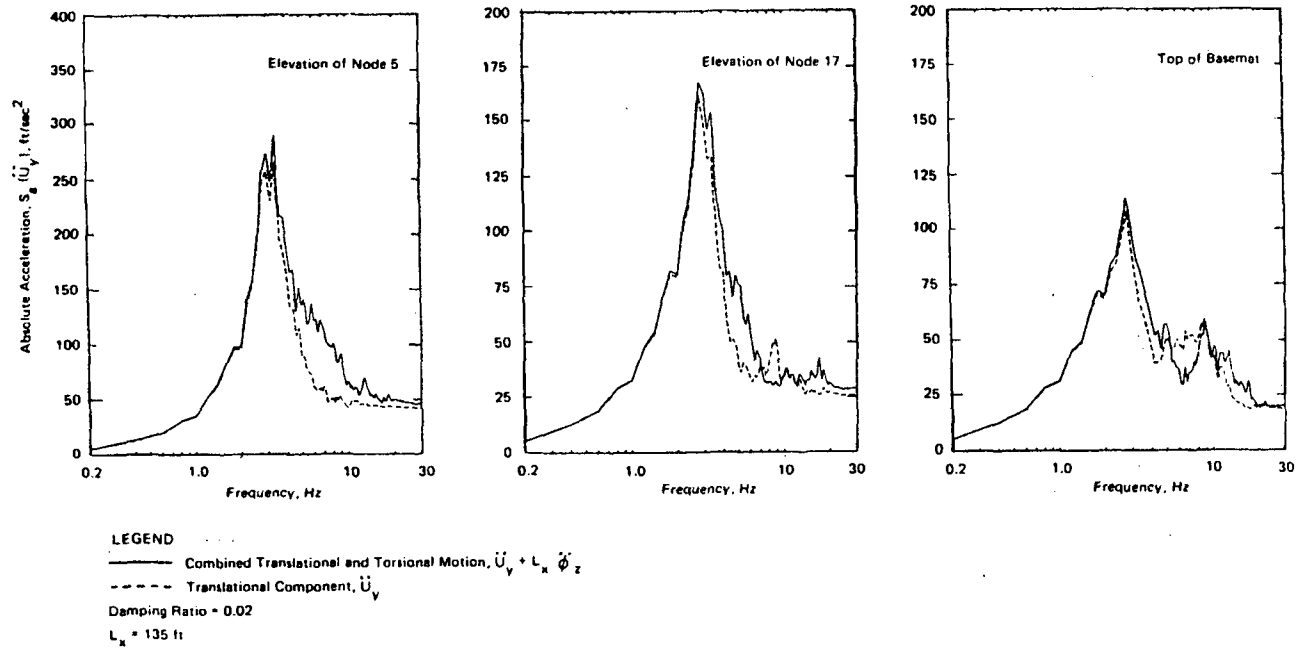
EXPLANATION

- With Kinematic Interaction
- Without Kinematic Interaction

Damping Ratio = 0.02
L = 63.6 ft

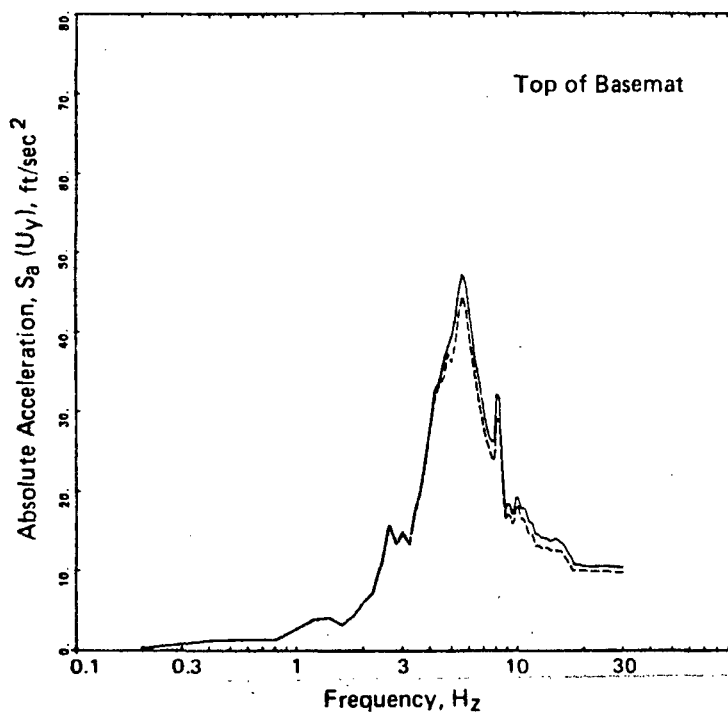
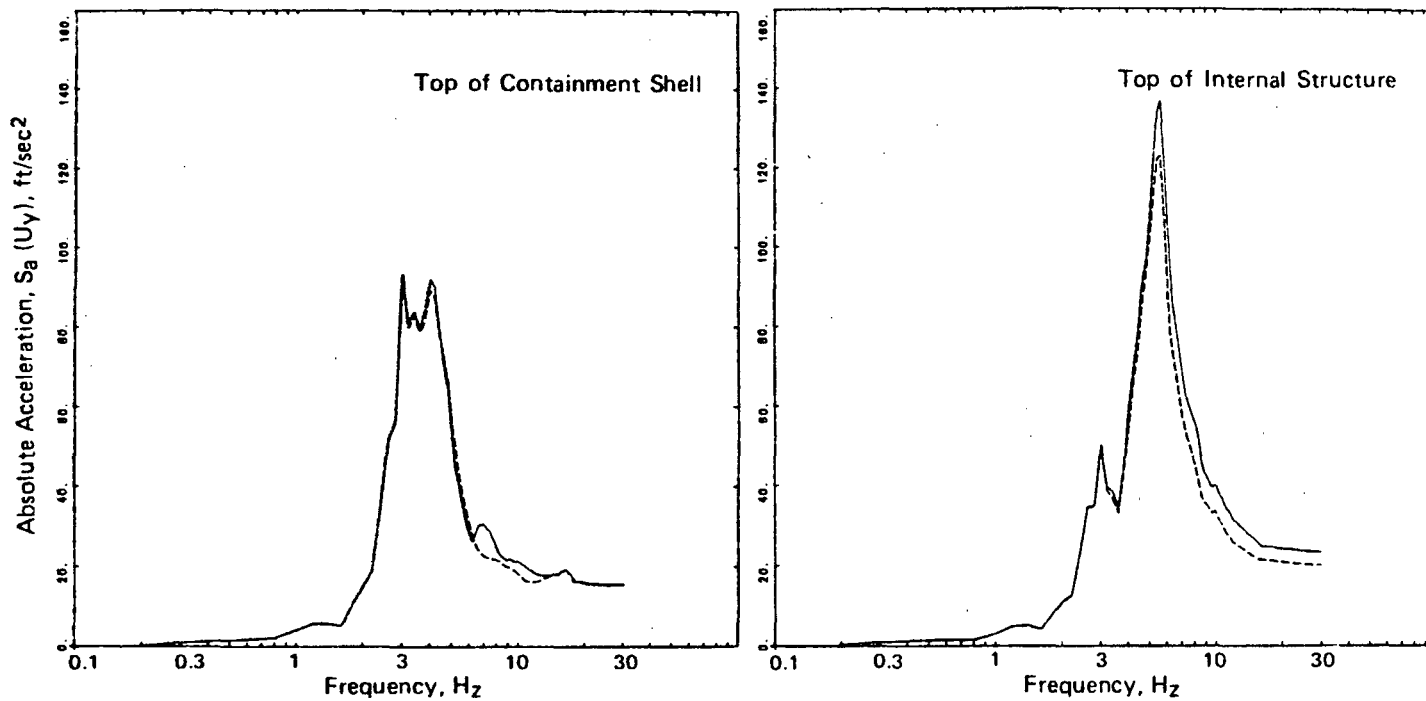
Based on Luco et al. (1986)
(Vol. 4 of NUREG/CR-3805)

Figure 3-30. Comparison of Floor Response Spectra of Reactor Building from Analyses with and without Consideration of Kinematic Interaction, Artificial Reg.Guide 1.60 Excitation, Soil Profile III (40 ft Embedment, Vertical Incidence)



From Luco et al. (1986)
 (Vol. 4 of NUREG/CR-3805)

Figure 3-31. Comparison of Response Spectra of Combined Translational and Torsional Motion and Translational Component, Auxiliary Building, Soil Profile III, Nonvertically Incident Waves ($C_y = 3 \text{ km/sec}$), Artificial Reg. Guide 1.60 Excitation



LEGEND

———— Combined Translational and Torsional Motion, $\ddot{U}_y \pm L \ddot{\phi}_z$

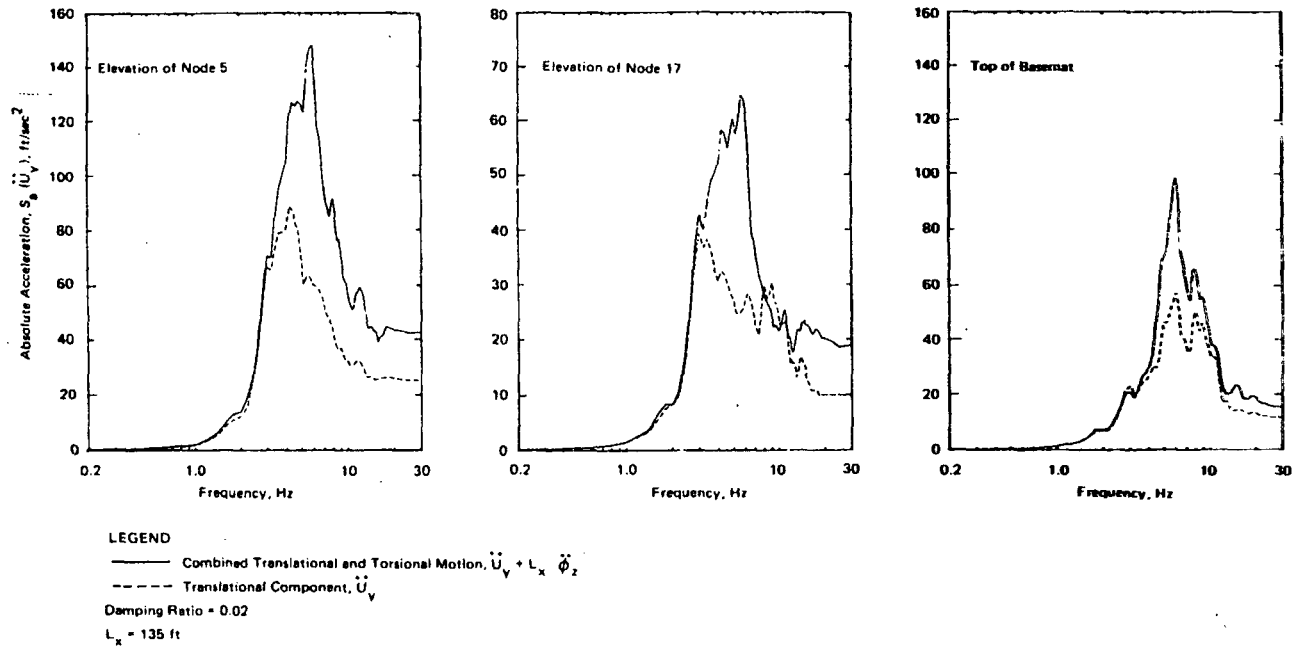
----- Translational Component, \ddot{U}_y

Damping Ratio = 0.02

$L = 63.6$ ft

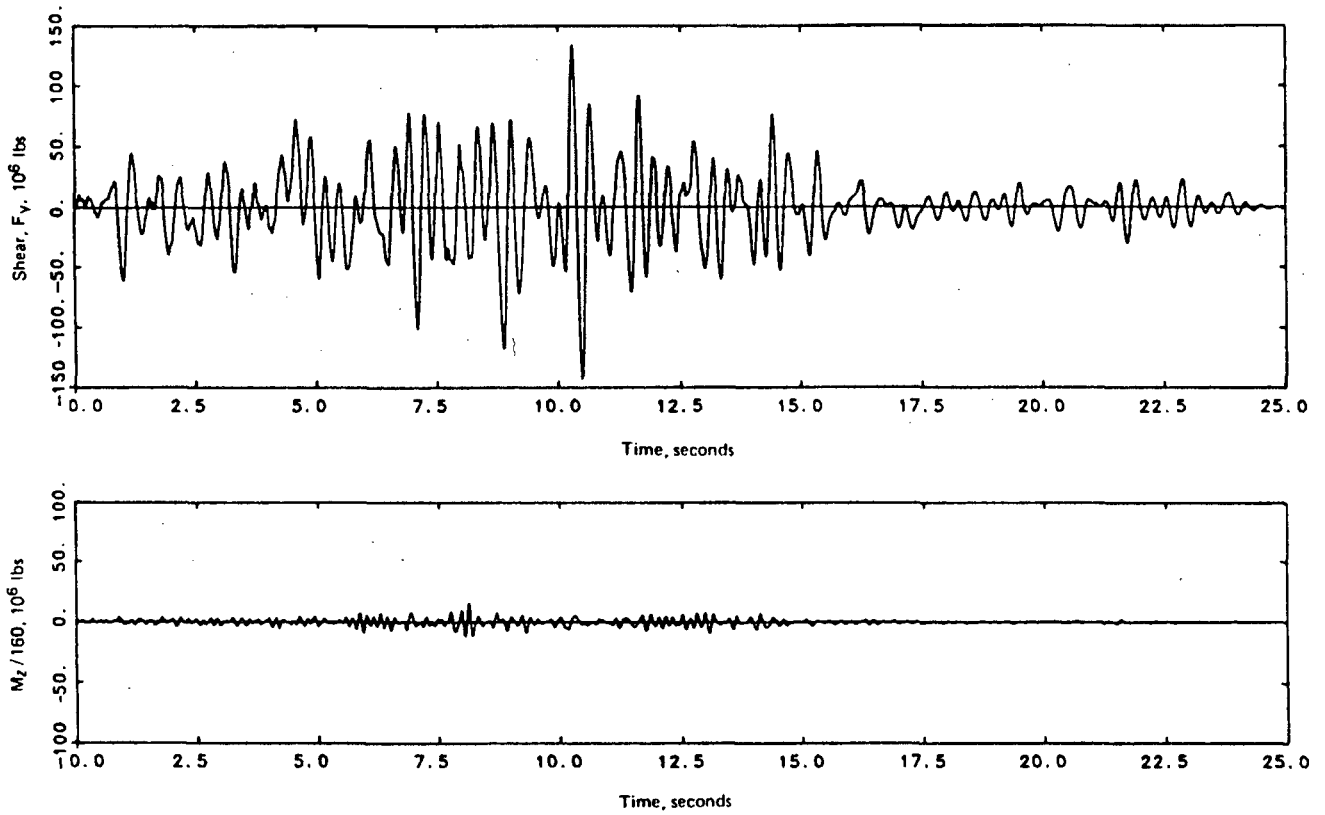
Based on Luco et al. (1986)
(Vol. 4 of NUREG/CR-3805)

Figure 3-32. Comparison of Response Spectra of Combined Translational and Torsional Motion and Translational Component, Reactor Building, 40 ft Embedment, Soil Profile II, Nonvertically Incident Waves ($C_y = 3$ km/sec), Melendy Ranch Excitation



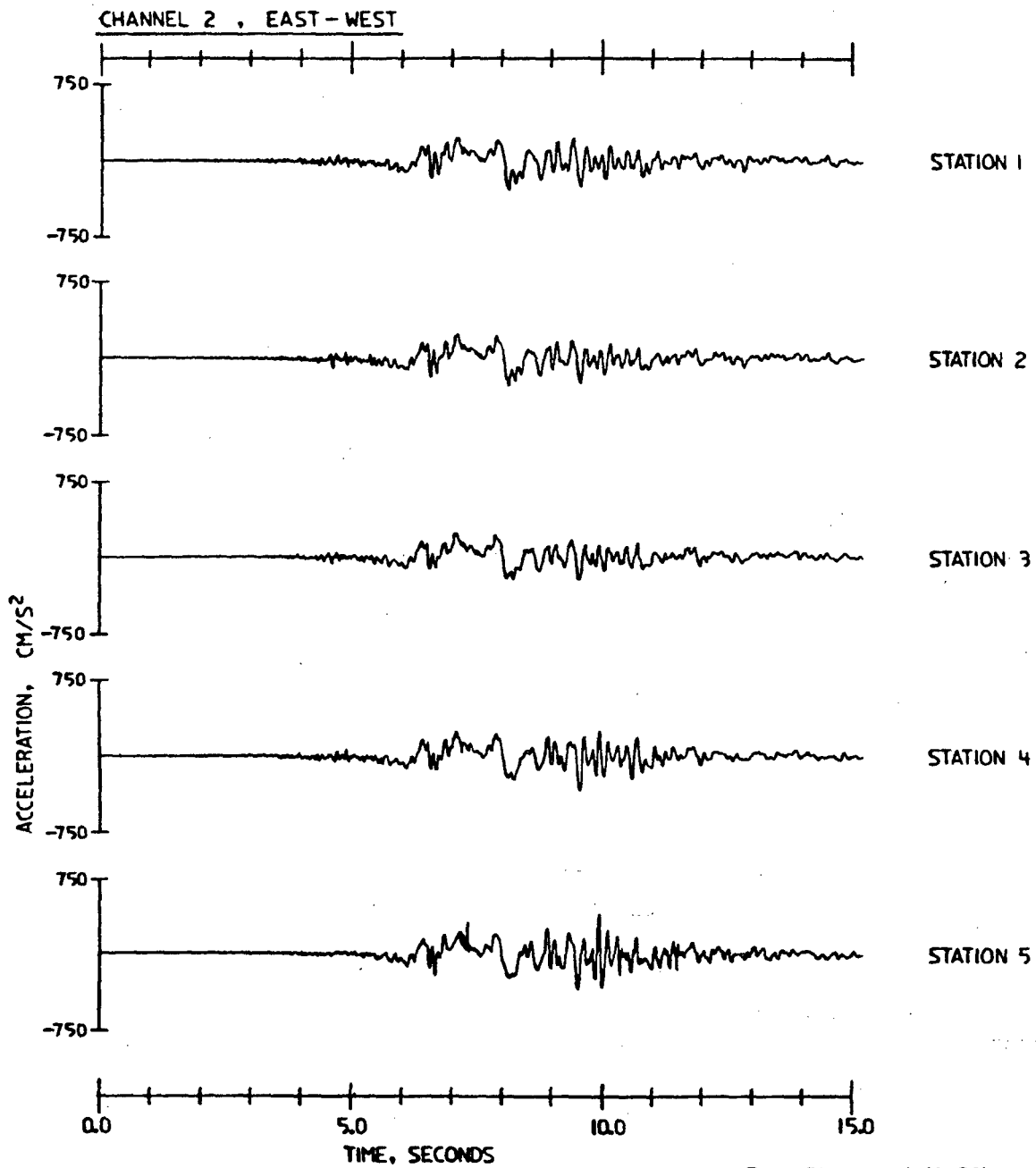
From Luco et al. (1986)
 (Vol. 4 of NUREG/CR-3805)

Figure 3-33. Comparison of Response Spectra of Combined Translational and Torsional Motion and Translational Component, Auxiliary Building, Soil Profile III, Nonvertically Incident Waves ($C_y = 3$ km/sec), Melendy Ranch Excitation



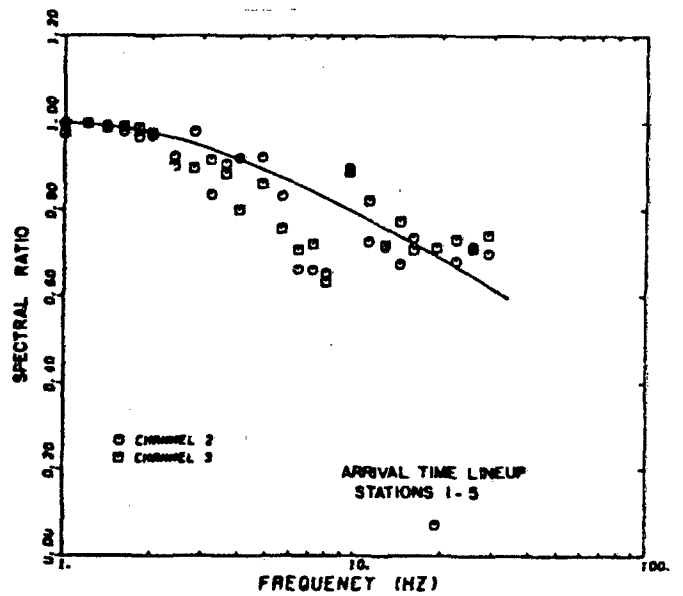
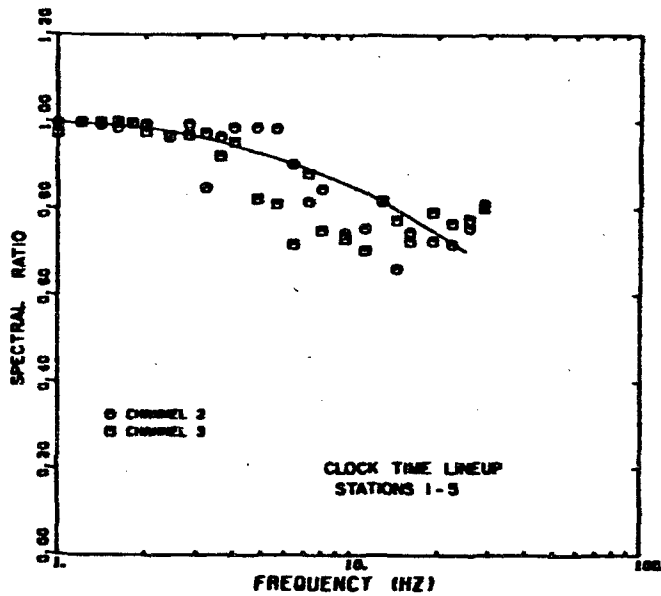
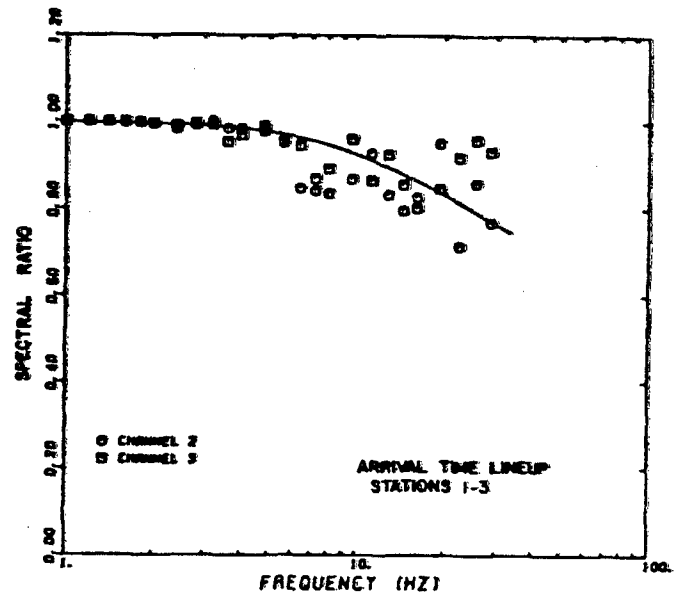
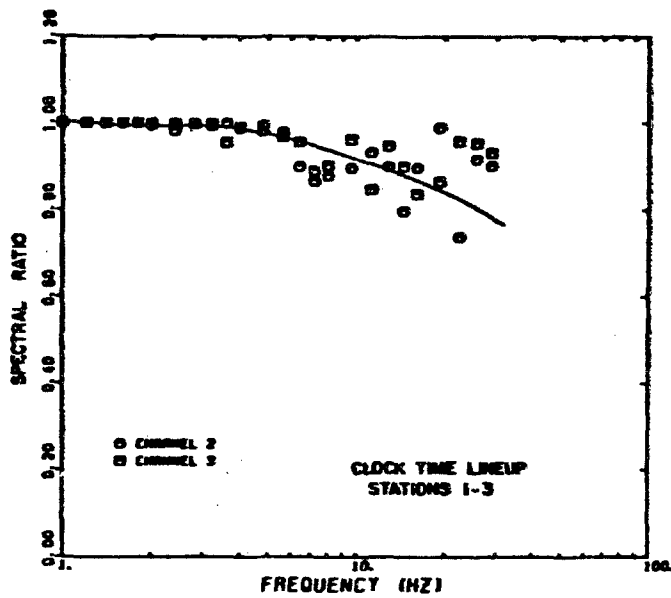
From Luco et al. (1986)
 (Vol. 4 of NUREG/CR-3805)

Figure 3-34. Time Histories of Base Shear and Torque (normalized by $d = 160$ ft), Auxiliary Building, Soil Profile III, Nonvertically Incident Waves ($C_y = 3$ km/sec), Artificial Reg. Guide 1.60 Excitation



From Chang et al. (1986)
(Vol. 3 of NUREG/CR-3805)

Figure 3-35. Acceleration Time Histories for Channel 2 (East-West Component), El Centro Differential Array, the 1979 Imperial Valley Earthquake. (After Smith et al., 1982)



From Chang et al. (1986)
 (Vol. 3 of NUREG/CR-3805)

Figure 3-36. Ratio of the Response Spectra for the Array Sum to the Average of the Individual Response Spectra for the Horizontal Components (Channels 2 and 3), El Centro Differential Array (After Smith et al., 1982).

4. SUMMARY AND CONCLUSIONS

This study has the objective of providing guidance on procedures to be used for the engineering characterization of earthquake ground motion for the design of nuclear power plant structures. The engineering characterization of ground motion has been related in this study to two basic considerations: the inelastic response and performance of structures; and spatial variations of ground motion and soil-structure interaction. The main results and conclusions of the study as related to these considerations are presented in Sections 2 and 3 of this report. Summarized briefly in this section are the main findings of the study in four areas of ground motion characterization:

- Characterization of free-field control motion;
- Characterization of ground motion variations with depth;
- Characterization of variations of ground motion in a horizontal plane; and
- Characterization of ground motion for structural inelastic deformations.

CHARACTERIZATION OF FREE-FIELD CONTROL MOTION

- The studies have emphasized strongly the importance of frequency content of ground motion in determining structural response. As summarized in Section 2, structural inelastic response is importantly influenced by the frequency content of ground motion over a frequency range from the structural elastic frequency to a lower frequency corresponding to a "softened" structure that has attained a certain amount of inelastic deformation or ductility. As summarized in Section 3, some elastic response quantities for a structure in a soil-structure system, such as containment shell base shear force, may be largely determined by the ground motion frequency content in the vicinity of the fundamental characteristic frequency of the soil-structure system, which is

lower than the structural elastic fixed-base frequency. Thus both the studies of inelastic structural response and soil-structure interaction point to the importance of adequately characterizing the frequency content of ground motion at frequencies lower than the structural elastic frequency, as well as at the structural elastic frequency. However, frequency content over a broad frequency range is important for floor response spectra.

- Duration of strong ground shaking was found to be a significant factor influencing structural inelastic response, although secondary in comparison to the influence of frequency content. The small effect of duration in comparison to frequency content on inelastic structural response is partly the result of use in this study of displacement ductility as the measure of structural damage. For a damage measure consisting of the total hysteretic energy absorbed by a structure during inelastic response, duration increases in importance. It should also be noted that in some extreme cases, such as earthquake ground motions in Mexico City during the 1985 Mexico earthquake, duration may play a larger role in affecting inelastic structural response than for the ground motions used in this study.

- Because frequency content as well as duration of ground motion are strongly dependent on site-specific factors, including earthquake source characteristics, source-to-site wave propagation characteristics, and local soil conditions, the study emphasizes the importance of site-specific ground motion characterizations, rather than using standard, non-site-specific characterizations such as Reg. Guide 1.60 response spectra shapes. Uncertainty must be recognized and allowed for in any site-specific ground motion characterization, regardless of whether the characterization is derived based on recorded ground motion data, theoretical modeling, or both.

CHARACTERIZATION OF VARIATIONS OF GROUND MOTION WITH DEPTH

- There is a good body of data to show that, in general, both peak accelerations and response spectra decrease significantly with depth in the depth range of typical embedment depths of nuclear power plant structures.
- Comparisons of data and analysis indicate that deconvolution procedures assuming vertically propagating shear waves provide reasonable and apparently somewhat conservative estimates of the variations of ground motion with depth. The current practice of conducting deconvolution analyses incorporating rather wide parametric variations in soil shear modulus appears to result in conservative estimates of the variations of ground motion with depth.
- The practice of excluding ground motion variations with depth, as has been done in a number of instances in nuclear power plant design practice, is not founded on a physical basis and appears to uniformly lead to additional conservatism and overestimation of structural response.
- On the basis of these studies, it is concluded that appropriate variations of ground motion with depth should be included in characterizing foundation input motions and carrying out soil-structure interaction analyses for embedded structures. Current analysis procedures that incorporate deconvolution of ground surface motions in the free field may appropriately be used. It is also concluded that incorporating soil property variations in parametric deconvolution and soil-structure interaction analyses is an appropriate way not only to incorporate effects of uncertainties in the properties on foundation stiffness and inertial interaction but also to reasonably incorporate effects of uncertainties in the characterization of ground motion variations with depth.

CHARACTERIZATION OF VARIATIONS OF GROUND MOTION IN A HORIZONTAL PLANE

- The effects of phase differences of ground motion across foundation widths on foundation and structural response, sometimes called "wave passage effects", are clearly related to the apparent horizontal propagation velocity of the seismic waves. The slower the velocity, the greater is the difference in response relative to response for vertically propagating waves (for which apparent horizontal wave velocities are infinite). The limited available data indicate that the apparent horizontal velocities of predominant propagating seismic energy are generally high, in the range of about 2.5 to 5.5 km/sec.
- For such high velocities, it appears that, in most cases, effects of phase differences in ground motion in a horizontal plane on structural translation and rocking responses are small enough to be neglected and effects on torsional response are adequately incorporated by the common design practice of assuming a 5 percent accidental eccentricity of the induced base shear force. Thus, in general, it would appear to be satisfactory to analyze assuming vertically propagating waves except for providing a nominal 5 percent accidental eccentricity. However, the study also suggests that a more significant torsional response due to non-vertically incident waves may occur for the case of a high-frequency, narrow-banded, short duration ground motion input to a structure on a soil site.
- Incoherence of ground motion is manifested by differences in the frequency content (response spectra) of ground motion horizontally from point to point. It appears that due to incoherence, a large foundation will experience average translational motions that are reduced from the free-field motions. This reduction, which has been termed a "base-averaging" effect, increases with frequency, foundation size, and heterogeneity of the local soil conditions,

and appears to be larger for horizontal motions than for vertical motions. The base averaging effect may also depend on the relative rigidity of the foundation and the underlying soil deposit, increasing as the relative rigidity increases.

- Effects of incoherence on foundation input motions could be incorporated as a frequency-dependent reduction in the translational input motions. Although the amount of reduction is not well quantified at present due to limited data, the available data indicate that for a 50 m wide foundation on a relatively uniform soil site, reductions in horizontal spectral acceleration of about 20 percent at frequencies between 20 and 30 Hz, 10 to 15 percent at frequencies between 10 and 20 Hz, 5 percent at frequencies between 5 and 10 Hz, and no reduction at frequencies below 5 Hz are reasonable. Data are not presently available to ascertain effects of incoherence on rotational foundation input motions.

CHARACTERIZATION OF GROUND MOTION FOR STRUCTURAL INELASTIC RESPONSE

- The study included a literature review of the performance of structures during past earthquakes. The review indicated that characterization of ground motion by low-damped elastic response spectra is not sufficient to describe the damage potential of the ground motion. The review indicated that well-designed structures could experience ground motions at least 2.5 times those that would just cause structural yielding (just reach elastic capacity), even for ground motions of relatively long duration.
- From findings and correlations developed during the study between inelastic structural response and ground motion characteristics, procedures were developed for constructing inelastic response spectra, i.e., reduced response spectra that if designed for elastically, would result in the attainment of a certain ductility

in a structure if the structure experienced the actual ground motion. The reduction factors for obtaining inelastic response spectra from elastic response spectra are a strong function of the shape of the response spectrum and a lesser function of the duration of the ground motion. For the shear wall-type resistance functions used in this study, it was found that the recommended procedures for constructing inelastic response spectra are significantly improved over other commonly used approaches. These procedures may also be conservatively used for braced frames and other structural systems, as long as these systems do not exhibit greater stiffness degradation and pinching behavior than the resistance-deformation functions used in this study for shear walls.

- Although the procedures for characterizing ground motions with respect to their structural damage potential and constructing inelastic response spectra were developed based on analyses of simple structures, these procedures can also be used, with some degree of uncertainty, to estimate the inelastic response of multi-degree-of-freedom structures. Uncertainty in the use of the procedures increases with increased nonuniformity of elastic computed demand to capacity ratios throughout the structure (i.e., increased uncertainty when the structure has "weak links"), increased sensitivity of inelastic response to incremental changes in the amplitude of the input accelerogram, and apparently with the presence of soil-structure interaction effects. The methods are quite efficient when a number of parametric studies are to be conducted. However, if only one or a few analyses are to be conducted, it is equally or more efficient as well as more accurate to conduct a nonlinear time history analysis than to use these simplified procedures to estimate inelastic response.

- With respect to inelastic structural response effects on floor spectra, it was found that if floor spectra show highly amplified narrow spikes, then inelastic structural response will reduce

them. However, if such spectral spikes are not present either because of soil-structure interaction effects or lack of frequency content of the input motion, then the effects of structural inelastic response on floor spectra will be small.

- The study is indicative that the portion of the seismic safety margin of a structure due to inelastic response capacity may be smaller for a structure embedded in soil than for a structure on rigid rock (fixed-base condition). Consequently, if seismic margins due to soil-structure interaction effects and structural inelastic response capacity are being combined, this needs to be done carefully in order not to double-count in obtaining the overall seismic margin.

REFERENCES

- Bolt, B.A., Loh, C.H., Penzien, J., Tsai, Y.B. and Yeh, Y.T. (1982). Preliminary Report on the SMART 1 Strong Motion Array In Taiwan, Report No. UCB/EERC-82/13, Earthquake Engineering Research Center, University of California, Berkeley.
- Bouchon, M. and Aki, K. (1982). Strain, Tilt, and Rotation Associated with Strong Motion in the Vicinity of Earthquake Fault, Bulletin of the Seismological Society of American, Vol. 72, No. 5 pp. 1717-1738.
- Campillo, M. and Bouchon, M. (1983). A Theoretical Study of the Radiation from Small Strike-Slip Earthquake at Close Distances, Bulletin of the Seismological Society of America, Vol. 73, No. 1, pp. 83-96.
- Chang, C.-Y., Power, M.S., Idriss, I.M., Somerville, P.G., Silva, W. and Chen, P.C. (1986). Engineering Characterization of Ground Motion, Task II: Observational Data on Spatial Variations of Earthquake Ground Motion, NUREG/CR-3805, Vol. 3, Prepared for U.S. Nuclear Regulatory Commission.
- Gulkan, P. and Sozen, M.A. (1974). Inelastic Responses of Reinforced Concrete Structures to Earthquake Motions, ACI Journal, Vol. 71, No. 12, pp. 604-610, December.
- Iwan, W.D. (1980). Estimating Inelastic Response Spectra From Elastic Spectra, Earthquake Engineering & Structural Dynamics, Vol. 8, pp. 375-399.
- Kennedy, R.P., Short, S.A., Merz, K.L., Tokarz, F.J., Idriss, I.M., Power, M.S., and Sadigh, K. (1984). Engineering Characterization of Ground Motion, Task I: Effects of Characteristics of Free-Field Motion on Structural Response, NUREG/CR-3805, Vol. 1, Prepared for U.S. Nuclear Regulatory Commission.
- Kennedy, R.P., Kincaid, R. H., and Short, S.A. (1985). Engineering Characterization of Ground Motion, Task II: Effects of Ground Motion Characteristics on Structural Response Considering Localized Structural Nonlinearities and Soil-Structure Interaction Effects, NUREG/CR-3805, Vol. 2, Prepared for U.S. Nuclear Regulatory Commission.
- Kim, Y.-S. (1984). Effect of Embedment on Seismic Motions of Buildings, M.S. Thesis, University of Texas, Austin.
- King, J.L. and Tucker, B.E. (1982). Analysis of Differential Array Data from El Centro, USA and Garm, USSR, Proceedings of the 3rd International Earthquake Microzonation Conference, II, pp. 611-622.

- Luco, J.E., and Wong, H.L. (1982). Response of Structures to Nonvertically Incident Seismic Waves, Bulletin of the Seismological Society of America, Vol. 72, No. 1, pp. 275-302.
- Luco, J.E., Wong, H.L., Chang, C.-Y., Power, M.S., and Idriss, I.M. (1986). Engineering Characterization of Ground Motion, Task II: Soil-Structure Interaction Effects on Structural Response, NUREG/CR-3805, Vol. 4, Prepared for U.S. Nuclear Regulatory Commission.
- Luco, J.E., and Sotiropoulos, D.A. (1980). Local Characterization of Free-Field Ground Motion and Effect of Wave Passage, Bulletin of the Seismological Society of America, Vol. 70, No. 6, pp. 2229-2244.
- Mohraz, B., (1976). A Study of Earthquake Response Spectra for Different Geological Conditions, Bulletin of the Seismological Society of America, Vol. 66, No. 3, June, pp. 915-936.
- Newmark, N.M., and Hall, W.J. (1978). Development of Criteria for Seismic Review of Selected Power Plants, NUREG/CR-0098, Newmark Consulting Engineering Services, Urbana, Illinois, May.
- Newmark, N.M., and Hall, W.J., and Morgan, J.R. (1977). Comparison of Building Response and Free Field Motion in Earthquakes, Proceedings of the 6th World Conference on Earthquake Engineering, 3, pp. 1-6.
- O'Rourke, M.J., Bloom, M.C., and Dobry, R. (1982). Apparent Propagation Velocity of Body Waves, Earthquake Engineering and Structural Dynamics, 10, pp. 283-294.
- Riddell, R. and Newmark, N.M. (1979). Statistical Analysis of the Response of Nonlinear Systems Subjected to Earthquakes, SRS 468, Department of Civil Engineering, University of Illinois, Urbana, August.
- Roesset, J.M. (1980). Seismic Safety Margins Research Program (Phase I), Project III - Soil - Structure Interaction, A Review of Soil-Structure Interaction, Report No. UCRL-15262 prepared for Lawrence Livermore Laboratory; also in NUREG/CR-1780.
- Seed, H.B. and Idriss, I.M. (1969). The Influence of Soil Conditions on Ground Motions During Earthquakes, Journal of Soil Mechanics and Foundations Division, ASCE, Vol. 94, No. SM1, pp. 99-137.
- Seed, H.B. and Lysmer, J. (1980). The Significance of Site Response in Soil-Structure Interaction Analyses for Nuclear Facilities, Proceedings of the ASCE Specialty Conference, Knoxville, Tennessee. Also, the Seismic Soil-Structure Interaction Problem for Nuclear Facilities, Report NUREG/CR-1780, UCRL-53011.

- Seed, H.B., Ugas, C., and Lysmer, J. (1976). Site-Dependent Spectra for Earthquake-Resistant Design, Bulletin of the Seismological Society of America, Vol. 66, No. 1, February, pp. 221-243.
- Shibata, A. and Sozen, M.A. (1976). Substitute-Structure Method for Seismic Design in R/C, Journal Structural Division, ASCE, Vol. 102, ST1, pp. 1-18, January.
- Smith, S.W., Ehrenberg, J.E., Hernandez, E.N. (1982). Analysis of the El Centro Differential Array for the 1979 Imperial Valley Earthquake, Bulletin of the Seismological Society of America, Vol. 72, pp. 237-258.
- Tajirian, F.F., Tabatabaie, M. and Lysmer, J. (1984). Truly Three-Dimensional Soil-Structure-Interaction Analysis of the Humboldt Bay Power Plant, Proceedings, International Symposium of Dynamic Soil-Structure Interaction, Minneapolis, Minnesota, pp. 147-152.
- Tera Corporation. (1980). Reduction in Free Field Ground Motion Due to the Presence of Structures, Report Submitted to Southern California Edison Company.
- Tsai, N.C. (1974). Modal Damping for Soil-Structure Interaction, Journal of the Engineering Mechanics Division, ASCE, Vol. 100, No. EM2, Proc. Paper 10490, pp. 323-341.
- Valera, J.E., Seed, H.B., Tsai, C.F., and Lysmer, J. (1977). Soil-structure Interaction Effects at the Humboldt Power Plant in the Ferndale Earthquake of June 7, 1975, Report No. UCB/EERC 77/02, Earthquake Engineering Research Center, University of California, Berkeley.
- Wong, H.L. and Luco, J.E. (1981). Identification of Sensitive Parameters for Soil-Structure Interaction, Report NUREG/CR-3044, UCRL-15493, Prepared for Lawrence Livermore National Laboratory, Livermore, California.
- Wong, H.L., and Luco, J.E. (1980). Soil-Structure Interaction: A Linear Continuum Mechanics Approach (CLASSI), Report CE 79-03, Department of Civil Engineering, University of Southern California, Los Angeles, California.

APPENDIX A

CALCULATIONS OF ACCIDENTAL ECCENTRICITY

In this study, limited analyses were made to examine the effect of phasing of the time histories of torque and base shear on the apparent accidental eccentricity for both the reactor building and auxiliary building due to non-vertically incident wave excitation analyzed by Luco et al. (1986). Results of these analyses are summarized in this appendix. The accidental eccentricity was calculated by an approximate procedure described as follows:

- (1) Calculation of effective base shear force, $(F_y)_e$, for non-vertically incident wave cases. The shear force in an individual shear wall resulting from a total shear force, $F_y(t)$, and a total torque, $M_z(t)$, can be expressed in terms of an effective shear, $(F_y)_e(t)$, given by

$$(F_y)_e(t) = |F_y(t)| + \frac{|M_z(t)|}{d} \quad (A-1)$$

where d is a characteristic length appropriate for the shear wall and depends on all other shear walls also present at a given elevation. In the case of a single circular ring wall of diameter, D :

$$d = D \quad (A-2)$$

However, with multiple ring walls, $d < D$. For typical walls in the reactor building analyzed in this study, d is assumed to be greater than 60 ft and less than 120 ft. In the case of a rectangular building with dimensions $a \times b$ and only a single solid exterior wall:

$$d = (a + b)/2 \quad (A-3)$$

For the auxiliary building analyzed in this study, d is assumed to be greater than 80 ft and less than 180 ft. For a given d , Eq. (A-1) is used to determine the maximum value of $|(F_y)_e|_{\max}$.

- (2) Determination of maximum values of base shear force, $|F_{yv}|_{\max}$, and torque, $|M_{zv}|_{\max}$, without combining them, for the vertically incident wave case. For a symmetric structure, the torque is zero.
- (3) Calculation of eccentricity, e , such that for the same d value used in Step 1, the following equation is satisfied:

$$|(F_y)_e|_{\max} = |F_{yv}|_{\max} + \frac{|M_{zv}|_{\max} + |F_{yv}|_{\max}e}{d} \quad (A-4)$$

where $|(F_y)_e|_{\max}$ is obtained from Eq. (A-1) in Step 1.

- (4) Repeating Steps 1 through 3 for other values of d in the range considered. The largest e required to satisfy Eq. (A-4) and divided by the maximum building plan dimension (127 ft for the reactor building and 270 ft for the auxiliary building) represents the accidental eccentricity from nonvertically incident waves.

ACCIDENTAL ECCENTRICITY FOR REACTOR BUILDING AND AUXILIARY BUILDING

As described in Section 3.3.1.2, parametric soil-structure interaction analyses were made during this study (Luco et al., 1986) to examine the effects of non-vertically incident waves on the response of a reactor building and an auxiliary building. Accidental eccentricities were calculated by using the approximate procedure described in this appendix for the reactor building analyzed for soil profile II and for the auxiliary building analyzed for soil profile III. The cases examined

are for an apparent horizontal velocity of 3 km/sec associated with SH-waves (designated as case b).

For purposes of examining the relative magnitude and phasing between the base shear forces and the torques induced by the non-vertically incident wave excitation, time histories of the base shear forces, $F_y(t)$, and the torques divided by a characteristic length, d , ($M_z(t)/d$), are compared in Figures A-1 and A-2 for the reactor building and Figures A-3 and A-4 for the auxiliary building. As shown in Figures A-1 and A-3, the out-of-phasesness of the torque and base-shear time histories of responses of the reactor building and the auxiliary building due to the broad-banded Reg. Guide 1.60 input is apparent. The relatively small contribution of the torque to the shear forces is also apparent in these figures from the comparisons of the amplitudes of the time histories of $M_z(t)/d$ and $F_y(t)$.

However, for the narrow-banded, short-duration Melendy Ranch input shown in Figures A-2 and A-4, peak torque and shear responses were out of phase in some cases (for the containment shell of the reactor building) and nearly in phase in other cases (for the internal structure of the reactor building and for the auxiliary building). Also, the figures indicate a larger contribution of the torque to the base shear force for the Melendy Ranch input than for the Reg. Guide 1.60 input.

The accidental eccentricities calculated for the reactor building and the auxiliary building using the approximate procedure described in this appendix are summarized in Table A-1. Accidental eccentricities were larger for the Melendy Ranch input than for the Reg. Guide 1.60 input. For cases using the Reg. Guide 1.60 input, the accidental eccentricities were less than 1 percent for the cases examined. For cases using the Melendy Ranch input, the accidental eccentricities were approximately 0.5 percent for the containment shell and approximately 3 percent for the internal structure of the reactor building, and approximately 15 percent for the auxiliary building.

Table A-1

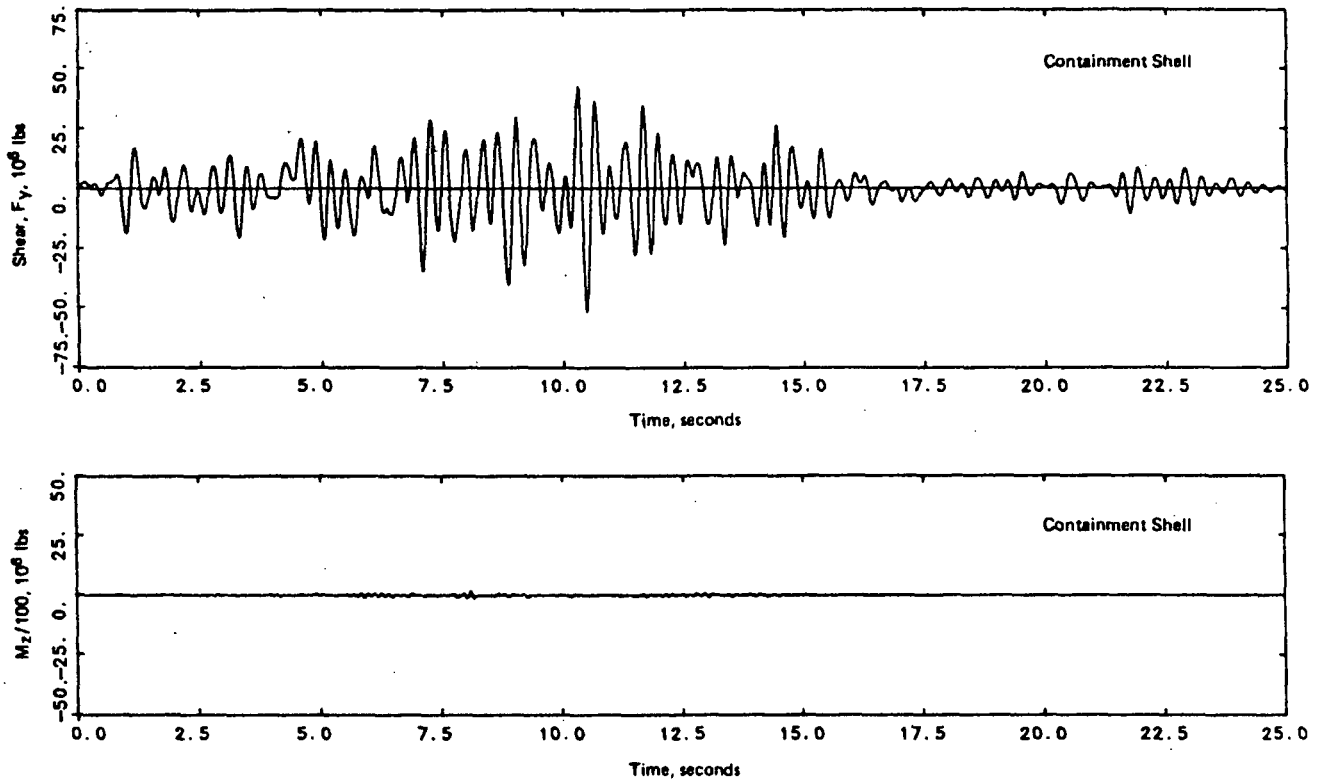
(1)

ACCIDENTAL ECCENTRICITY FOR NON-VERTICALLY INCIDENT EXCITATIONS

	Reactor Building		Auxiliary Building
	<u>Containment Shell</u>	<u>Internal Structure</u>	
Reg. Guide 1.60	0	0.8 - 0.9	0 - 0.2
Melendy Ranch	0.4 - 0.6	3 - 4	15 - 17

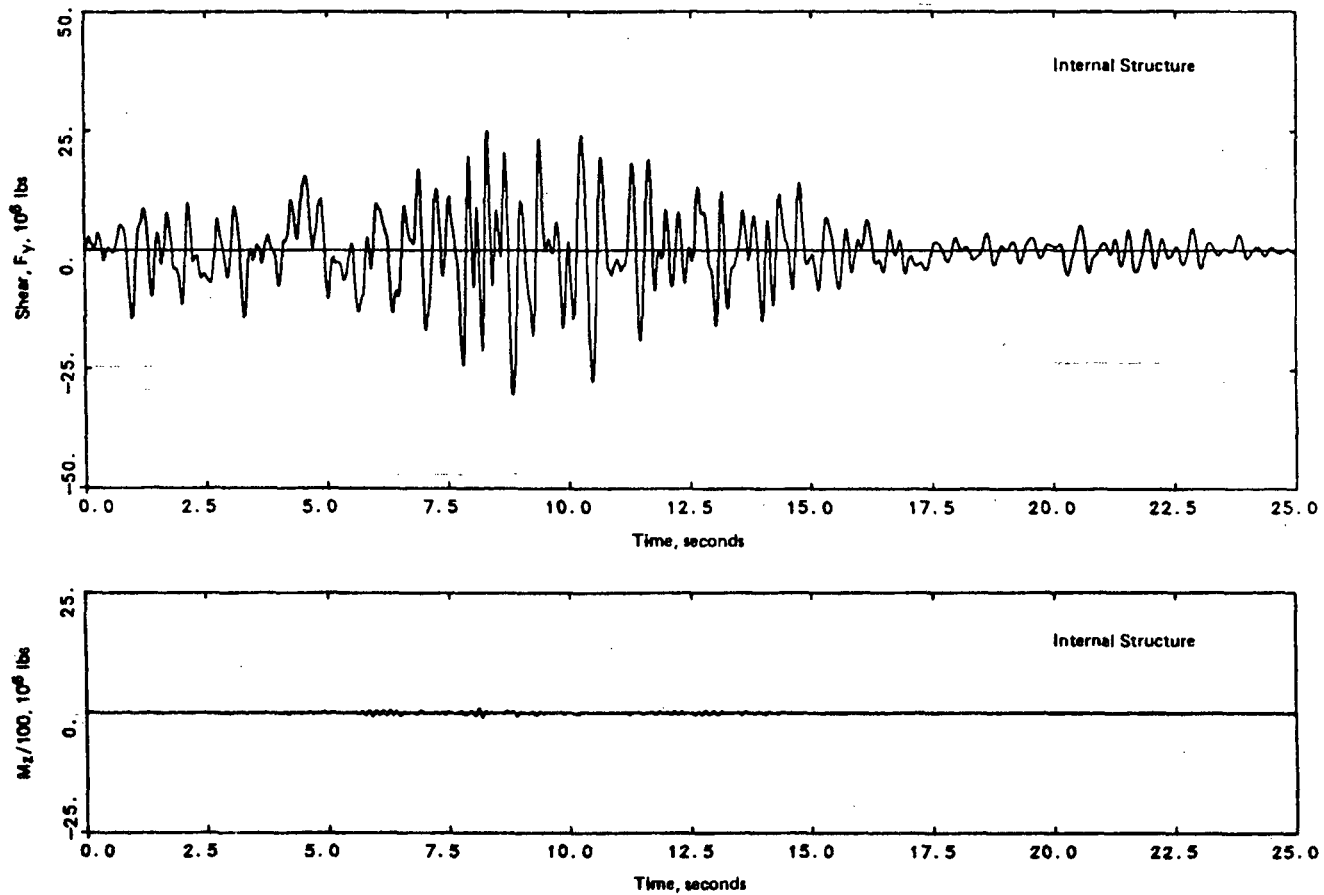
Note:(1) Accidental eccentricity is defined as a percentage of a characteristic dimension of the building. For the reactor building, a dimension equal to the diameter of the basemat ($2 L = 127$ ft) was used. For the auxiliary building, the maximum building plan dimension of 270 ft was used. Cases analyzed correspond to non-vertically incident wave excitation with an apparent horizontal propagation velocity of 3 km/sec associated with SH-waves (case b).

Based on Luco et al. (1986) (Vol. 4 of NUREG/CR-3805)



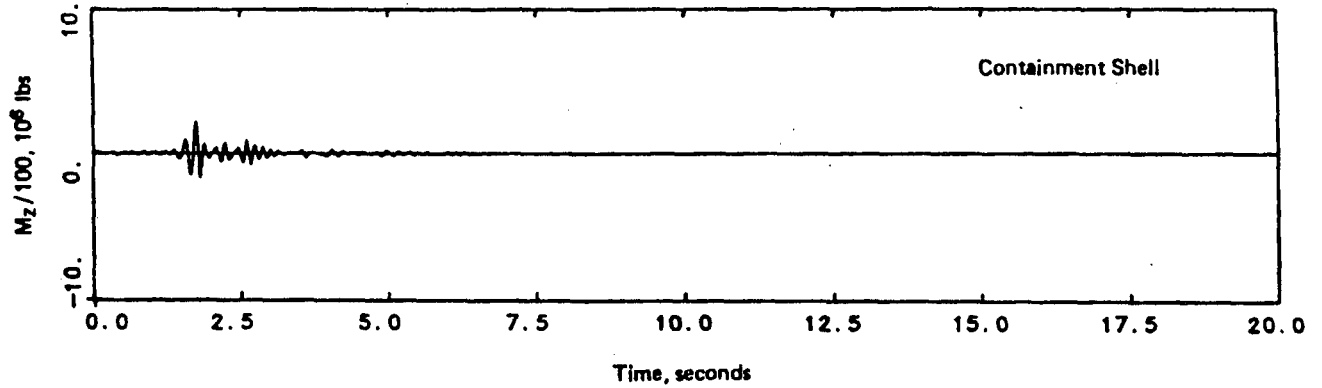
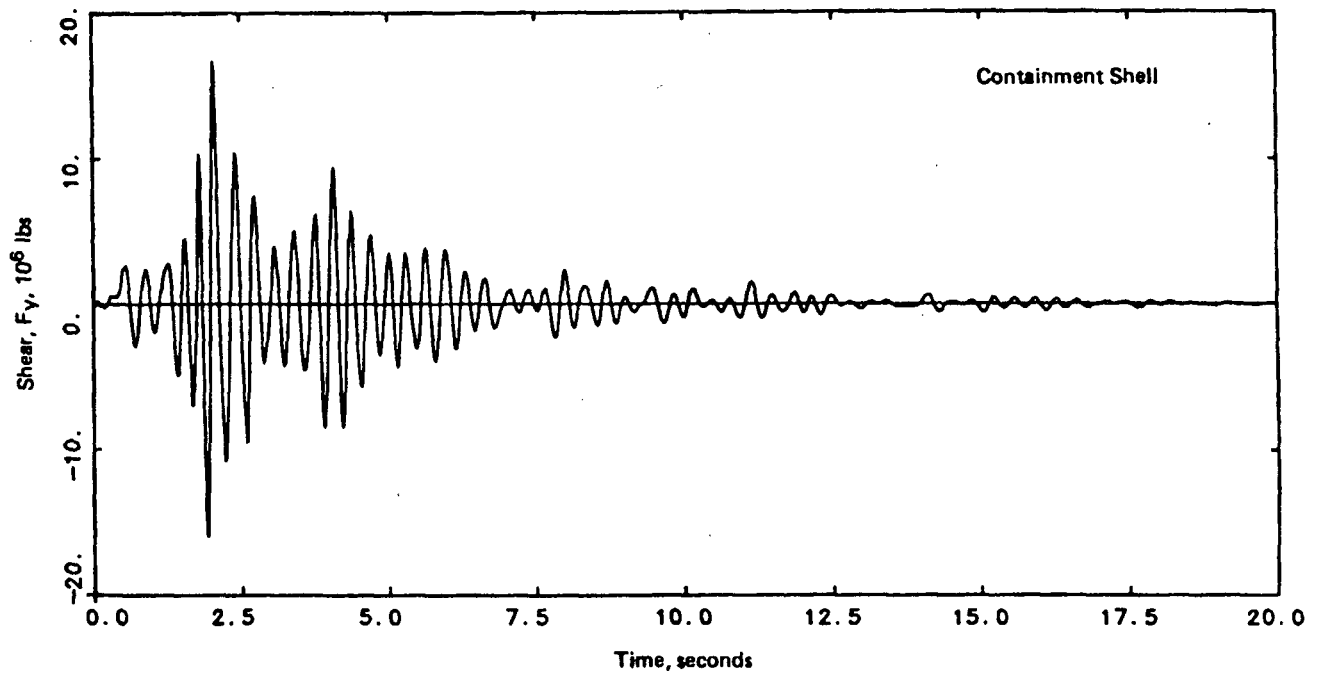
Based on Luco et al. (1986)
 (Vol. 4 of NUREG/CR-3805)

Figure A-1a. Time Histories of Base Shear and Torque (normalized by $d = 100$ ft), Reactor Building, 40 ft Embedment, Soil Profile II, Nonvertically Incident Waves ($C_y = 3$ km/sec), Artificial Reg. Guide 1.60 Excitation



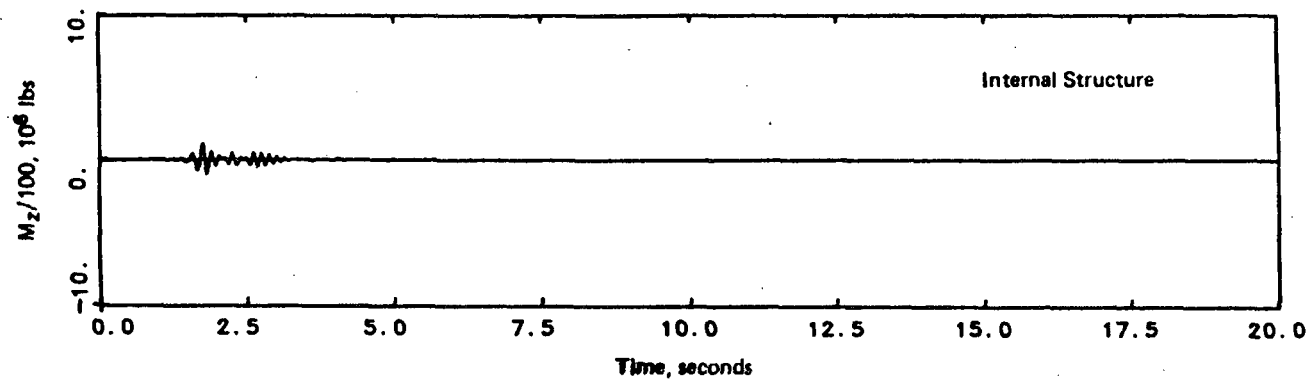
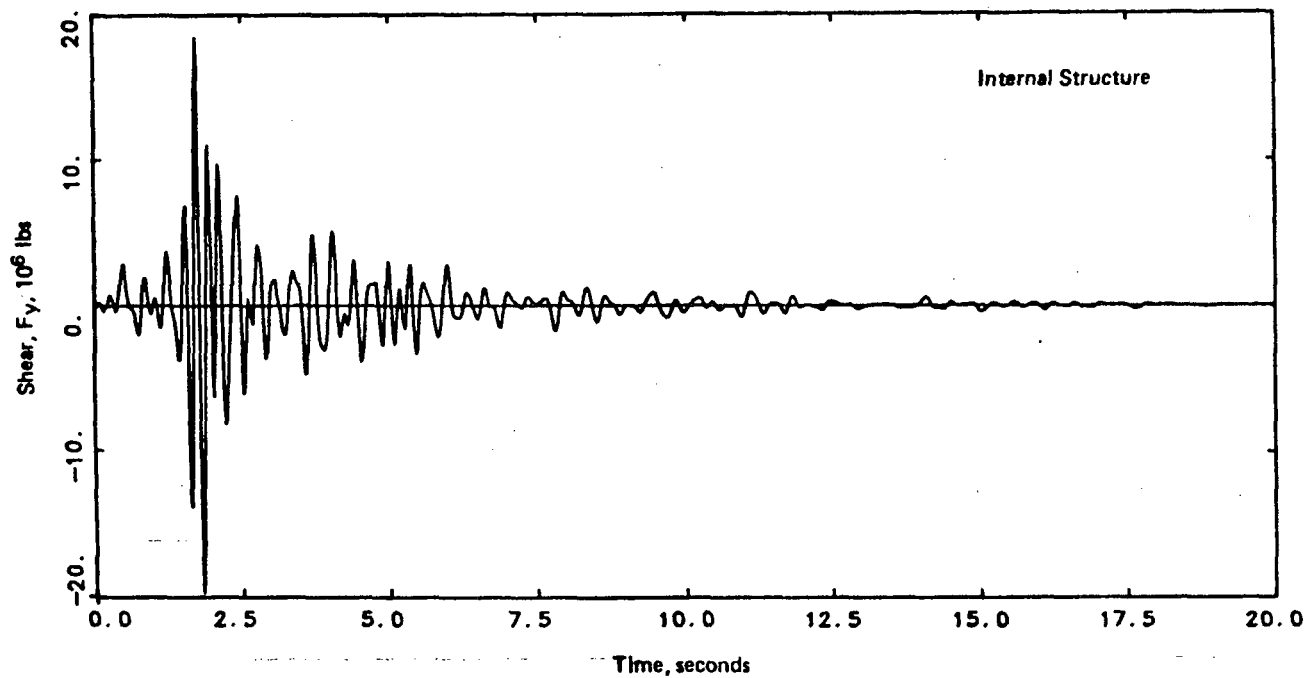
Based on Luco et al. (1986)
 (Vol. 4 of NUREG/CR-3805)

Figure A-1b. Time Histories of Base Shear and Torque (normalized by $d = 100$ ft)
 Reactor Building, 40 ft Embedment, Soil Profile II, Nonvertically
 Incident Waves ($C_y = 3$ km/sec), Artificial Reg. Guide 1.60 Excitation



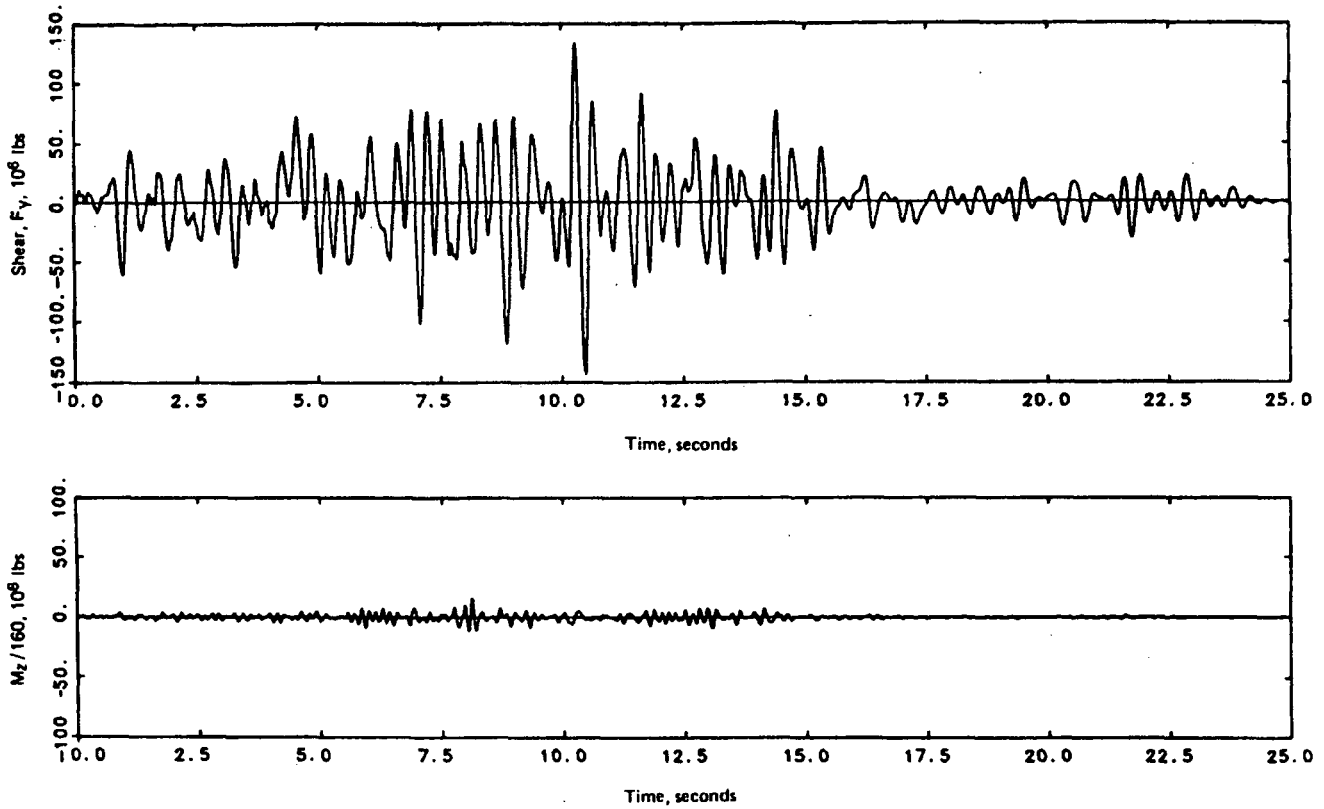
Based on Luco et al. (1986)
 (Vol. 4 of NUREG/CR-3805)

Figure A-2a. Time Histories of Base Shear and Torque (normalized by $d = 100$ ft), Reactor Building, 40 ft Embedment, Soil Profile II, Nonvertically Incident Waves ($C_y = 3$ km/sec), Melendy Ranch Excitation



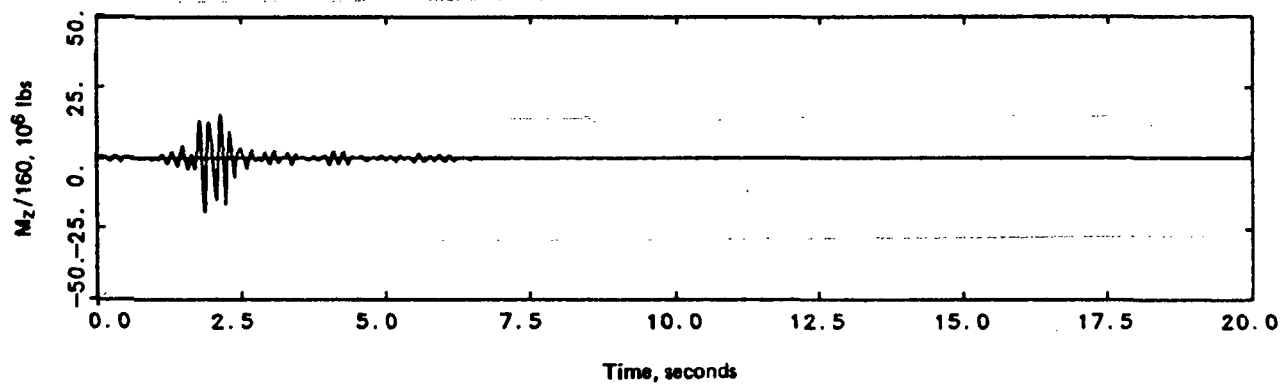
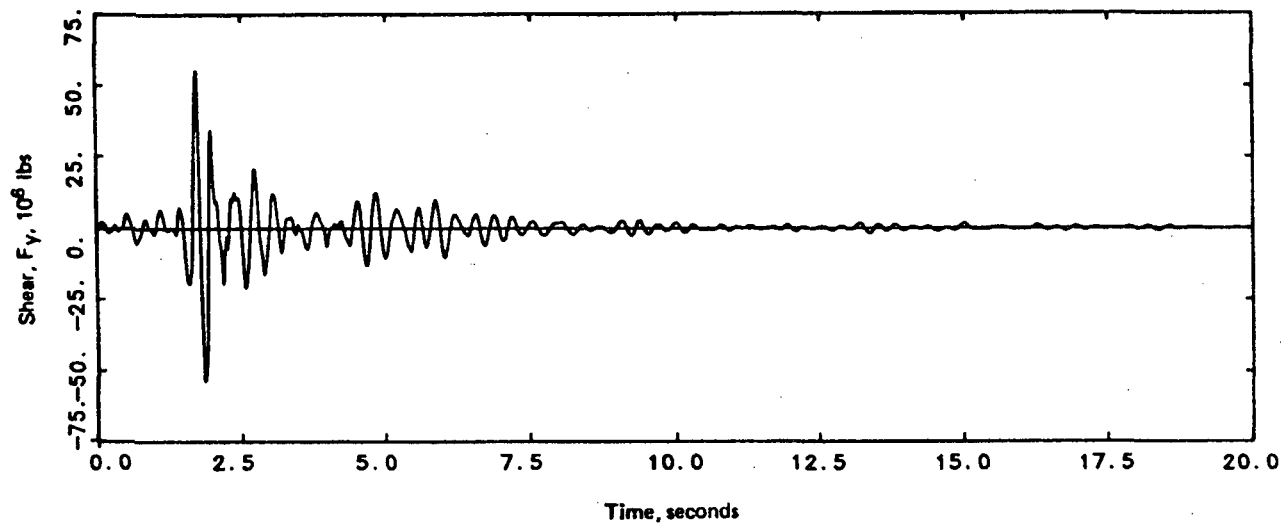
Based on Luco et al. (1986)
 (Vol. 4 of NUREG/CR-3805)

Figure A-2b. Time Histories of Base Shear and Torque (normalized by $d = 100$ ft), Reactor Building, 40 ft Embedment, Soil Profile II, Nonvertically Incident Waves ($C_y = 3$ km/sec), Melendy Ranch Excitation



Based on Luco et al. (1986)
 (Vol. 4 of NUREG/CR -- 3805)

Figure A-3. Time Histories of Base Shear and Torque (normalized by $d = 160$ ft), Auxiliary Building, Soil Profile III, Nonvertically Incident Waves ($C_y = 3$ km/sec), Artificial Reg. Guide 1.60 Excitation



Based on Luco et al. (1986)
 (Vol. 4 of NUREG/CR-3805)

Figure A-4. Time Histories of Base Shear and Torque (normalized by $d = 160$ ft), Auxiliary Building, Soil Profile III, Nonvertically Incident Waves ($C_y = 3$ km/sec), Melendy Ranch Excitation

NRC FORM 336 (2-84) NRCM 1102, 3201, 3202	U.S. NUCLEAR REGULATORY COMMISSION	1. REPORT NUMBER (Assigned by TIDC, add Vol. No., if any)				
BIBLIOGRAPHIC DATA SHEET		NUREG/CR-3805, Vol. 5				
SEE INSTRUCTIONS ON THE REVERSE		3. LEAVE BLANK				
2. TITLE AND SUBTITLE Engineering Characterization of Ground Motion Task II: Summary Report		4. DATE REPORT COMPLETED				
5. AUTHOR(S) M.S. Power, C.-Y. Chang, I.M. Idriss / WCC R.P. Kennedy / SMAI		<table border="1" style="width: 100%; border-collapse: collapse;"> <tr> <td style="width: 50%; text-align: center;">MONTH</td> <td style="width: 50%; text-align: center;">YEAR</td> </tr> <tr> <td style="text-align: center;">June</td> <td style="text-align: center;">1986</td> </tr> </table>	MONTH	YEAR	June	1986
MONTH	YEAR					
June	1986					
7. PERFORMING ORGANIZATION NAME AND MAILING ADDRESS (Include Zip Code) Woodward-Clyde Consultants Structural Mechanics 100 Pringle Avenue, Suite 300 Associates, Inc. Walnut Creek, California 94596 Newport Beach, CA 92660		8. PROJECT/TASK/WORK UNIT NUMBER				
10. SPONSORING ORGANIZATION NAME AND MAILING ADDRESS (Include Zip Code) Division of Engineering Technology Office of Nuclear Regulatory Research U.S. Nuclear Regulatory Commission Washington, D.C. 20555		9. FIN OR GRANT NUMBER <p style="text-align: center;">FIN B6680</p>				
12. SUPPLEMENTARY NOTES		11a. TYPE OF REPORT <p style="text-align: center;">Technical</p>				
13. ABSTRACT (200 words or less)		b. PERIOD COVERED (Inclusive dates) <p style="text-align: center;">1983 - 1985</p>				
<p>This report presents the results of part of a two-task study on the engineering characterization of earthquake ground motion for a nuclear power plant design. Task I of the study, which is presented in NUREG/CR-3805, Vol. I, developed a basis for selecting design response spectra taking into account the characteristics of free-field ground motion found to be significant in causing structural damage. Task II incorporates additional considerations of effects of spatial variations of ground motion and soil-structure interaction on foundation motions and structural response. The results of Task II are presented in four parts: (1) effects of ground motion characteristics on structural response of a typical PWR reactor building with localized nonlinearities and soil-structure interaction effects; (2) observational data on spatial variations of earthquake ground motion; (3) soil-structure interaction effects on structural response; and (4) summary based on Tasks I and II studies. This report presents the results of the fourth part of Task II.</p>						
14. DOCUMENT ANALYSIS - a. KEYWORDS/DESCRIPTORS		15. AVAILABILITY STATEMENT				
earthquake engineering earthquake ground motion effective peak acceleration soil-structure interaction spatial variations		<p style="text-align: center;">Unlimited</p>				
b. IDENTIFIERS/OPEN ENDED TERMS		16. SECURITY CLASSIFICATION				
		<table border="1" style="width: 100%; border-collapse: collapse;"> <tr> <td style="text-align: center;">(This page)</td> <td style="text-align: center;">Unclassified</td> </tr> <tr> <td style="text-align: center;">(This report)</td> <td style="text-align: center;">Unclassified</td> </tr> </table>	(This page)	Unclassified	(This report)	Unclassified
(This page)	Unclassified					
(This report)	Unclassified					
17. NUMBER OF PAGES		18. PRICE				